Blood Flow and The Mammalian Embryo

Thesis by

Elizabeth Anne Vincent Jones

In Partial Fulfillment of the Requirements

For the Degree of

Doctor of Philosophy

In Chemical Engineering

California Institute of Technology

Pasadena, CA

2005

(Defended January 13th, 2005)

Acknowledgements

I would like to thank Scott for his help over the years. On many occasions, meeting with Scott gave an instant answer to a problem I had been agonizing over for weeks. He truly is one of the most intelligent people I have ever met. I will also miss his sense of humour. They say that you have to worry when Scott stops making fun of you. I never did feel worried.

I would also like to thank Mary Dickinson. Our brain-storming sessions advanced my projects and helped me to get out of here quickly. She's been there when things were going well and she's learnt to stay clear when I'm grumpy. I wish her all the best as she begins her solo career and hope that Texas treats her well. I think we have learnt a lot together over the years and I hope that all her future students have as wonderful an experience as I have had.

I would like to thank the rest of my committee as well. To Marianne Bronner-Fraser, who has been insightful and who has thoroughly supported me throughout my years here. To Mory Gharib, who has always made me feel that my research was exciting and important. To John Brady, for all the times I came to his office, asking questions. He was very open and always available to help me. And to Anand Asthagiri, for asking perceptive questions during committee meetings that helped me along on my research path.

I would like to thank all my labmates. To David Koos, who spend endless hours with me when nothing was working and asked nothing in return. To Helen McBride, who has

read every word I've ever written and came up with experiments for me to try when I was stuck. You really keep the Fraser lab running. To Carole and Christie, who smile and bring silliness into my life (and sometimes bellydance). To Raj, who makes me speak Spanish even though I don't really know how to. To Melanie Martin, who has now left the Fraser lab, for singing Canadian children's songs in lab with me and sharing the Seder with me every year. I would also like to thank the technical staff in the lab and at Caltech in general. To Chris Waters, who has put up with my mood swings and ignored me when I stole his lab supplies. To Mary Flowers, who is a lab mom par excellence. You are patient and understanding of the moods of a scientist. To Gary Belford, who has calmed me down when everything around me was crashing, or at least all the computers were. You are generous with your time and make our lives a lot easier. To Aura Keeter, who works behind the scenes and is always helpful and available.

I would like to thank my parents. They have been very supportive and I know they are proud of me. To my brother, Greg, and his fiancée Michelle, I wish you both a lot of happiness. To James, who has been my shoulder to cry on when things were bad and who has forgivingly taken all the crap I've slung his way. To James again, who did a far bit of slinging of his own. To Amber and Jason, who found me when I was lonely and stayed to keep me company. I love the both of you. To the bellydancing crew, who stole me away from lab and made me shake and jingle my butt.

Abstract

Hemodynamics, or blood fluid dynamics, is of great importance in vascular biology and its role is well recognized in events ranging from atherosclerosis to wound healing. The importance of hemodynamics during embryonic development, however, is less clear. The early vertebrate vasculature is established through two processes; vasculogenesis, which is the de novo formation of vessels and angiogenesis, which is the sprouting of new vessels from existing vessels and the remodeling of existing vessels. The latter process, angiogenesis and vascular remodeling, is dependent on blood flow and does not occur if cardiac output is blocked. As well, if blood flow is altered, such as with mutations that affect cardiac contraction, the early vessels also fail to remodel. Flowing blood imparts a physical force, called shear stress, on the endothelial lining of the blood vessels. Many genes known to be regulated by shear stress are important for vascular remodeling in the embryo. In this work, we investigate the role of shear stress on the remodeling process.

Studying the role of shear stress in embryos requires the ability to measure changes in both fluid dynamics and vascular morphology as well as methods to alter shear stress levels. In this work, we use an optical technique for the quantitative analysis of hemodynamics during early organogenesis in the mouse embryo. We established the morphological changes that occur in the vasculature during remodeling and link these to the fluid dynamics that are present. We establish the mechanical cues that are available to the endothelial cells and the type of flow present at various stages of development. In order to understand how these mechanical cues affect embryonic development, we examine altered shear stress during development using a mutant mouse model in which the atrial cardiac contraction is lacking as well as inducing specific changes in shear

stress through chemical manipulation of the embryonic cardiovascular system. These studies establish a link between the pattern of blood flow within the vasculature and the stage of cardiovascular development and enable analysis of the influence of mechanical forces during development.

Table of Contents

Chapter 1

Introduction

The cardiovascular system is the first functional organ system to develop in the embryo and is critical to embryonic survival [1]. Malformations of the circulatory system are thought to account for approximately 10% of still births in humans. In live births, there is a reported incidence of blood vessel and heart defects of 1%, making this the most common human birth defect [2]. In addition, gene ablation studies in mice show that when genes important to cardiovascular development are ablated, the embryos die at mid-gestation [3]. Though formation of a functional cardiovascular system is so critical to development, the mechanism through which the cardiovascular system is established is poorly understood.

For the cardiovascular system to function properly, several components must merge and integrate, blood as the fluid, vessels as the conduits and the heart as the pump. As such, the study of cardiovascular development can be divided into four areas, hematopoiesis or blood formation, vasculogenesis or the de novo formation of vessels, angiogenesis also called vessel sprouting, and heart development. Understanding how these four fields come together, however, is essential for understanding how an operational cardiovascular system arises.

Much of current cardiovascular research focuses on genes that are necessary for the formation of the developing cardiovascular system. However, elucidation of the genetic mechanisms only reveals part of the picture. Proper formation of the cardiovascular system requires many dynamic input, some which are genetically encoded, others that arise by the transport of nutrients, and others still which are derived from the mechanical forces generated by blood flow. I have focused my studies specifically on the

importance of blood flow and the possible regulatory role that fluid dynamics play during cardiovascular development.

Cardiovascular Development

Shortly after the mouse embryo implants into the uterine wall at 4.5 days of gestation (E4.5), the embryo gastrulates, whereby the three primary cell layers of the embryo are formed. These cell layers are called ectoderm, mesoderm and endoderm. Ectodermal derivatives include skin and neural tissue. Cells that form most of the organs in the embryo are of mesodermal origin. Endoderm derivatives include the lungs, liver, stomach, intestines and other components of the digestive system. After gastrulation, the embryo enters a period of development called organogenesis. It is during this period of development that most of the organs of the embryo form.

Vertebrate embryos in organogenesis are often staged by the number of somites present. Somites are blocks of mesodermal cells that give rise to muscle and skeletal tissue. The first somite appears in a mouse embryo at 8 days of gestation (E8.0) and then one somite forms every 1.5 hours thereafter. Organogenesis begins at 7 days of gestation (E7.0) and at this point in development, the cardiovascular cells, both hematopoietic (blood-forming) and endothelial, are formed.

Hematopoietic and endothelial precursors form in the mesodermal tissue of the embryo, receiving signals from the endoderm [4]. The induction of this differentiation seems to be largely driven by a protein called FGF-2 [5]. As these precursor cells form, they clump together, with the inner cells becoming erythroblasts, or primitive red blood cells,

and the outer cells flattening to become endothelial cells [6]. These precursors localize to the yolk sac, an extra-embryonic membrane that surrounds the developing embryo, and form a tight band of cells called the blood islands (Figure 1, pre-somitic stage). The common inductive signals [7-11] and the co-localization of hematopoietic and endothelial cells have led to the idea of the hemangioblast, a common precursor of both cell types [12, 13].

Primitive hematopoiesis in the blood islands is very different from hematopoiesis in the mature organism. Blood islands in the yolk sac produce mainly erythroblasts, or primitive red blood cells [14], though some megakaryocytes [15] and primitive macrophages may also be produced [16, 17]. In addition, these primitive erythroblasts differ from mature red blood cells in that they produce different haemoglobin than mature red blood cells, and are larger in size and nucleated [18]. Because these early red blood cells are nucleated, they are rounded rather than disc-like in shape. Mammals represent the only vertebrate species that have enucleated red blood cells [19] and the evolutionary advantage of enucleated red blood cells is unclear.

Endothelial precursors begin to expand from the blood islands much earlier than the hematopoietic cells (Figure 1, 1 somite stage) [20, 21]. It is not known if these precursor cells retain any “hemangioblast” characteristics once they leave the blood islands, though there is evidence that some cells of the endothelium throughout the embryo can produce erythroblasts during early cardiovascular development [22]. How the population of cells expands has not been established either, whether it is by de novo induction of endothelial precursor in the rest of the yolk sac or by cell division and migration from the

blood islands. In the chick embryo, it has been shown that angioblasts undergo extensive migration [23]. Similarities in mouse embryo development suggest that endothelial precursors in mammals have similar migratory capabilities. The endothelial precursors coalesce into strands that are referred to as the angioblastic cords (Figure 1, 3 to 4 somite stage). The formation of these cords can also be induced *in vitro* by culturing endothelial cells on Matrigel, a membrane matrix [24]. These *in vitro* structures resemble capillaries, and given a high enough seeding population, will link to form vascular networks that are morphologically similar to the early vessels of the embryo. Interestingly, the formation of these networks can be modeled based on paracrine growth factor production and diffusion [25]. The formation of angioblastic cords in mouse embryos begins at E8.0 (0 somites) and the entire yolk sac is covered in angioblastic cords 6 hours later at 4 somites [21]. Hematopoietic cells, however, are still clustered in the blood islands (Figure 1, 4 somites).

In order to produce functional blood vessels, the angioblastic cords must then lumenize. The process of lumenization involves the formation of “slit-like spaces” between angioblasts [26]. The contents of these slits forms the primordial blood plasma [27]. The exact timing of lumenization has not been firmly established and the mechanism of lumenization is poorly understood. It is generally believed that the lumen forms by the production and coalescence of vacuoles within the endothelial cells [28]. Once lumens have formed within the endothelial cells, proper channels for blood flow are present.

At the same time as endothelial and hematopoietic cells are forming in the yolk sac, the heart arises in the embryo proper (Figure 1). As with hematopoietic and endothelial

precursors, heart tissue is derived from mesodermal tissue by late gastrulation [29]. These initial heart cells are recognizable as an epithelial layer that forms a crescent between the embryonic and extra-embryonic regions of the embryo (Figure 1, 1 somite) [30]. By the 4 somite stage, the two sections of this crescent migrate to the midline and fuse to form a linear heart tube (Figure 1, 4 somite) [31]. The heart begins contractile activity essentially as it is forming, with the first beating cardiomyocytes being present at 3 somites [32].

Though there is a beating heart present by 3 somites, the exact onset of erythroblast circulation is not known. Early hematopoietic cells are tightly associated with the endothelial cells through junctional proteins [28]. These cells must lose their attachment and become free within the vessel [28]. As such, the exact timing of the entry of erythroblasts into circulation has not been established. Studies on fixed samples by McGrath *et al*., have indicated that circulation begins between 4 and 6 somites because erythroblasts can be found outside the blood islands at this stage (Figure 1, 4 to 6 somites). Using Doppler Ultrasound, fluid motion can be detected at the 7 somite stage [33], but it may be difficult to detect initial flows with this method. The entry of erythroblasts into circulation changes many of the characteristics of the blood, such as the viscosity [34], and therefore, the exact timing of these events is essential.

After the onset of blood flow, the initial capillary plexus undergoes a remodeling process culminating in the formation of large vessels such as the vitelline veins and arteries (Figure 2). Remodeling is characterized by changes in vessel morphology including the formation of large vessels, and recruitment of peripheral cell types [35]. The process of

remodeling is heavily dependent on flow. Nearly a hundred years ago, Chapman showed by surgically removing the heart before the commencement of circulation that the peripheral vasculature formed, but failed to remodel without blood flow and pressure [36]. Manner *et al.,* surgically removed the heart of young chicken embryos and incubated the embryos in high levels of oxygen to remove the effects of hypoxia, and found that though there were fewer deformities in the embryo proper, the remodeling of the vasculature still did not occur [37]. In the Ncx1 knockout mouse, the heart is formed but does not beat. In these embryos, the plexus forms in the yolk sac, but is never remodeled into vessels, even though other aspects of development, such as limb and organ development, are normal [38] .

There are three main hypotheses as to why blood flow is important to remodeling. The first is that unnourished tissue releases hypoxic signals that induce the alteration of the blood vessels. The second possibility is that the commencement of the blood flow increases delivery of nutrients and signaling molecules that induce growth in endothelial cells. Lastly, the forces created by the flow itself could signal angiogenesis in the embryos. Forces from blood flow have been shown to cause changes in morphology, cytoskeleton organization, ion channel activation and gene expression within endothelial cells [39] and turbulent flows have been shown to increase cell turnover rates [40]. This research will explore the possibility that mechanical forces are necessary for vessel remodeling by measuring forces caused by flowing blood and correlating these forces with observed changes in vascular remodeling.

Shear Stress in the Cardiovascular System

The vascular endothelium is the interface in the cardiovascular system between the blood vessel wall and the flowing blood. As such, these cells are exposed to both shear stress, the tangential force caused by the flowing of the blood, and blood pressure, a force perpendicular to the vessel wall. These forces can act as a signaling mechanism upregulating or activating many genes including genes that are important to cardiovascular development such as PDGF-β [41], connexin43 [42] and Flk1 [42]. Understanding what intracellular changes occur when cells are exposed to shear stress is an active area of research.

One of the open questions in the field is how endothelial cells can sense the presence of shear stress. This ability to sense shear stress, called mechanotransduction, may result from ion channels expressed on endothelial cells, which can be activated by the stretch caused by the flowing blood. Activation of the channels causes an increase in polarization of the cells and an increase in intracellular calcium [43]. This signaling mechanism appears consistent with many of the genes that are activated within minutes of the onset of flow, however, it does not explain many of the long term changes associated with exposure of endothelial cells to shear. The most likely candidates for mechanotransduction of shear stresses are the junctional complexes that link endothelial cells to each other or to the extra-cellular matrix. The cytoskeleton anchors to other cells through adherens junctions [44]. Shear stress induces changes in the organization of the adherens junctions and causes complex formation which include VE-cadherin and β-catenin [45]. Connections between the cytoskeleton and the extra-cellular matrix

through integrins are also important. Activation of various integrins has been shown to be essential for many shear stress responses (for review, see [46]). Though the exact mechanism of shear response remains elusive, it seems likely that changes in the cytoskeleton and its connection to the surrounding environment are crucial to the process.

Understanding the role of shear stress in biology is complicated by the fact that different types of flow seem to differentially induce gene expression (for review, see [46]). Thus, it is not enough to analyze the level of shear stress present, but one must also look at whether the flow is laminar or turbulent, and the role of oscillatory shear stress. The presence of laminar flow, which is a type of fluid flow where the streamlines of the fluid motion are parallel, has been found to have atheroprotective effects on blood vessels [47]. Laminar shear stress reduces levels of apoptosis [48] and induces many anti-apoptotic genes, such as Bcl-X_L [49]. Though laminar flow prevents apoptosis, it also keeps cells from proliferating by inhibiting DNA synthesis [50, 51]. Through microarray analysis, it is known that physiological levels of laminar shear stress downregulates more genes than it upregulates [52]. Disturbed flow, a term which includes both turbulent flow and eddies caused by laminar flow separation, is a much more biologically active flow. It is rarely seen in the mammalian cardiovascular system and is generally indicative of disease. Vessel bifurcations are prone to flow separation and eddy formation, and it was observed that atherosclerotic plaques formed preferentially at these locations [53]. From *in vitro* work, it was found that large gradients of shear stress, such as those present during oscillatory flow, caused endothelial cell migration and proliferation [54]. Turbulence induces apoptosis by the activation genes such as the Fas

receptor [55], and increases cell proliferation rates [40]. Thus, the type of shear stress, the gradients of shear stress and the magnitude of shear stress are all important considerations when analyzing endothelial cells' response to shear stress.

The flow patterns present in blood vessels are highly complex and variable. As such, *in vitro* studies are inherently limited to approximations of flows that cells would normally experience. Analysis of shear stress response *in vivo*, however, is difficult. Work using cDNA microarrays has been used to quantify changes in gene expression *in vivo* when flow is chronically increased or decreased and these results agree with many of the gene changes seen *in vitro* [56]. To correlate these results to the levels of shear stress or the type of flow present in the blood vessel requires a better understanding of the flow dynamics present *in vivo*.

Blood Fluid Dynamics

The mature vasculature is made up of arteries, arterioles, capillaries, venules and veins. The arterioles, venules and capillaries make up the microcirculation, which is defined as any vessel with a diameter less than 180 μm [57]. In the early embryonic plexus, the range of vessel diameter present is between 10 and 100 μm and therefore the flow is most similar to flow in mature microcirculation than any other vessels of the adult. Much of the research into blood fluid dynamics, however, has focused on larger structures such as the heart and major vessels because measurements are problematic in the

smallest vessels. As such, the knowledge of the blood fluid dynamics that is applicable to the embryonic case is limited.

One of the characteristic of flow in microcirculation is the presence of very low Reynold's number flow. The Reynold's number is the ratio of the viscous forces to inertial forces in a flowing fluid. As inertial forces become more important, and the Reynold's number increases, flow will become turbulent. The switch to turbulent flow occurs at a Reynold's number of approximately 2100 for flow in tubes. The exceedingly low Reynold's number in embryonic blood vessels (<<1) indicates that viscous forces dominate. In such a flow regime, inertial effects can effectively be ignored.

The other parameter of importance in establishing the type of flow present in a blood vessel is the Womersley number (α). The Womersley number describes the relative importance of the transient inertial forces due to the pulsatility of the flow as compared to the viscous forces [58]. When flow oscillates, the velocity must be equal to zero at the wall of the vessel because of high frictional forces. This causes a viscous boundary layer to be present near the vessel wall. Flow in the centre of the vessel, however, is inertial and pulsatile. The Womersley number describes the relative thickness of the viscous boundary layer as compared to the diameter of the vessel. In embryonic blood flow, because the pulse is slow (~1 beat per second) and the vessel diameters are small, the Womersley number is very small (<< 1). As such, a quasi-steady state can be assumed where the viscous effects dominate throughout the entire vessel and fully developed laminar flow is expected to be present throughout the cardiac cycle [59].

With very small Reynold's and Womersley number, an analytical solution to the basic equations of flow is possible. The law of conservation of momentum as applied to a fluid is called the Navier Stoke's equation. It states that:

$$\rho \frac{D\vec{v}}{Dt} = \mu \nabla^2 \vec{v} - \nabla p + \rho g \, .$$

Given the relative importance of viscous forces over inertial forces, both transient and convective acceleration can be ignored from the equations of flow. As well, the gravitational term can be ignored because of the low Reynold's number. This simplifies the Navier Stoke's equation to:

$$\mu \nabla^2 \vec{v} = \nabla p \, .$$

This equation is known as Stoke's equation. The simplifications make the equation linear and no longer dependant on time. From these equations, we expect blood flow to have a laminar velocity profile throughout the cardiac cycle. Laminar flow in a pipe has a parabolic velocity profile described by the equation:

$$V = V_{\max} \left(1 - \frac{r^2}{R^2} \right),$$

where V_{max} is the velocity at the centre of the vessel.

The assumption in these equations is that blood behaves as a Newtonian fluid. Newtonian fluids have a constant viscosity at all shear rates. Blood, however, consists of particles, or the red blood cells, suspended in the blood plasma. In large blood vessels, this primarily causes an increase in the viscosity and the fluid can be treated as a homogenous Newtonian fluid [60]. In smaller vessels and at low shear rates, the presence of red blood cells causes blood to exhibit non-Newtonian behavior [34]. As the diameter of the vessels approaches the diameter of a red blood cell, the fluid motion can no longer be thought of as a homogenous fluid [61]. The boundary layer, in which no blood cells are found, is no longer a small fraction of the total tube diameter. Vessels as small as 22 μm, however, can be considered as homogeneous liquids with an apparent viscosity determined by the shear rate and tube hematocrit, or volume fraction of red blood cells [62]. Most vessels within the embryo fall within this range and therefore blood can be treated as homogenous.

Another important consideration when analyzing the rheology of blood in embryos is that early erythroblasts are spherical, rather than bi-concave [18], which affects the visco-elastic characteristics of blood. Many of the non-Newtonian properties of blood are due to the elasticity and shape of the red blood cells. For bi-concave cells, the hematocrit, or volume percent of the blood taken up by red blood cells, can be as high as 58% without deformation of the cells [63]. Spherical blood cells, however, do not allow for such a high packing density. Research has been done comparing other enucleated forms of blood, such as avian blood, to human nucleated blood and no significant effect of the nucleation was found at hematocrits below 50% [64]. As such, the nucleation of

erythroblasts in embryonic development is not expected to have significant effects on the visco-elastic properties of the blood.

There are many important morphological differences between vessel of microcirculation and of the embryo that affect the flow properties. Pulsatile flow is not present in mature microcirculation because the pulses are attenuated by the time they reach the capillaries [65]. Since all vessels in the embryo fall within the category of microcirculation, pulsatile flow is often found in these vessels.

In addition to differences in hemodynamic properties, there are many important morphological differences between mature microcirculation and embryonic vasculature. Mature capillaries are surrounded by support cell types, such as pericytes and smooth muscle cells, that affect the vessel's elasticity and reaction to hemodynamic stimuli. These are not present in the embryo until after remodeling has occurred [6, 66]. Also, mature vasculature is lined with a layer of glycoproteins called the glycocalyx as well as a much thicker layer of absorbed plasma proteins called the endothelial surface layer [67]. The endothelial cell layer increases microvascular resistivity [68]. It is not known whether the embryonic blood vessels contain a glycocalyx, however, the much thicker (500 nm vs. 70 nm [67]) endothelial surface layer is unlikely to be present since many of the proteins known to form the layer are not expressed in the early embryo. Thus, embryonic vasculature represents a much simpler situation than mature circulation. Whereas the vessels of mature microcirculation could be described as elastic, reactive tubes that are lined with a porous solid, the embryonic vasculature resemble more a simple rigid tube of endothelial cells.

Based on the above considerations, it is possible to calculate many of the hemodynamic parameters of the flow through embryonic vasculature. This calculation requires knowledge of the velocity profile in the blood vessels and the hematocrit, or packing density of the red blood cells. Only by measuring these quantities within the embryo will it be possible to understand the role of hemodynamics in vascular remodeling.

Design Principles of Vascular Beds

Not only can individual cells react to fluid dynamics and shear stress, it is also known that networks of vessels adapt to chronic changes in flow. It is important to note that the flow rate in any given vessel is not only dependent on the flow resistance of the given vessel, but also on the flow resistance of all vessels upstream or downstream from it. If flow is reduced in a vessel, there is a chronic decrease in the vessel diameter [69-71]. Though the flow and diameter change in these experiments, measured wall shear rate remains constant [71] indicating the ability of the network to normalize shear stress upon chronic changes in flow. As such, the reaction of endothelial cells to shear stress is most relevant when considering it as part of a whole network.

A common method for predicting the final configuration of vascular networks is to minimize a cost function. When the cost function is configured to minimize the total energy required to drive and maintain blood, the results describe the relation between

the diameters of parent and daughter branches in the vasculature, such that:

$$D_o^{\,3} = D_1^{\,3} + D_2^{\,3}.$$

This is known as Murray's law [72]. A consequence of Murray's law is that a constant shear stress should be present within the vascular system [73]. In the chick embryo, it was found that Murray's law does hold within the early vasculature, even before the appearance of smooth muscle cells that actively regulate diameter with respect to shear stress [74]. Regression of the diameter data did, however, predict an actual exponent closer to 2.8. This value for the exponent can be obtained if wall tissue mass is chosen as the cost function to be minimized. In fact, it has been suggested that the production of vessel wall tissue is a limiting factor during embryonic development [75]. The fact that embryonic vasculature can be modeled by cost functions, however, indicates that even at very early stages the vasculature can respond to hemodynamic load on the vessels.

Though Murray's law predicts constant shear stress within the vasculature, measurements on mature cardiovascular system have shown that shear stress in arteries and capillaries is fairly constant, however shear stress levels are much lower in veins [76]. One of the largest differences between the arterial and venous system is the level of pressure in the system. It is well established that vascular networks react to both shear stress and pressure. Chronic elevation in shear stress leads to increased vessel diameter, whereas chronic increases in pressure lead to decreased vessel diameter [77, 78]. This work has led to a pressure-shear hypothesis whereby shear stress levels are a function of local pressure [76].

There are several important considerations when applying design principles developed for microcirculation to embryonic vessels. In mature vasculature, functional requirements, such as nutrient and oxygen delivery, must have priority over the energy costs of the flowing blood. Many of the metabolic needs of the embryo, however, are met by diffusion from the maternal circulation. In addition, mature vascular networks have the ability to transmit information from one vessel segment to another through gap junctions, which are intercellular channels [79]. The importance of this communication in embryos, however, is not clear since mice that lack vascular gap junctions survive until about birth (Simon & McWhorter, 2002). Establishing the vascular design principles that control embryonic remodeling is therefore essential to the understanding of cardiovascular development.

Hemodynamics in Embryos

The role of fluid dynamics and shear stress in embryonic development is even less clear than in mature circulation. Recent work has shown however that proper fluid dynamics are essential, even at the earliest stages of development. Hove *et al*. analyzed the fluid dynamics present during zebrafish heart development and perturbed the fluid dynamics by inserting beads within the flow in the heart [80]. This perturbation resulted in the heart failing to undergo looping, a process involved in heart chamber formation, and failing to form the third chamber of the fish heart called the bulbus. Blood flow patterns in the heart and dorsal aorta of the developing mouse embryo have also been investigated using ultrasound-biomicroscopy [33, 59, 81, 82]. This work has been

extended to mutant phenotypes, analyzing flow velocities in the NFATc1$^{-/-}$ mutant in which the aortic and pulmonary valves fail to form resulting in abnormal circulatory patterns and embryonic lethality [83]. Taken together, the work from these labs shows that proper hemodynamic conditions are essential for normal development, and that a failure to establish proper flow leads to embryonic mortality.

Work on the blood vessels, rather than the heart, is even more limited. Over one hundred years ago, Thoma (1893) observed that within embryos, vessels that carry the most blood flow enlarge, while vessels that carry little flow regress [84]. Twenty years later, Chapman (1918) theorized from his experiments where the heart of chick embryos was surgically removed, that the initial vasculature was laid down by purely hereditary principles and the subsequent development occurred purely by mechanical forces [36]. Measurements of hemodynamic parameters in chick embryos have also been reported in the literature [75, 85], however these are generally limited to older embryos because of the difficulty in measuring flow and pressure in young embryos. If the role of blood fluid dynamics in development is to be understood, it will require the development of new techniques specific to the problem. In this work, I present two such techniques, one which gives researchers access to developing mammalian embryos through embryonic culture, and a second which allows the velocity of flowing embryonic erythroblasts to be measured.

Concluding Remarks

The main aim of this research is to expand the knowledge of how blood flow relates to embryonic development. The role of hemodynamics has been recognized in several cardiovascular diseases, such as atherosclerosis, and in normal function, such as microvascular remodeling. What is less clear is whether these same forces play roles in other areas of the cardiovascular system. Many diseases, such as pancreatic cancer [86], are caused by the improper reactivation of developmental gene cascades. Though such a large quantity of research shows that blood flow is biologically active, it is generally believed that signals from hypoxic, or oxygen starved, tissues are the cause of remodeling and that the forces caused by blood flow have no role in the early embryo. As such, this work endeavors to show that:

1. Blood flow initiates remodeling of the vascular plexus.
2. Increases in shear stresses caused by the onset of erythroblast circulation are necessary for remodeling to occur.
3. Altered hemodynamic conditions alone can cause defects in vascular remodeling within the embryo.

By imaging fluid dynamics and assessing the forces on the endothelial cells during the period of development where the heart begins to beat, the relation between the flow forces and the restructuring that occurs can be investigated. This has been done using a static embryo culture technique (Chapter 2, [87]) that allows embryos to be observed over a period of 24 hours. In order to measure flow profiles, a technique developed for measuring blood flow in adult microcirculation has been adapted to embryonic blood

flow. In this method, a confocal laser scanning microscope is used to scan a single line perpendicular to the flow in a vessel to measure flow velocity (Chapter 3, [88]). This work allows us to characterize vascular and hematopoietic development, as well as to characterize the flow dynamics present in these early vessels (Chapter 4, Jones *et al*., submitted). The work also compares these forces during normal development to fluid forces present during abnormal development in order to understand how mutants differ from the normal developmental course (Chapter 5, Jones *et al*., in preparation).

The development of the mature vasculature is a complex, multi-step process. By focusing on one aspect, the earliest flow, some of the most important physical forces on the vasculature are explored. There is a great need for this research. With cardiovascular disease so common a congenital defect, it is essential to understand the causes of normal and abnormal development. This research goes beyond past experiments where the normal flow patterns are explored and instead links these flows to changes in the vasculature during development.

References

1. Risau, W. and I. Flamme, Vasculogenesis*. Annual Review of Cell & Developmental Biology*, 1995. 11: 73-91.
2. Olson, E.N. and D. Srivastava, Molecular pathways controlling heart development*. Science*, 1996. 272(5262): 671-6.
3. Conway, S.J., A. Kruzynska-Frejtag, P.L. Kneer, M. Machnicki, and S.V. Koushik, What cardiovascular defect does my prenatal mouse mutant have, and why? *Genesis*, 2002. 35: 1-21.
4. Wilt, F.H., Erythropoiesis in the Chick Embryo: The Role of Endoderm*. Science*, 1965. 147: 1588-90.
5. Cox, C.M. and T.J. Poole, Angioblast differentiation is influenced by the local environment: FGF-2 induces angioblasts and patterns vessel formation in the quail embryo*. Dev Dyn*, 2000. 218(2): 371-82.
6. Gonzalez-Crussi, F., Vasculogenesis in the chick embryo. An ultrastructural study*. Am J Anat*, 1971. 130(4): 441-60.
7. Eichmann, A., C. Corbel, V. Nataf, P. Vaigot, C. Breant, and N.M. Le Douarin, Ligand-dependent development of the endothelial and hemopoietic lineages from embryonic mesodermal cells expressing vascular endothelial growth factor receptor 2*. Proc Natl Acad Sci USA*, 1997. 94(10): 5141-6.
8. Young, P.E., S. Baumhueter, and L.A. Lasky, The sialomucin CD34 is expressed on hematopoietic cells and blood vessels during murine development*. Blood*, 1995. 85(1): 96-105.

9. Kallianpur, A.R., J.E. Jordan, and S.J. Brandt, The SCL/TAL-1 gene is expressed in progenitors of both the hematopoietic and vascular systems during embryogenesis. *Blood*, 1994. 83(5): 1200-8.

10. Orkin, S.H., GATA-binding transcription factors in hematopoietic cells. *Blood*, 1992. 80(3): 575-81.

11. Watt, S.M., S.E. Gschmeissner, and P.A. Bates, PECAM-1: its expression and function as a cell adhesion molecule on hemopoietic and endothelial cells. *Leuk Lymphoma*, 1995. 17(3-4): 229-44.

12. Choi, K., M. Kennedy, A. Kazarov, J.C. Papadimitriou, and G. Keller, A common precursor for hematopoietic and endothelial cells. *Development*, 1998. 125(4): 725-32.

13. Sabin, F., Studies on the origin of blood vessels and of red blood corpuscles as seen in the living blastoderm of chicks during the second day of incubation. *Contrib Embryol Carnegie InstWashington.*, 1920. 9: 214–262.

14. Wong, P.M., S.W. Chung, D.H. Chui, and C.J. Eaves, Properties of the earliest clonogenic hemopoietic precursors to appear in the developing murine yolk sac. *Proc Natl Acad Sci USA*, 1986. 83(11): 3851-4.

15. Xu, M.J., S. Matsuoka, F.C. Yang, Y. Ebihara, A. Manabe, R. Tanaka, M. Eguchi, S. Asano, T. Nakahata, and K. Tsuji, Evidence for the presence of murine primitive megakaryocytopoiesis in the early yolk sac. *Blood*, 2001. 97(7): 2016-22.

16. Cline, M.J. and M.A. Moore, Embryonic origin of the mouse macrophage. *Blood*, 1972. 39(6): 842-9.

17. Shepard, J.L. and L.I. Zon, Developmental derivation of embryonic and adult macrophages*. Curr Opin Hematol*, 2000. 7(1): 3-8.

18. Ingram, V.M., Embryonic red blood cell formation*. Nature*, 1972. 235(5337): 338-9.

19. Gulliver, G., Observations on the sizes and shapes of the red corpuscles of the blood of vertebrates, with drawings of them to a uniform scale, and extended and revised tables of measurements. *Proc Zool Soc London*, 1875: 474-495.

20. Drake, C.J. and P.A. Fleming, Vasculogenesis in the day 6.5 to 9.5 mouse embryo*. Blood*, 2000. 95(5): 1671-9.

21. Ferkowicz, M.J., M. Starr, X. Xie, W. Li, S.A. Johnson, W.C. Shelley, P.R. Morrison, and M.C. Yoder, CD41 expression defines the onset of primitive and definitive hematopoiesis in the murine embryo*. Development*, 2003. 130(18): 4393-403.

22. Sequeira Lopez, M.L., D.R. Chernavvsky, T. Nomasa, L. Wall, M. Yanagisawa, and R.A. Gomez, The embryo makes red blood cell progenitors in every tissue simultaneously with blood vessel morphogenesis*. Am J Physiol Regul Integr Comp Physiol*, 2003. 284(4): R1126-37.

23. Rupp, P.A., A. Czirok, and C.D. Little, Novel approaches for the study of vascular assembly and morphogenesis in avian embryos*. Trends Cardiovasc Med*, 2003. 13(7): 283-8.

24. Folkman, J. and C. Haudenschild, Angiogenesis in vitro*. Nature*, 1980. 288(5791): 551-6.

25. Serini, G., D. Ambrosi, E. Giraudo, A. Gamba, L. Preziosi, and F. Bussolino, Modeling the early stages of vascular network assembly. *Embo J*, 2003. 22(8): 1771-9.

26. Houser, J.W., G.A. Ackerman, and R.A. Knouff, Vasculogenesis and erythropoiesis in the living yolk sac of the chick embryo. A phase microscopic study. *Anat Rec*, 1961. 140: 29-43.

27. Downs, K.M., Florence Sabin and the mechanism of blood vessel lumenization during vasculogenesis. *Microcirculation*, 2003. 10(1): 5-25.

28. Haar, J.L. and G.A. Ackerman, A phase and electron microscopic study of vasculogenesis and erythropoiesis in the yolk sac of the mouse. *Anat Rec*, 1971. 170(2): 199-223.

29. Kinder, S.J., T.E. Tsang, G.A. Quinlan, A.K. Hadjantonakis, A. Nagy, and P.P. Tam, The orderly allocation of mesodermal cells to the extraembryonic structures and the anteroposterior axis during gastrulation of the mouse embryo. *Development*, 1999. 126(21): 4691-701.

30. Redkar, A., M. Montgomery, and J. Litvin, Fate map of early avian cardiac progenitor cells. *Development*, 2001. 128(12): 2269-79.

31. DeRuiter, M.C., R.E. Poelmann, I. VanderPlas-de Vries, M.M. Mentink, and A.C. Gittenberger-de Groot, The development of the myocardium and endocardium in mouse embryos. Fusion of two heart tubes? *Anat Embryol (Berl)*, 1992. 185(5): 461-73.

32. Linask, K.K., M.D. Han, M. Artman, and C.A. Ludwig, Sodium-calcium exchanger (NCX-1) and calcium modulation: NCX protein expression patterns and regulation of early heart development. *Dev Dyn*, 2001. 221(3): 249-64.

33. Ji, R.P., C.K. Phoon, O. Aristizabal, K.E. McGrath, J. Palis, and D.H. Turnbull, Onset of cardiac function during early mouse embryogenesis coincides with entry of primitive erythroblasts into the embryo proper*. Circ Res*, 2003. 92(2): 133-5.

34. Chien, S., S. Usami, H.M. Taylor, J.L. Lundberg, and M.I. Gregersen, Effects of hematocrit and plasma proteins on human blood rheology at low shear rates*. J Appl Physiol*, 1966. 21(1): 81-7.

35. Risau, W., Mechanisms of angiogenesis*. Nature*, 1997. 386(6626): 671-4.

36. Chapman, W.B., The effect of the heart-beat upon the development of the vascular system in the chick. *Am. J. Anat.*, 1918. 23: 175-203.

37. Manner, J., W. Seidl, and G. Steding, Formation of the cervical flexure: an experimental study on chick embryos*. Acta Anat*, 1995. 152(1): 1-10.

38. Wakimoto, K., K. Kobayashi, O.M. Kuro, A. Yao, T. Iwamoto, N. Yanaka, S. Kita, A. Nishida, S. Azuma, Y. Toyoda, K. Omori, H. Imahie, T. Oka, S. Kudoh, O. Kohmoto, Y. Yazaki, M. Shigekawa, Y. Imai, Y. Nabeshima, and I. Komuro, Targeted disruption of Na+/Ca2+ exchanger gene leads to cardiomyocyte apoptosis and defects in heartbeat*. J Biol Chem*, 2000. 275(47): 36991-8.

39. Chiu, J.J., D.L. Wang, S. Chien, R. Skalak, and S. Usami, Effects of disturbed flow on endothelial cells*. J Biomech Eng*, 1998. 120(1): 2-8.

40. Davies, P.F., A. Remuzzi, E.J. Gordon, C.F. Dewey, Jr., and M.A. Gimbrone, Jr., Turbulent fluid shear stress induces vascular endothelial cell turnover in vitro*. Proc Natl Acad Sci USA*, 1986. 83(7): 2114-7.

41. Resnick, N., T. Collins, W. Atkinson, D.T. Bonthron, C.F. Dewey, Jr., and M.A. Gimbrone, Jr., Platelet-derived growth factor B chain promoter contains a cis-

acting fluid shear-stress-responsive element. *Proc Natl Acad Sci USA*, 1993. 90(10): 4591-5.

42. Gabriels, J.E. and D.L. Paul, Connexin43 is highly localized to sites of disturbed flow in rat aortic endothelium but connexin37 and connexin40 are more uniformly distributed. *Circ Res*, 1998. 83(6): 636-43.
43. Lehoux, S. and A. Tedgui, Signal transduction of mechanical stresses in the vascular wall. *Hypertension*, 1998. 32(2): 338-45.
44. Bazzoni, G. and E. Dejana, Endothelial cell-to-cell junctions: molecular organization and role in vascular homeostasis. *Physiol Rev*, 2004. 84(3): 869-901.
45. Shay-Salit, A., M. Shushy, E. Wolfovitz, H. Yahav, F. Breviario, E. Dejana, and N. Resnick, VEGF receptor 2 and the adherens junction as a mechanical transducer in vascular endothelial cells. *Proc Natl Acad Science USA*, 2002. 99(14): 9462-7.
46. Resnick, N., H. Yahav, A. Shay-Salit, M. Shushy, S. Schubert, L.C.M. Zilberman, and E. Wofovitz, Fluid shear stress and the vascular endothelium: for better and for worse. *Prog Biophys Mol Biol.*, 2002. 81(3): 177-99.
47. Berk, B.C., J.I. Abe, W. Min, J. Surapisitchat, and C. Yan, Endothelial atheroprotective and anti-inflammatory mechanisms. *Ann N Y Acad Sci*, 2001. 947: 93-109; discussion 109-11.
48. Dimmeler, S., J. Haendeler, V. Rippmann, M. Nehls, and A.M. Zeiher, Shear stress inhibits apoptosis of human endothelial cells. *FEBS Lett*, 1996. 399(1-2): 71-4.
49. Bartling, B., H. Tostlebe, D. Darmer, J. Holtz, R.E. Silber, and H. Morawietz, Shear stress-dependent expression of apoptosis-regulating genes in endothelial

cells. *Biochemical & Biophysical Research Communications*, 2000. 278(3): 740-6.

50. Levesque, M.J., R.M. Nerem, and E.A. Sprague, Vascular endothelial cell proliferation in culture and the influence of flow. *Biomaterials*, 1990. 11(9): 702-7.

51. Akimoto, S., M. Mitsumata, T. Sasaguri, and Y. Yoshida, Laminar shear stress inhibits vascular endothelial cell proliferation by inducing cyclin-dependent kinase inhibitor p21(Sdi1/Cip1/Waf1). *Circ Res*, 2000. 86(2): 185-90.

52. Garcia-Cardena, G., J. Comander, K.R. Anderson, B.R. Blackman, and M.A. Gimbrone, Jr., Biomechanical activation of vascular endothelium as a determinant of its functional phenotype. *Proc Natl Acad Sci USA*, 2001. 98(8): 4478-85.

53. Cornhill, J.F. and M.R. Roach, A quantitative study of the localization of atherosclerotic lesions in the rabbit aorta. *Atherosclerosis*, 1976. 23(3): 489-501.

54. DePaola, N., M.A. Gimbrone, Jr., P.F. Davies, and C.F. Dewey, Jr., Vascular endothelium responds to fluid shear stress gradients. *Arteriosclerosis & Thrombosis*, 1992. 12(11): 1254-7.

55. Freyberg, M.A., D. Kaiser, R. Graf, and P. Friedl, Vascular endothelial cells express a functional fas-receptor due to lack of hemodynamic forces. *Apoptosis*, 2001. 6(5): 339-43.

56. Wesselman, J.P., R. Kuijs, J.J. Hermans, G.M. Janssen, G.E. Fazzi, H. van Essen, C.T. Evelo, H.A. Struijker-Boudier, and J.G. De Mey, Role of the Rhoa/Rho kinase system in flow-related remodeling of rat mesenteric small arteries in vivo. *J Vasc Res*, 2004. 41(3): 277-90.

57. Berger, S.A., W. Goldsmith, and E.R. Lewis, *Introduction ot bioengineering*. 2000, New York: Oxford Univeristy Press.

58. Fung, Y.C., *Biomechanics: circulation*. 2nd ed. 1997, New York: Springer-Verlag. 571.

59. Phoon, C.K., O. Aristizabal, and D.H. Turnbull, Spatial velocity profile in mouse embryonic aorta and Doppler-derived volumetric flow: a preliminary model*. Am J Physiol Heart Circ Physiol*, 2002. 283(3): H908-16.

60. Chien, S., S. Usami, R.J. Dellenback, and M.I. Gregersen, Shear-dependent deformation of erythrocytes in rheology of human blood*. Am J Physiol*, 1970. 219(1): 136-42.

61. Srivastava, V.P. and M. Saxena, Suspension model for blood flow through stenotic arteries with a cell- free plasma layer*. Math Biosci*, 1997. 139(2): 79-102.

62. Skalak, R., N. Ozkaya, and T.C. SKalak, Biofluid Mechanics*. Ann Rev Fluid Mech*, 1989. 21: 167-204.

63. Burton, A.C., *Physiology and Biophysics of the Circulation*. 1965, Chicago: Year Book Medical Publishers, Inc.

64. Usami, S., V. Magazinovic, S. Chien, and M.I. Gregersen, Viscosity of turkey blood: rheology of nucleated erythrocytes*. Microvascular Research*, 1970. 2(4): 489-99.

65. Salotto, A.G., L.F. Muscarella, J. Melbin, J.K. Li, and A. Noordergraaf, Pressure pulse transmission into vascular beds*. Microvasc Res*, 1986. 32(2): 152-63.

66. Hirakow, R. and T. Hiruma, Scanning electron microscopic study on the development of primitive blood vessels in chick embryos at the early somite-stage*. Anat Embryol (Berl)*, 1981. 163(3): 299-306.

67. Pries, A.R., T.W. Secomb, and P. Gaehtgens, The endothelial surface layer. *Pflugers Arch*, 2000. 440(5): 653-66.

68. Pries, A.R., T.W. Secomb, H. Jacobs, M. Sperandio, K. Osterloh, and P. Gaehtgens, Microvascular blood flow resistance: role of endothelial surface layer. *Am J Physiol*, 1997. 273(5 Pt 2): H2272-9.

69. Langille, B.L. and F. O'Donnell, Reductions in arterial diameter produced by chronic decreases in blood flow are endothelium-dependent. *Science*, 1986. 231(4736): 405-7.

70. Buus, C.L., F. Pourageaud, G.E. Fazzi, G. Janssen, M.J. Mulvany, and J.G. De Mey, Smooth muscle cell changes during flow-related remodeling of rat mesenteric resistance arteries. *Circ Res*, 2001. 89(2): 180-6.

71. Wang, D.H. and R.L. Prewitt, Microvascular development during normal growth and reduced blood flow: introduction of a new model. *Am J Physiol*, 1991. 260(6 Pt 2): H1966-72.

72. Murray, C.D., The physiological principle of minimum work. I. The vascular system and the cost of blood volume. *Proc. Natl. Acad. Sci. USA*, 1926. 12: 207-214.

73. Zamir, M., Shear forces and blood vessel radii in the cardiovascular system. *J Gen Physiol*, 1977. 69(4): 449-61.

74. Taber, L.A., S. Ng, A.M. Quesnel, J. Whatman, and C.J. Carmen, Investigating Murray's law in the chick embryo. *J Biomech*, 2001. 34(1): 121-4.

75. Kurz, H., Physiology of angiogenesis. *J Neurooncol*, 2000. 50(1-2): 17-35.

76. Pries, A.R., T.W. Secomb, and P. Gaehtgens, Design principles of vascular beds. *Circ Res*, 1995. 77(5): 1017-23.

77. Folkow, B., Structure and function of the arteries in hypertension. *Am Heart J*, 1987. 114(4 Pt 2): 938-48.

78. Mulvany, M.J., Small artery remodeling in hypertension. *Curr Hypertens Rep*, 2002. 4(1): 49-55.

79. Simon, A.M. and D.A. Goodenough, Diverse functions of vertebrate gap junctions. *Trends Cell Biol*, 1998. 8(12): 477-83.

80. Hove, J.R., R.W. Koster, A.S. Forouhar, G. Acevedo-Bolton, S.E. Fraser, and M. Gharib, Intracardiac fluid forces are an essential epigenetic factor for embryonic cardiogenesis. *Nature*, 2003. 421(6919): 172-7.

81. Phoon, C.K., O. Aristizabal, and D.H. Turnbull, 40 MHz Doppler characterization of umbilical and dorsal aortic blood flow in the early mouse embryo. *Ultrasound in Med & Biol.*, 2000. 26(8): 1275-1283.

82. Phoon, C.K. and D.H. Turnbull, Ultrasound biomicroscopy-Doppler in mouse cardiovascular development. *Physiol Genomics*, 2003. 14(1): 3-15.

83. Phoon, C.K., R.P. Ji, O. Aristizabal, D.M. Worrad, B. Zhou, H.S. Baldwin, and D.H. Turnbull, Embryonic heart failure in NFATc1-/- mice: novel mechanistic insights from in utero ultrasound biomicroscopy. *Circ Res*, 2004. 95(1): 92-9.

84. Thoma, R., *Untersuchungen über die Histogenese und Histomechanikdes Gefässsytems*. 1893, Stuttgart: Ferdinand Enke.

85. Clark, E.B., *Functional characteristics of the embryonic circulation.*, in *The Development of the Vascular System*, R.N. Feinberg, G.K. Sherer, and R. Auerbach, Editors. 1991, Karger: Basel. p. 125–135.

86. Miyamoto, Y., A. Maitra, B. Ghosh, U. Zechner, P. Argani, C.A. Iacobuzio-Donahue, V. Sriuranpong, T. Iso, I.M. Meszoely, M.S. Wolfe, R.H. Hruban, D.W.

Ball, R.M. Schmid, and S.D. Leach, Notch mediates TGF alpha-induced changes in epithelial differentiation during pancreatic tumorigenesis. *Cancer Cell*, 2003. 3(6): 565-76.

87. Jones, E.A., D. Crotty, P.M. Kulesa, C.W. Waters, M.H. Baron, S.E. Fraser, and M.E. Dickinson, Dynamic in vivo imaging of postimplantation mammalian embryos using whole embryo culture. *Genesis*, 2002. 34(4): 228-35.

88. Dirnagl, U., A. Villringer, and K.M. Einhaupl, In-vivo confocal scanning laser microscopy of the cerebral microcirculation. *Journal of Microscopy*, 1992. 165(Pt 1): 147-57.

Figure 1 – Timeline of Cardiovascular Development. Changes in the embryo, as well as endothelial cells (blue), hematopoietic cells (red) and the heart are shown with respect to somite stage. Both endothelial and hematopoietic cells begin as a tight cluster in the proximal section of the yolk sac. Endothelial cells, however, begin to expand to cover the yolk sac earlier than hematopoietic cells. The heart begins as a crescent shaped tissue. Cardiac precursors then migrate to the midline to form a linear heart tube. The linear heart tube then undergoes a looping process as the first step in formation of a chambered heart.

Figure 2 – Vascular Remodeling. Blood vessels are highlighted using antibodies to PECAM, an endothelial marker. The network of the vasculature is initially patterned in honey-comb configuration (A). As the vessels mature, they organize such that larger vessels branch to feed smaller vessels (B) in a process known as vascular remodeling.

Figure 1

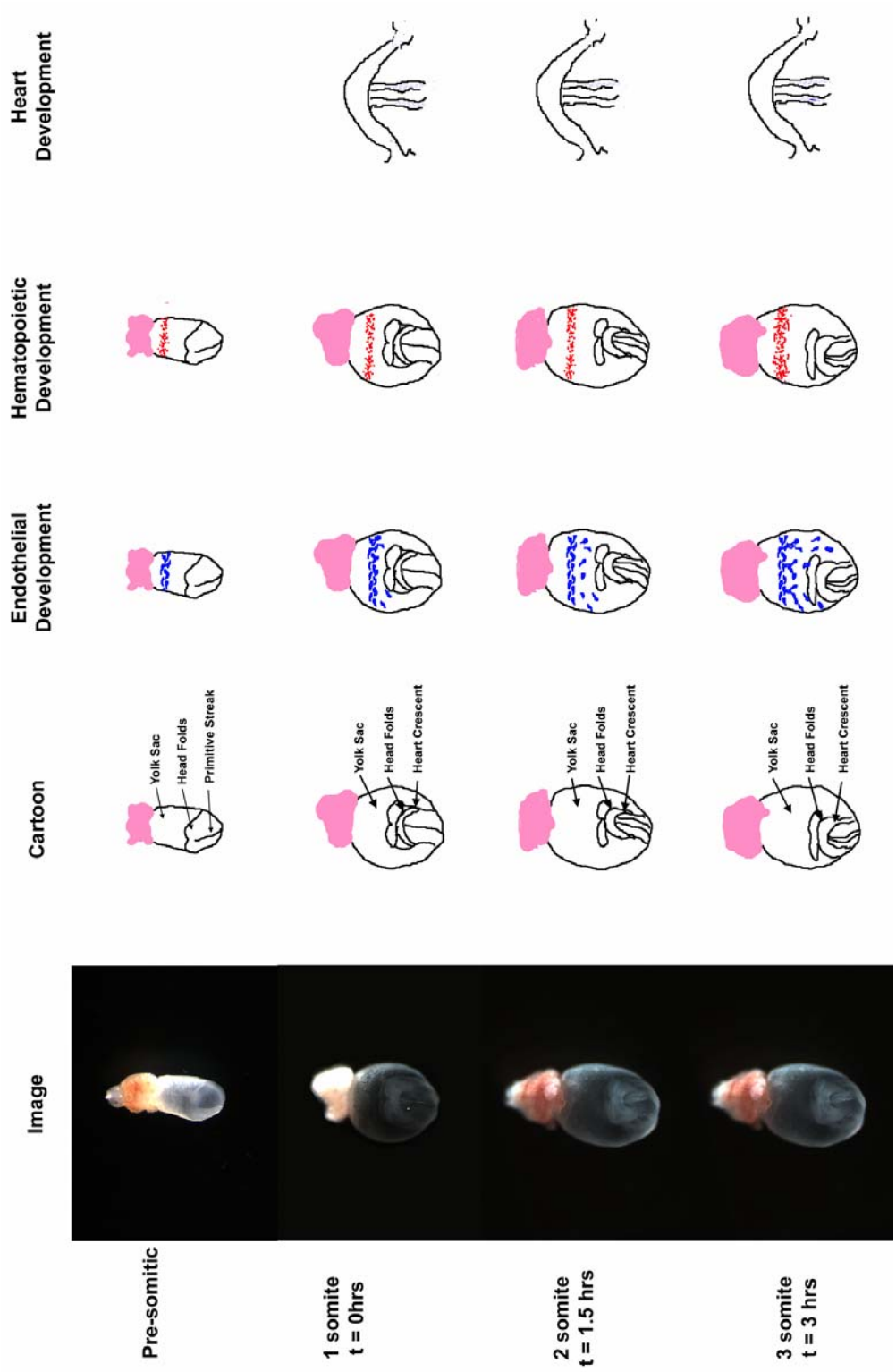
Heart Development
Hematopoietic Development
Endothelial Development
Cartoon
Image
Yolk Sac
Head Folds
Primitive Streak
Heart Crescent
Pre-somitic
1 somite t = 0hrs
2 somite t = 1.5 hrs
3 somite t = 3 hrs

Figure 1

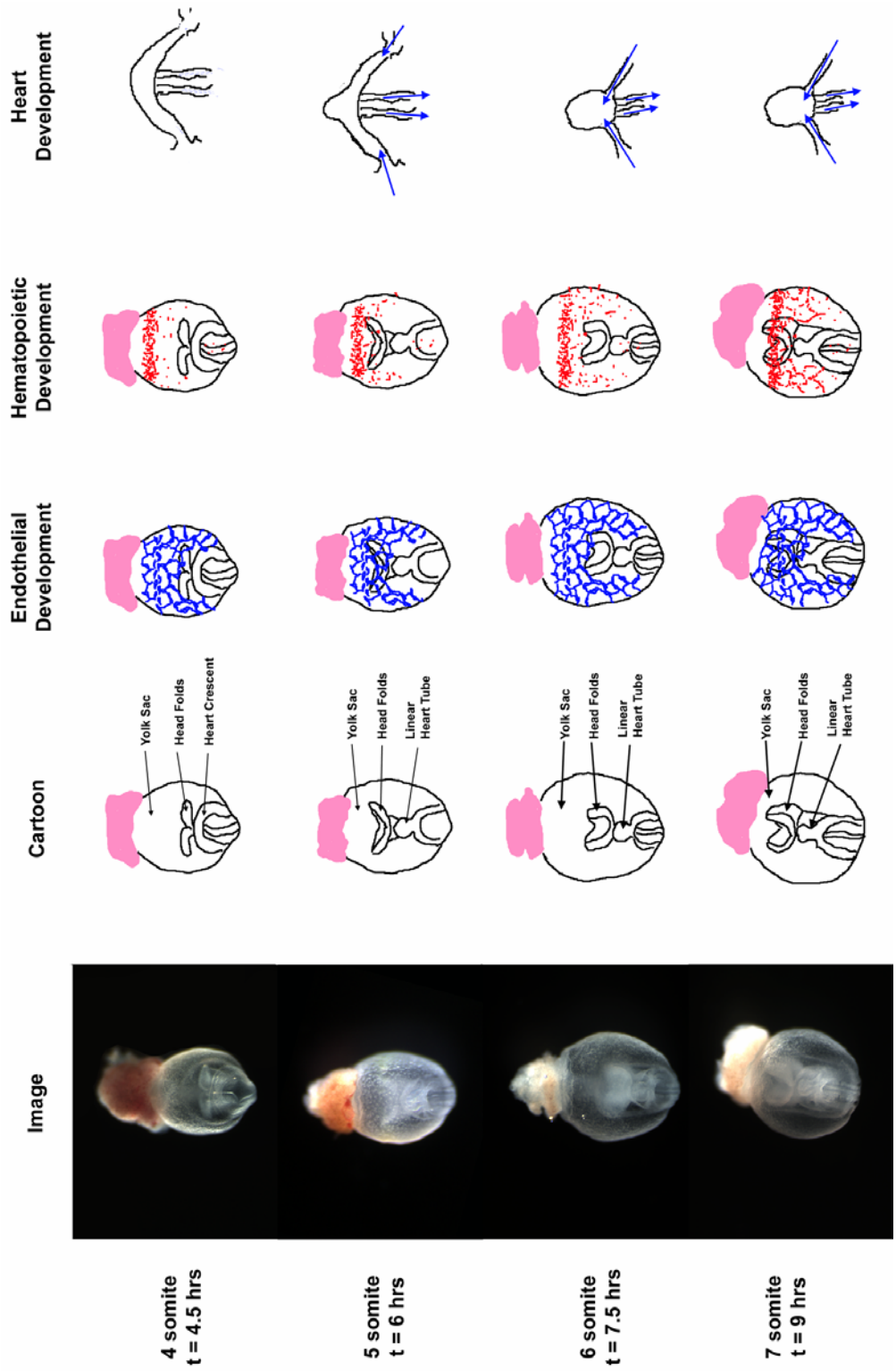
Heart Development
Hematopoietic Development
Endothelial Development
Cartoon
Image
Yolk Sac
Head Folds
Heart Crescent
Linear Heart Tube
4 somite t = 4.5 hrs
5 somite t = 6 hrs
6 somite t = 7.5 hrs
7 somite t = 9 hrs

Figure 1

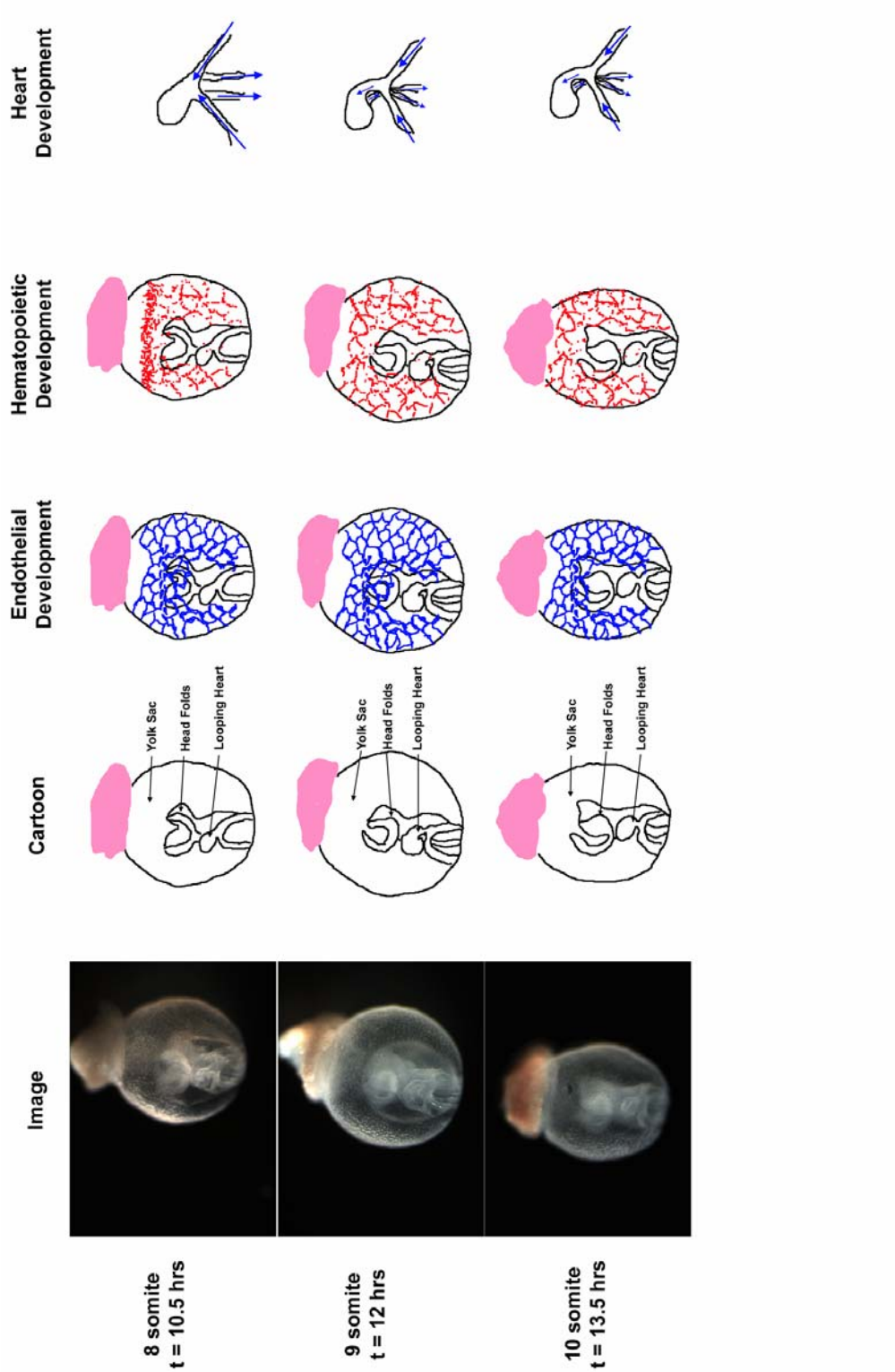
Heart Development
Hematopoietic Development
Endothelial Development
Cartoon
Yolk Sac
Head Folds
Looping Heart
Image
8 somite
t = 10.5 hrs
9 somite
t = 12 hrs
10 somite
t = 13.5 hrs

Figure 2

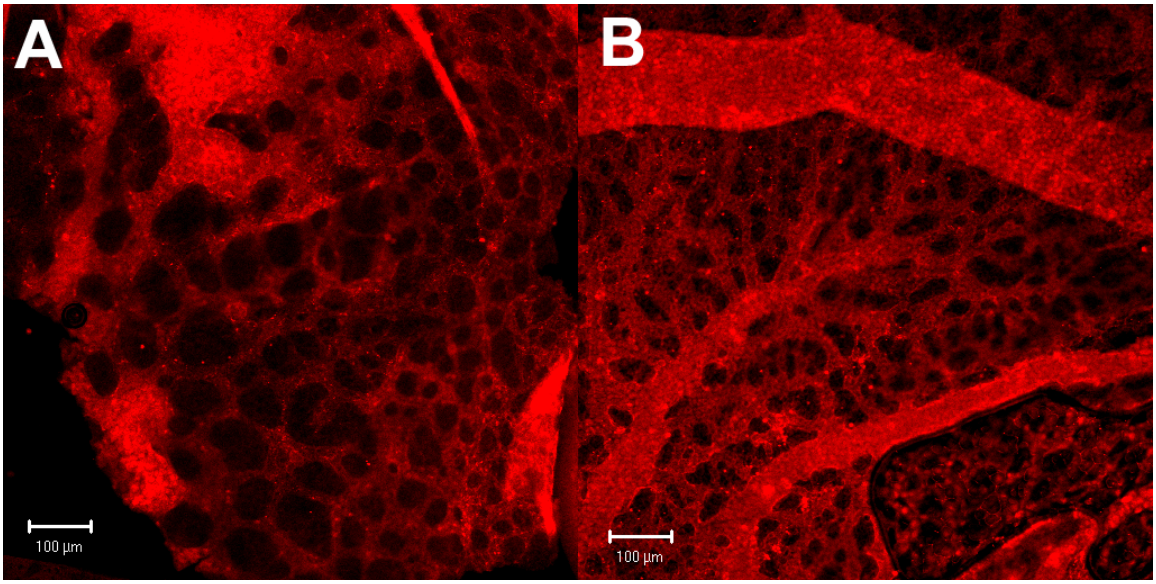

Chapter 2

Dynamic *In Vivo* Imaging of Post-Implantation Mammalian Embryos Using Whole Embryo Culture

Summary

Due to the internal nature of mammalian development, much of the research performed is of a static nature and depends on interpolation between stages of development. This approach cannot explore the dynamic interactions that are essential for normal development. While roller culture overcomes the problem of inaccessibility of the embryo, the constant motion of the medium and embryos makes it impossible to observe and record development. We have developed a static mammalian culture system for imaging development of the mouse embryo. Using this technique, it is possible to sustain normal development for periods of 18-24 hours. The success of the culture has been evaluated based on the rate of embryo turning, heart rate, somite addition, and several gross morphological features. When this technique is combined with fluorescent markers, it is possible to follow the development of specific tissues or the movement of cells. To highlight some of the strengths of this approach, we present time-lapse movies of embryonic turning, somite addition, closure of the neural tube and fluorescent imaging of blood circulation in the yolk sac and embryo.

Introduction

Through sophisticated genetic manipulation and examination of naturally occurring mutations, hundreds of genes have been identified that play key roles in early mouse development. As more is learned about genetic hierarchies that control morphogenesis, additional questions arise concerning how cells behave in response to both molecular and environmental cues. Mutations can cause a multitude of results, from absence of certain structures to malformations of embryonic tissues. Defects can result from changes in cell fate, apoptosis of progenitor cells, lack of differentiation of progenitors or from incorrect cell migration. Thus, it is important to understand how cells interact in normal development and how mutations change these interactions, resulting in abnormal development.

Because mouse embryos develop *in utero*, most of what is known about dynamic events such as gastrulation and neural tube closure has been deduced from static images of embryos at successive stages of development. Dynamic cellular interactions have been studied in other, more accessible systems, such as Xenopus, zebrafish or avian embryos. In these systems, labeled cells can be visualized over time using time-lapse light microscopy to determine migration trajectories and behaviors, to observe cell-cell contacts, as well as to determine cell fate relationships. Such approaches have been limited in the early mouse embryo because culture conditions suitable for time-lapse microscopy have not been established. While embryos up to late 7.5 days post coitum (dpc) can be grown in static cultures suitable for imaging, older embryos, from 8.5-dpc onwards, have traditionally been cultured in roller flasks [1]. It has generally been

thought that the gas exchange provided by roller culture was essential for normal embryonic development.

Here we present a robust, static culture method for embryos isolated from 8.5-dpc to 9.5-dpc. We show that by controlling pH, gas exchange and evaporation, embryos at these stages can be grown in a culture dish placed directly on the microscope stage, enabling time-lapse analysis of their development. Normal development is sustained for at least 18-24 hours. Several critical parameters of the growth media and culture environment were tested and are described here. Time-lapse movies of embryos in culture are provided, illustrating the success of the technique.

Results

The goal of these experiments is to provide a method for observation of the development of the post-implantation mouse embryos. For meaningful results, *in vitro* development must recapitulate *in utero* development. Because roller culture is an accepted means of culturing mouse embryos, the initial goal of this research was to develop growth conditions comparable to roller culture. Success was judged by several factors. For 8.5-dpc embryos, the ability of the embryos to turn was recorded and compared with *in vivo* and roller culture results. The embryos were also examined for normal head fold closure, heart looping, vascular development and heart rates, as compared to *in vivo* growth. Embryos were staged using a system that consisted of 22 stages defined by images of freshly dissected 8.5-dpc embryos (described in Table 1, images not shown). A more traditional staging system, such as the one proposed by Brown & Fabro [2] was

not used since the system requires the removal of the yolk sac to evaluate many features. Since 8.5-dpc embryos were cultured with the yolk sac intact, it would not have been possible to evaluate the initial age. For 9.5-dpc embryos, rate of somite addition and heart rate were used as the main criteria for normal development. Since somite addition relates linearly to embryonic growth, we used this criterion to assess extent of embryonic growth [2]. Heart rates were measured throughout the culture period.

Culture Chambers and Temperature Control of Embryos on the Microscope Stage

Embryos were cultured in Labtek chambers consisting of two plastic culture wells attached to a coverslip via a silicon gasket. Embryos were imaged from below, through the coverslip, with an inverted microscope. Embryos were cultured three per chamber. In order to keep the medium static, yet enable aeration and pH regulation, the inside of the culture chamber was supplied continuously with heated humidified gas. The whole system, including the microscope optics, was kept at constant temperature using a chicken egg incubator heater enclosed within a mylar-insulated box (Figure 1; described in detail in the Materials and Methods section).

Culture Media and Additives

The first culture condition that was optimized was the composition of the medium. The literature on roller culture highlighted the need for high quality rat serum, as well as a wide range of possible media additives [3]. These included vitamins [4], glucose [1] [4], transferrin [5], inositol [1], albumin [5] and HEPES buffer. Complete DMEM/F12 medium

was chosen as a starting point for the medium formulation because it already contained vitamins, glucose and inositol.

As with other published culture methods, a high concentration of rat serum in the medium was found to be essential [3]. Commercial sources of rat serum were tested and results compared to those obtained from serum freshly prepared in our own lab (see Table 2). Commercial sources of rat serum were adequate for normal culture of 9.5-dpc embryos, resulting in the development of embryos with normal heart rates and somite addition rates (Table 2). After optimization with the 9.5-dpc embryos, the best of these commercial sera, from Seracare, was then tested for culture of 8.5-dpc embryos. These embryos never completed the turning process in the commercial sera. Therefore, our homemade serum was used for all subsequent studies.

We tested HEPES buffer solution as a means to regulate pH fluctuations in the medium. Two different concentrations (5 and 10 mM) were tested. For both concentrations, similar final pH values were measured at the end of the culture period (average pH for 5mM HEPES was 7.5 ($\pm$0.3, n=34); 7.6 ($\pm$0.2, n=20) for 10 mM HEPES). The desired pH should be between 7.0 and 7.2. As such, a greater level of control over the pH is necessary and will be discussed later. A concentration of 10 mM HEPES was used for all subsequent cultures.

Transferrin is an iron storage protein produced both by maternal tissues and by the yolk sac [6]. Based on previously reported uses of transferrin in whole embryo culture [7], a concentration of 10 μg/mL was tested. Embryos cultured in the presence of 10 μg/mL of transferrin had significantly lower heart rates (average of 40 beats per minute or bpm,

n=12 for 8.5-dpc, n=6 for 9.5-dpc) by the end of the culture period. Therefore, transferrin was omitted from subsequent cultures.

Albumin is an essential blood component and is also known to deteriorate quickly in preparations of rat serum [5]. We therefore tested whether the addition of albumin could improve the culture. Albumin collected from chicken egg whites was added at a range of concentrations, from 50 μL to 250 μL per mL of media. The embryos cultured under these conditions had no heartbeats after 24 hrs of culture (n=12), even though temperature and pH were kept constant for the entire culture period.

Based on these experiments the preferred medium composition consists of 50% rat serum, 50% DMEM/F12, supplemented with HEPES and Pen-Strep (see Materials and Methods).

Aeration of Culture Chamber

Because roller culture offers better gas exchange than static culture, the effects of aeration and diffusion were investigated. Even with proper medium formulation, static cultures were still not as successful as cultures in roller flasks. pH levels were too high by the end of culture (average of 7.6 compared with a desired 7.2, as previously reported) and the percentage of 8.5-dpc embryos that turned was also low (11%, n=38).

It has previously been reported that the yolk sac becomes a barrier to nutrient transport after the embryo has turned [8]. We tested whether the yolk sac was hindering nutrient transport by culturing 9.5-dpc embryos with and without yolk sacs (n= 12, n=70 respectively), and found that the presence of the yolk sac impedes development. 9.5-dpc embryos cultured with yolk sacs did not survive 24 hours in culture (as defined by

the absence of a heartbeat). Therefore, the yolk sac was removed for 9.5-dpc embryos, while younger embryos were cultured with intact yolk sacs.

The effects of gas flow rate were also investigated since gas transfer rates are lower in static culture. Rapid evaporation from the medium was observed at high flow rates. However, even at low flow rates, some evaporation occurred and was found to be detrimental to the embryonic development, suggesting that embryos are sensitive to even small changes in the concentration of medium components or secreted waste products. Evaporation causes yolk sacs of 8.5-dpc embryos to become wrinkled and caused the circulation in the yolk sac to stop. Under these conditions, the embryos did not complete the turning process. Evaporation is apparently not a problem in roller culture where the embryo chambers are maintained at higher backpressures. The backpressure creates a resistance to the flow, resulting in lower inlet gas flow rates. Static culture maintains the chamber pressure at atmospheric levels and so gas flow rates are much higher.

Several steps were taken to minimize evaporation of the medium. The gas mixture was bubbled through a heated humidifier before it entered the culture chamber. The chamber was sealed with Teflon tape, allowing gas to exit, but trapping moisture. The gas flow rate was also set as low as the regulator would allow. These conditions worked well for 9.5-dpc embryos. For the earlier embryos, it was necessary to take additional steps to minimize evaporation. This was achieved by placing a thin layer of mineral oil over the medium. This layer helped maintain pH at normal levels (7.0 to 7.2). Under these conditions, the percentage of embryos that turned rose from 10.5% (n=38) to 41.4% (n=82) (Table 3). The yolk sacs of the embryos cultured with mineral oil were

smooth and circulation in the yolk sac was constant. Heart rates of the embryos cultured in mineral oil were also more in line with previously published rates for freshly dissected embryos [9].

Development of 8.5-dpc Embryos in Culture

During normal embryogenesis, in the 24 hours between 8.5-dpc and 9.5-dpc, many important developmental changes occur. Most notably, the heart begins to beat and the embryos turns, becoming physically separated from the yolk sac. These milestones were recorded to assess normal growth. Embryos grown for 24 hours in culture (Figure 2, a-b) were compared to freshly dissected 9.5-dpc embryos (Figure 2, c). The cultured embryos were found to match freshly dissected embryos both in size and appearance.

In all cultured embryos (n=82), blood flow could readily be observed in the vascular channels of the yolk sac and embryo as well as in the heart. During culture, the heart rate increased from 92.2 $\pm$ 21.7 to 107.2 $\pm$ 27.1 bpm, as stated in Table 3. These rates do not vary significantly from rates published for freshly dissected embryos [9]. Even after 24 hours in culture, the embryos still had very strong heartbeats and good flow through their blood vessels. This can also be observed in several of the time-lapse movies presented in the subsequent section.

To assess the extent of embryonic turning, we compared our static culture technique with roller culture. Our culture conditions resulted in 41.4% of embryos turning (n=82), as compared to 58.3% of embryos turning in roller culture (n=19). Only embryos older than stage 9 (first heart fibrillations visible) were included in these statistics. It is thought that all embryos above stage 9 have the ability to turn in culture, although error could be

introduced since it is difficult to pre-determine an embryo's potential to turn. The average initial stage of the embryos was 13.1 ± 2.6 for static culture and 12.9 ± 3.0 for roller culture. Turning has, in the past, been the largest impediment to static culture for embryos this age. The high rate at which embryos turned in static culture highlight the success of this technique.

Development of 9.5-dpc Embryos in Culture

Development of 9.5-dpc embryos is characterized by the onset of organogenesis, significant changes in embryonic size and the maturation of many of the head features. The size and morphological traits of cultured 9.5-dpc embryos (Figure 2, e) and freshly dissected 10.5-dpc embryos (Figure 2, f) are grossly indistinguishable.

During normal embryonic development, somites are added at a rate of approximately one pair every hour and a half [10]. The somite addition rate can be taken as a "biological clock" and was monitored as a sign of embryonic health during culture. As seen in Figure 4, somite addition rates measured in culture were quite consistent with the somite addition rates reported for embryonic development *in vivo* [3]. After 24 hours, the tissue becomes quite opaque, possibly because of the initiation of tissue necrosis late in culture. As such, 9.5-dpc embryos should not be cultured past 18 hours.

Because heart rates appear to be very sensitive to small changes in the local environment, the heart rate was again used as an indicator of embryonic health. Heart rates are shown in Figure 3 for 9.5-dpc embryos cultures and are compared to previously published data [9]. The published rate for 9.5-dpc was measured in whole embryos, however the rate for 10-dpc embryos was measured in isolated hearts [9].

Embryo heart rates in static culture appeared to remain constant over the 24-hour incubation period. The difference between our rates and published rates after 24 hours, though not statistically significant, could be due to the comparison of whole embryo heart rates and those from isolated hearts. After 24 hours in culture, the standard deviation of the heart rates of the cultured embryos became quite large. Therefore, the culture period was never extended beyond 24 hours.

Time-Lapse Movies

Because this static embryo culture system was developed with the aim of using fluorescent or bright field imaging to observe mammalian development, several movies were made to demonstrate the success of the technique. These are provided here in panel form and as time-lapse movies in the supplemental material that is presented on the Internet.

In the first movie (Figure 5, also see the supplementary video 1), we show neural tube closure in the hindbrain region. The neural folds approximate in a caudal to rostral manner, as occurs *in vivo*. Interestingly, small, dynamic groups of cells are evident at the midline during closure, indicating that some cells may delaminate during this process.

Another major event in the development of 8.5-dpc embryos is axial rotation or turning (Figure 6, shown in the supplementary video 2). The embryo is clearly seen rotating its upper body away from the yolk sac. The body detaches from the yolk sac in a rostral-caudal direction, leaving only the caudal end attached. Clearly highlighted is the

posterior closure of the ventral side. The head and heart disappear and then reappear below the caudal end of the embryo.

The addition of somites was followed (Figure 7, see also supplementary video 3) in 9.5-dpc embryos. Embryos typically start off with 12 somites and progressively add somites through the culture period. The somites are labeled as they are added using asterisks (Figure 7). The rate of somite addition matches that reported for freshly dissected embryos [10].

The last movie highlights the main strength of this technique, which is the ability to follow fluorescently labeled cell movements in tissues. The embryo shown carries a green fluorescent protein (GFP) reporter that is expressed specifically in primitive erythroblasts [11]. This allows the direct observation of blood flow in the yolk sac and the embryo and reveals normal circulation (Figure 7, as well as supplementary video 4). Careful inspection also provides insight into early changes in vascular morphology. By including a marker such as a GFP, it is now possible to observe dynamic interactions in mammalian embryos that lead to the formation of differentiated tissues.

Discussion

It has generally been assumed that the most significant limitation of static culture of post-implantation embryos is diffusion. We present results that clearly show that this problem is not as restrictive as was previously thought. This is especially highlighted by the high rate at which 8.5-dpc embryos were able to complete the turning process under static

conditions and the constant rate of somite addition in the 9.5-dpc embryos. Though the ability to culture embryos of this stage under static conditions in incubators was reported previously [12], the technique had never been expanded to direct microscopic observation. With this goal in mind, we have optimized environmental conditions for normal embryonic development on the microscope stage.

It is not solely the diffusion limitation of static culture that prevents proper development on microscopic stages, but the greater difficulties in controlling environmental conditions. In roller culture, high pressure reduces gas flow rates to very low levels, minimizing evaporation. Similarly, in tissue incubator cultures, the extremely humid environment minimizes evaporation and concentration of the medium. Since it is not feasible to reach a humidity level similar to tissue incubators during culture on the microscope stage, it was necessary to take further steps to prevent evaporation, through the addition of a very thin layer of mineral oil.

The ability to culture mouse embryos within a chamber accessible to microscopy overcomes the limitations of visualizing the cellular dynamics of mouse development. While the technique is limited in providing an 18-24 hour window on development, it improves upon roller culture in that embryos can be continuously observed over this period. With the growing number of transgenic mouse lines expressing fluorescent marker proteins, it should be possible to observe the localization of any gene product and to track the movement and development of cells expressing that gene.

We are working to extend this technique in two ways. First, preliminary results using 7.5-dpc embryos (n=9, data not shown) show promise that younger embryos too can develop normally in static culture. Second, work is also underway using the technique to

observe cellular development in mutant strains. Through time-lapse imaging, we should be able to bridge the gap between gene function and the subsequent changes in morphology.

Materials and Methods

Dissection

Male breeder mice were mated with CD-1 females overnight. The presence of a vaginal plug was taken as 0.5-dpc. Embryos were collected on the morning of the eight or ninth day as noted in a plexiglass hood heated to 37°C with a chicken incubator heater (Lyon Electric Company # 115-20). Dissecting outside of the heated hood causes decreased viability. Dissecting medium was prepared by mixing 45 ml of D-MEM/F-12 (Gibco # 11330032) with 4.5 ml of heat-inactivated fetal bovine serum (Gibco # 16140063) and 0.5 ml of pen-strep solution (Irvine Scientific # 9366). The dissecting medium was warmed to 37°C prior to dissection. Females were euthanized with CO_2 followed by cervical dislocation. The uterine horns were dissected out and placed in warmed dissecting medium and the embryos isolated. Yolk sacs were left intact on 8.5-dpc embryos but were removed for 9.5-dpc embryos. For the imaging of neural tube closure, the yolk sac of 8.5-dpc embryo was removed.

Rat Serum

Though several sources of commercial rat serum were investigated, it was found that the best cultures came from serum that we made ourselves. Both the blood collection site

and the anesthetic in the commercial sources were presumed to be the cause of the lower quality serum. In particular, the use of ether as the anesthetic is likely to be essential because it can be completely eliminated by aeration [13].

Rat serum was prepared from blood collected from the dorsal aorta of male rats [3] using the following modifications. Blood was collected into vacutainer tubes (Becton-Dickinson # 366512) using a butterfly needle (Becton-Dickinson # 367283). After collection, the blood was centrifuged at 2500 rpm for 20 minutes. The plasma was isolated and supernatant from multiple rats were pooled. The serum was then centrifuged again at 2500 rpm for 10 minutes to remove remaining cells. The supernatant was heat-inactivated at 56°C for 30 minutes with the lid removed to allow the ether to evaporate. The serum was then filtered using a 0.45 μm filter and aliquoted into 1 mL samples. These samples were stored in a –80°C freezer.

Incubation and Culturing of Embryos

The culturing medium consisted of 1 mL D-MEM/F12, 1 mL heat-inactivated rat serum, 20 μL Pen-Strep and 20 μL HEPES buffer solution 1M (Irvine Scientific, Cat No. 9319). The medium was sterile filtered with a 0.2 μm filter and allowed to equilibrate, with the lid off, in a CO_2 incubator for 1 hour. The dissected embryos were then transferred to culture chambers (Nunc Lab-tek, 2 chambers/ coverglass, Cat No. 155380) with a minimal amount of the dissecting media using a transfer pipette. Three embryos were placed per chamber and 2 mL of the culturing media was added. For the 8.5-dpc embryos, the medium was then covered with a very thin layer of mineral oil (Sigma # M8410).

After transfer to the chamber slides, the embryos were pre-incubated for one hour at 37°C, 5% CO_2 in a tissue incubator and then still-photographed at 2.5x magnification. Initial heart rate and somite counts were made and the pH of the media was measured by removing a drop of medium. The pre-equilibration in a CO_2 incubator reliably adjusted the initial pH to 7.2.

In order to properly aerate the chambers, a hole was made in the side of the Lab-Tek chamber lid using a soldering iron. Inlet gas (5% CO_2, balance air) was passed through a bubbler to humidify the air. The bubbler was custom built by the Caltech Glass Shop, however, most commercially available gas-washing bottles can be used for this purpose. The flow rate was set as low as the regulator could operate. The chamber was sealed using Teflon tape.

The bubbler, culture chamber and a dissecting microscope were all placed within a heater box that was constructed around the microscope from cardboard (4mm thick) covered with thermal insulation (Reflectix Co.; 5/16" thick, foil-foil insulation). The temperature was set to 37 °C using an egg-incubator heater (Lyon Electric Company # 115-20) and allowed to warm for several hours before culture to prevent thermal drift of the microscope components. This arrangement is shown in Figure 1.

Static images of the embryos were taken at 6 hours, 12 hours and 24 hours. The heart rate and somite numbers were counted visually at these intervals. The intermediate measurements were found to harm the 8.5-dpc embryos and were eliminated in later studies. For the 8.5-dpc embryos, initial and final heart rates were measured and the extent of development was assessed by head fold closure, maturation of the vasculature

and ability to turn. After 24 hours, the embryos were fixed in 4% paraformaldehyde overnight at 4°C and then transferred to PBS (Ca^{2+} and Mg^{+} free) and stored at 4 °C.

Time-Lapse Imaging

In order to image the 8.5-dpc embryos, it was necessary to immobilize the embryos. This was done by tying a hair around the deciduas and resting the ends of the hair on the bottom of the chamber. Older embryos were more stable in the culture dish and therefore were not immobilized.

The embryos were imaged with either bright-field or confocal microscopy. Single images were taken every five minutes. The bright-field images were taken on an inverted microscope (Zeiss Axiovert) using a SIT camera (Hamamatsu) and acquired using VIDIM (VIDeo IMaging) software written by Scott Fraser, Jes Stollberg and Gary Belford for Imaging Technology Incorporated Series 151 image processors. The confocal images were taken on two distinct inverted confocal microscopes (BioRad MRC600; Zeiss LSM PASCAL). All images were taken at 5X magnification, except for the somite addition time-lapse, which is at 2.5X magnification.

Acknowledgements

The authors wish to acknowledge Carole Lu for help with the initial cultures, and Joaquin Gutierrez and Deanna Mohn for technical assistance. Research by the authors was supported by grants from the American Heart Association for D.C., from the National Institutes of Health to M.H.B., from the Human Frontiers S P grant to S.E.F. We would also like to thank Powell foundation for the partial support of this work through the option of bioengineering at Caltech.

References

1. Tam, P.P., Postimplantation mouse development: whole embryo culture and micro- manipulation. *Int J Dev Biol*, 1998. 42(7): 895-902.
2. Brown, N.A. and S. Fabro, Quantitation of rat embryonic development *in vitro*: a morphological scoring system. *Teratology*, 1981. 24: 65-78.
3. Copp, A.J. and D.L. Cockroft, *Postimplantation mammalian embryos : a practical approach*. The Practical approach series. 1990, Oxford ; New York: IRL Press. 357.
4. Martin, P. and D.L. Cockroft, Culture of postimplantation mouse embryos. *Methods Mol Biol*, 1999. 97: 7-22.
5. Katoh, M., R. Kimura, and R. Shoji, Embryogenesis-promoting factors in rat serum. *J Exp Zool*, 1998. 281: 188-200.
6. Janzen, R.G., G.K. Andrews, and T. Tamaoki, Synthesis of secretory proteins in developing mouse yolk sac. *Dev Biol*, 1982. 90(1): 18-23.
7. Bulic-Jakus, F., M. Vlahovic, G. Juric-Lekic, V. Crnek-Kunstelj, and D. Serman, Gastrulating rat embryo in a serum-free culture model: Changes of development caused by teratogen 5-azacytidine. *ATLA-Alternatives to Laboratory Animals*, 1999. 27: 925-933.
8. Eto, K. and N. Osumi-Yamashita, Whole embryo culture and the study of postimplantation mammalian development. *Develop Growth Differ*, 1995. 37: 123-132.

9. Porter, G.A., Jr. and S.A. Rivkees, Ontogeny of humoral heart rate regulation in the embryonic mouse*. Am J Physiol Regul Integr Comp Physiol*, 2001. 281(2): R401-7.

10. Hogan, B., R. Beddington, F. Costantini, and E. Lacy, *Manipulating the mouse embryo : a laboratory manual*. 2nd ed. 1994, Plainview, N.Y.: Cold Spring Harbor Laboratory Press. 497.

11. Dyer, M.A., S.M. Farrington, D. Mohn, J.R. Munday, and M.H. Baron, Indian hedgehog activates hematopoiesis and vasculogenesis and can respecify prospective neurectodermal cell fate in the mouse embryo*. Development*, 2001. 128(10): 1717-30.

12. Wan, Y.J., T.C. Wu, and I. Damjanov, Development of early somitic mouse embryos in static culture in vitro*. J Exp Zool*, 1982. 220(2): 219-25.

13. Sturm, K. and P.P.L. Tam, Isolation and culture of whole postimplantation embryos and germ layer derivatives. *Methods Enzymol*, 1993. 225: 164-190.

Tables

Table 1 – Summary of staging system used for 8.5 dpc embryos

Characteristic of Embryonic Development	Stage
Formation of neural plate	1
Appearance of first somite	4
Formation of linear heart tube	5
First heart beats	10
Commencement of head fold closure	11
Heart begins looping	12
Fusion of head folds	15
Beginning of axial rotation	17
Axial rotation 50% complete	19
Completion of axial rotation	22

Table 2 - Comparison of Rat Serum Collection Techniques

Supplier	Anesthetic	Source	Sex	No. of Somites After Culture of 9.5-dpc	Percent Turning at 8.5-dpc
Gibco (Carlsbad, CA)	CO_2	Jugular Bleed	Mixed sex	20.0 ± 2.4	N/A
Seracare, Inc. (Oceanside, CA)	CO_2	Cardiac collection	Male only	22.2 ± 4.0	0%
Biochemed Pharmacologicals, Inc. (Winchester, VA)	CO_2	Jugular Bleed	Mixed sex	23.2 ± 2.0	N/A
Home-made serum	Ether	Dorsal Aorta	Male only	21.3 ± 3.7	10.5%

Table 3 - Results from Culture With and Without Mineral Oil Addition

	Percent Turning	Initial Heart Rate (bpm)	Final Heart Rate (bpm)	n=
Static Culture without Mineral Oil	10.5	91.2 ± 26.5	60.3 ± 37.0	38
Static Culture with Mineral Oil	41.4	92.2 ± 21.7	107.23 ± 27.09	82
Freshly Dissected Embryos (Porter et Rivkees, 2001)	100	80 ± 2	91 ± 3	N/A

Figure 1. Experimental System. Modified Labtek chambers were placed on the microscope stage. The chambers were sealed with Teflon to prevent the evaporation of media. The gas mixture (5% CO_2, balance air) was humidified before flowing over the media. The entire setup was contained within an insulated box and heated to 37°C. The actual arrangement of the heater box (with top and side panels missing) is shown in frame A, as well as a schematic of the system in panel B.

Figure 2. Embryo Culture Comparison with Embryo Development *In Vivo*. 8.5-dpc (a) and 9.5-dpc (d) embryos before culture and after 24 hours in static culture (b & e), which are compared with embryos that have developed for an equivalent period in vivo from 8.5-dpc (c) and 9.5-dpc (f). Magnification is 4X for a-c, and 2.5X for frames d-f.

Figure 3. Heart Rates During Culture. Heart rates were followed as indicators of embryonic health and compared with data from Porter & Rivkees, 2001. The left-hand columns, which represent the 8.5-dpc embryos before and after culture (light gray), are compared with freshly dissected embryos (dark gray). On the right-hand side, columns represent the heart rate before and after culture for 9.5-dpc embryos (light gray) that are compared with freshly dissected embryos from the same age (dark gray).

Figure 4. Comparison of Somite Addition During Culture and In Vivo. The number of somites of 9.5-dpc embryos in culture were counted (solid line) at t=0, 6 and 12 hours and compared with the *in vivo* rates (dashed line). A final somite count at 24 hours was not performed because the embryos had become quite opaque and it was difficult to count somites accurately.

Figure 5. Time-Lapse of Neural Tube Closure in the Hindbrain Region. Panels illustrate hindbrain fusion in an 8.5-dpc embryo. The yolk sac was removed for this movie. The time-lapse covers a 14-hour period of time. The associated movie was imaged at a rate of one frame every 5 minutes and the panels present every 45th frame.

Figure 6. Time-Lapse of Embryonic Turning. The time-lapse covers an 11-hour period of time. In this time, the embryo goes from a being u-shaped to rotating into "fetal position." In the process, the embryo detaches from the yolk sac. The head (Hd), heart (Hrt) and somites (S) are labeled on the diagram. The imaging rate was one frame every 5 minutes, and the panels present every 40th frame.

Figure 7. Time-Lapse of Somite Addition. Frames illustrate somite addition in a 9.5-dpc embryo. The time-lapse covers a 13.5-hour period of time. The asterisk (*) marks new somites that have been added since the last panel. The addition of the somites is better seen in the accompanying time-lapse movie. The images in the movie were taken every five minutes, and the panels represent every 50th frame.

Figure 8. Blood Circulation in an 8.5-dpc Cultured Embryo. Panels illustrate the circulating red blood cells (in green) in an 8.5-dpc embryo that expresses GFP driven by the ε-globin promoter. [11] The time-lapse covers a 12.5-hour period of time during which the embryo is undergoing turning. The location of the anterior (A) and posterior (P) extremities of the embryo has been noted, as well as the dorsal aorta (DA) and the heart (H) when visible. The images were taken every 5 minutes, and the panels represent every 50th frame from the movie.

Figure 1

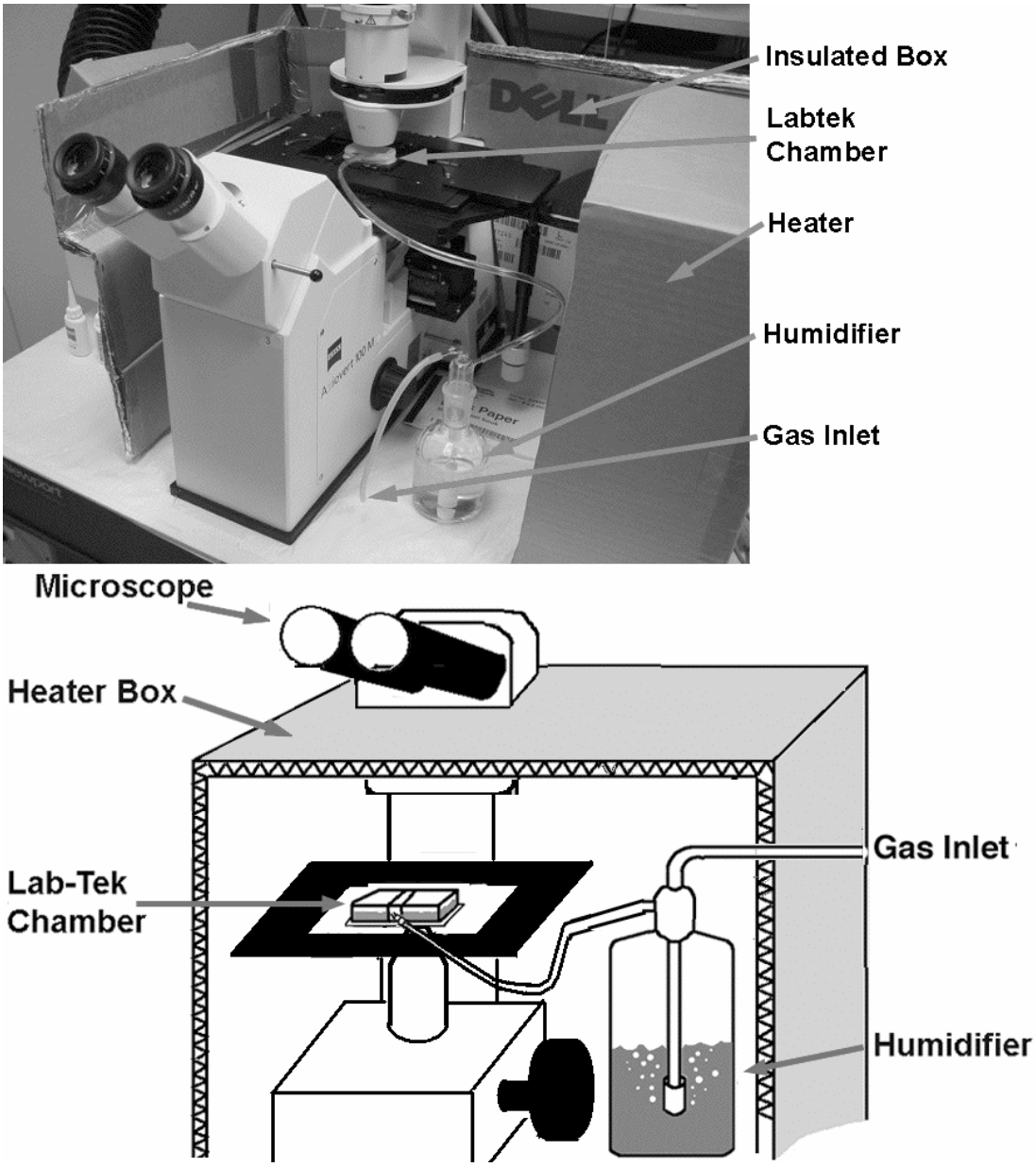
Insulated Box
Labtek Chamber
Heater
Humidifier
Gas Inlet
Microscope
Heater Box
Lab-Tek Chamber
Gas Inlet
Humidifier

Figure 2

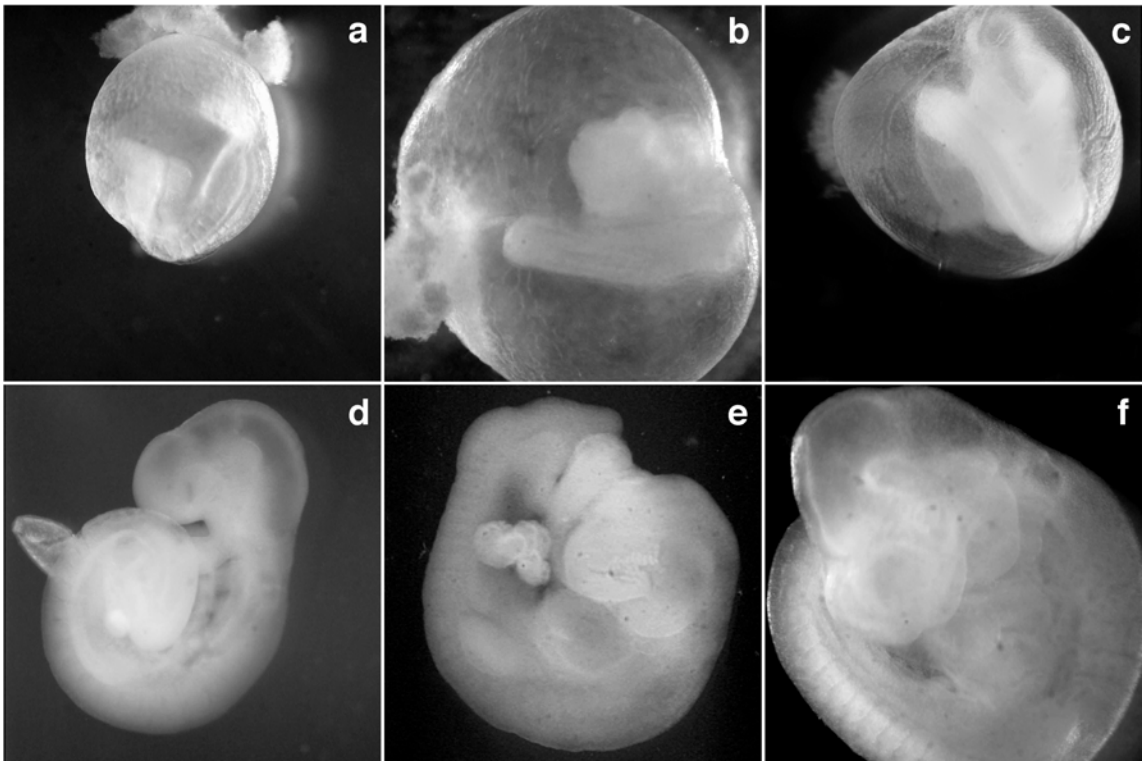

Figure 3

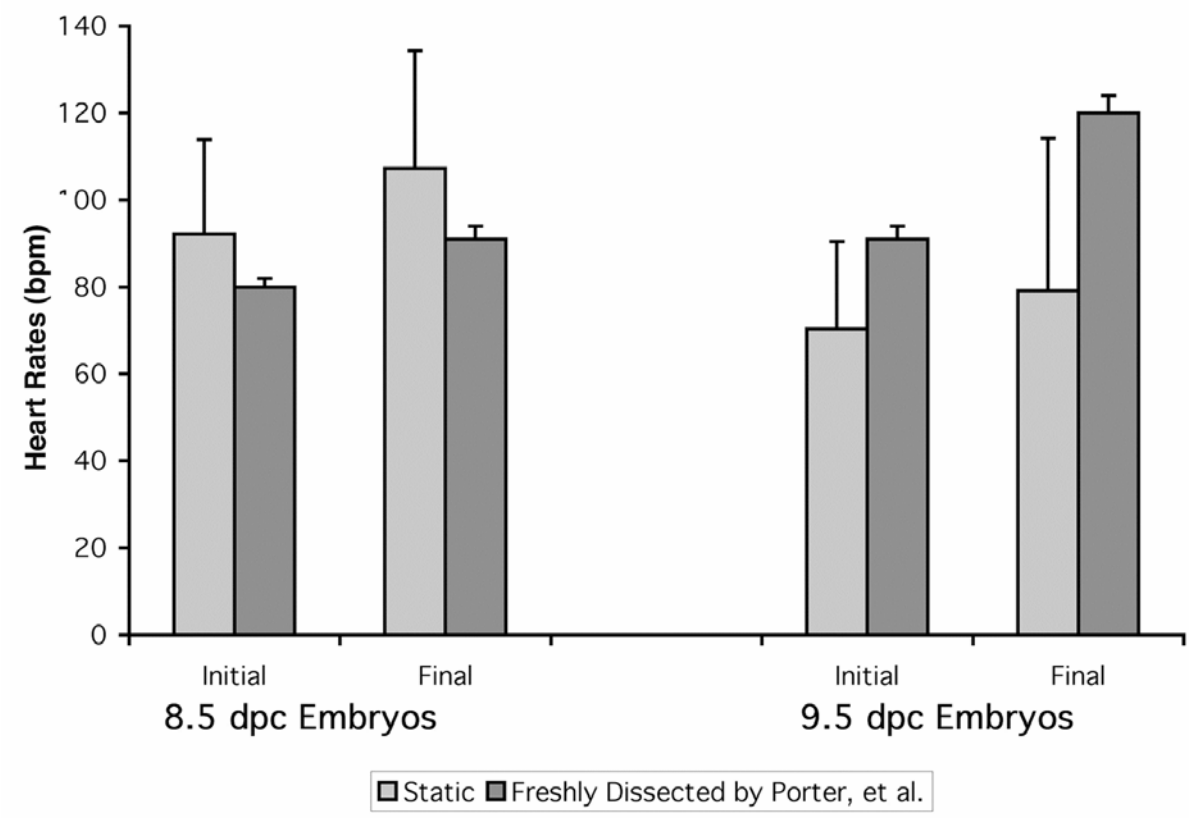
140
120
100
80
60
40
20
0
Heart Rates (bpm)
Initial
Final
Initial
Final
8.5 dpc Embryos
9.5 dpc Embryos
Static
Freshly Dissected by Porter, et al.

Figure 4

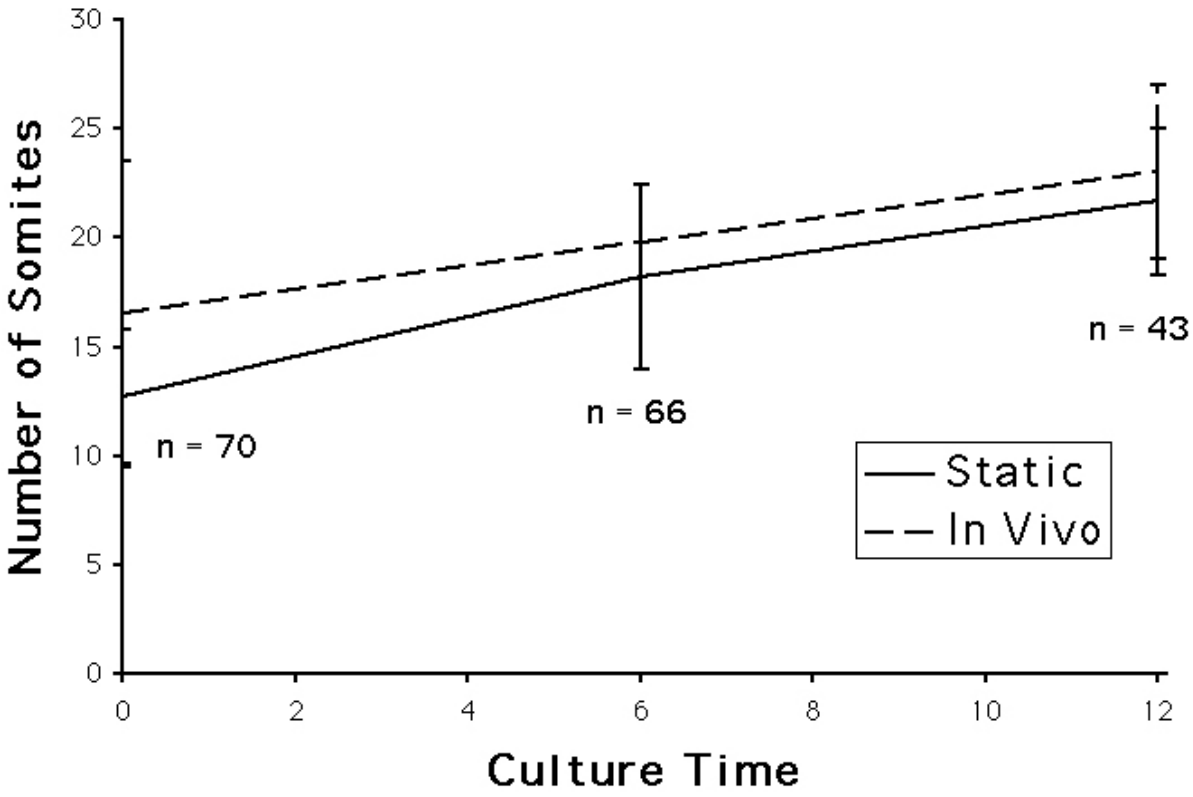
Number of Somites
30
25
20
15
10
5
0
0
2
4
6
8
10
12
Culture Time
n = 70
n = 66
n = 43
Static
In Vivo

Figure 5

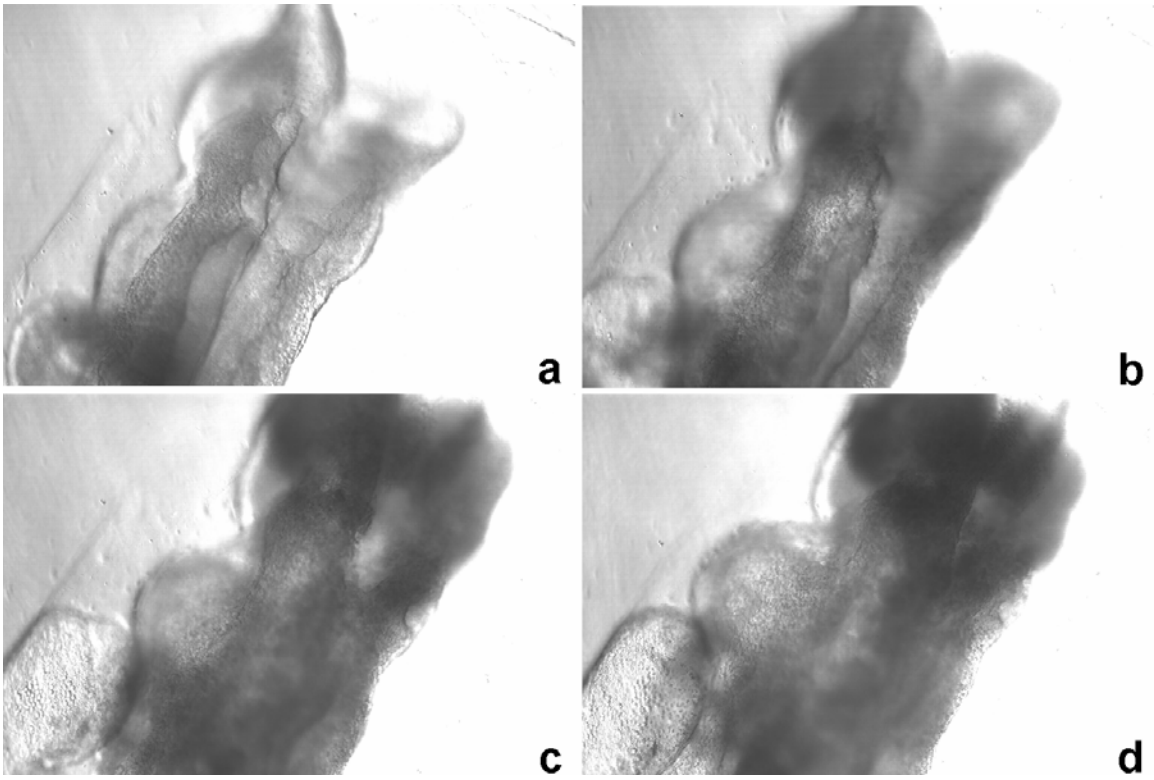

Figure 6

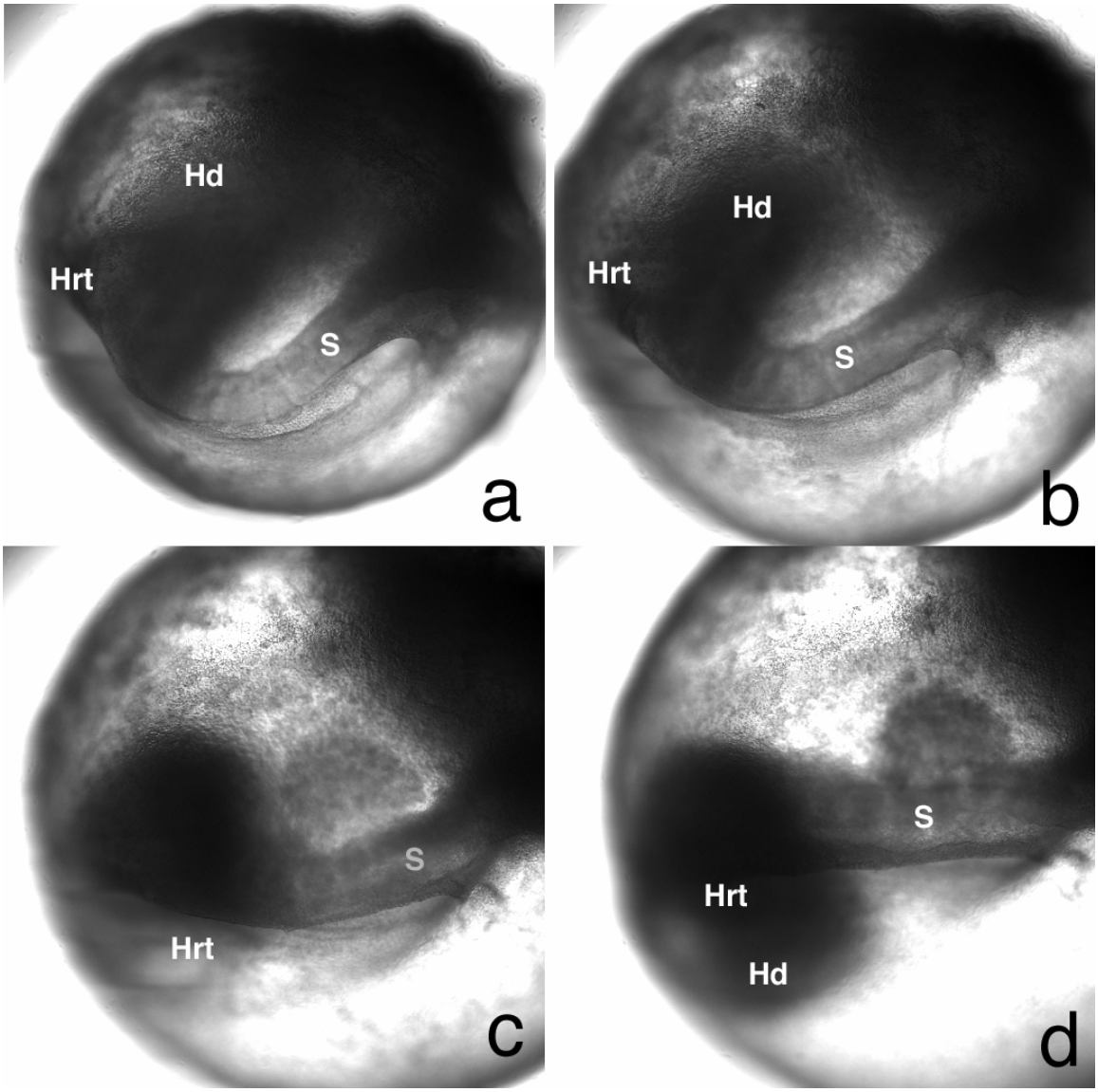

Figure 7

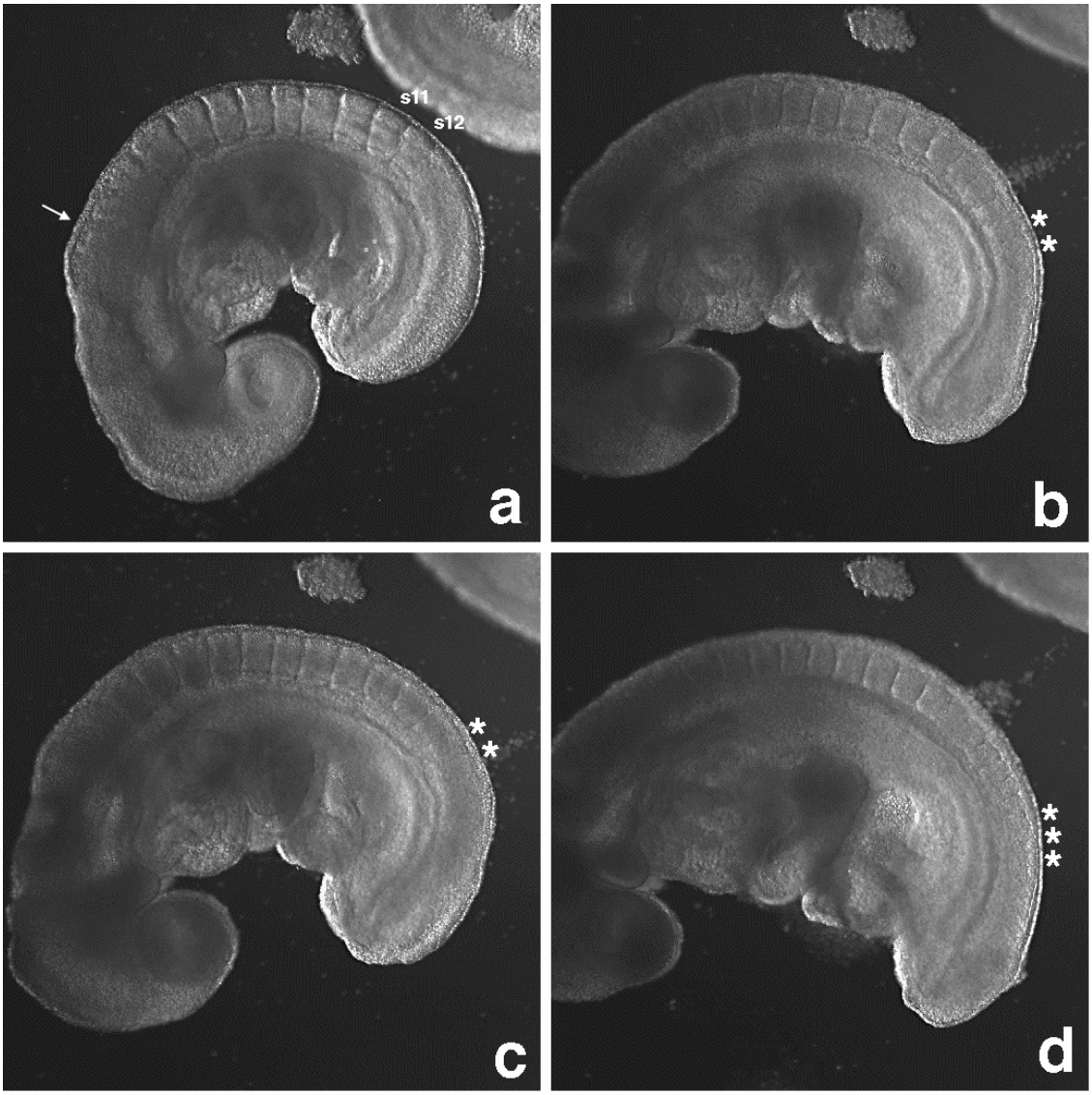

Figure 8

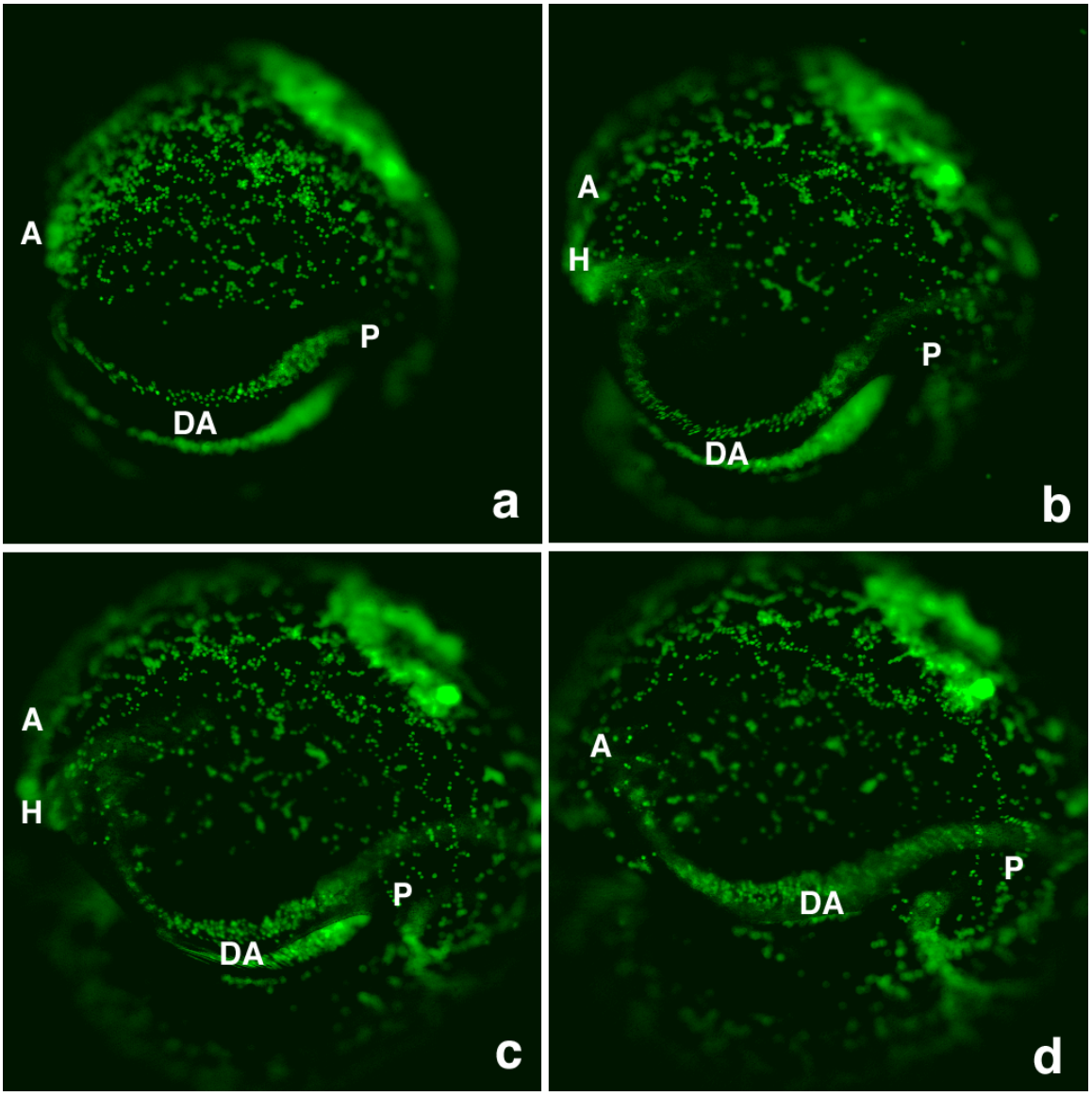

Chapter 3

Measuring Hemodynamic Changes During Mammalian Development

Summary

The pathogenesis of many congenital cardiovascular diseases involves abnormal flow within the embryonic vasculature, resulting either from heart malformations or from defects in the vasculature itself. Extensive genetic and genomic analysis in the mouse has led to the identification of an array of mutations that result in cardiovascular defects during embryogenesis. Many of these mutations cause secondary effects within the vasculature which are thought to arise because of altered fluid dynamics. Presumably, cardiac defects disturb or reduce flow**,** leading to the disruption of the mechanical signals necessary for proper vascular development. Unfortunately, a precise understanding of how disruptions in flow lead to secondary defects in the vasculature has been hampered by the inadequacy of existing analytical tools. Here we use a fast line-scanning technique for the quantitative analysis of hemodynamics during early organogenesis in the mouse embryo and present a model system for studying cellular responses during the formation and remodeling of the mammalian cardiovascular system. Flow velocity profiles can be measured as soon as the heart begins to beat, even in newly formed vessels. These studies establish a link between the pattern of blood flow within the vasculature and the stage of heart development and enable the analysis of the influence of mechanical forces during development.

Introduction

Abnormalities in the growth and development of the cardiovascular system are among the most common congenital birth defects [1, 2] and show a large degree of variability, indicating that cardiovascular development relies on a complex set of signals. Using model systems such as the mouse, great strides are being made in elucidating the molecular signaling pathways involved in early heart and blood vessel formation (for review, see [3]). Through both single gene targeting approaches and large scale screens (for review, [4]) a growing number of mutants are being identified with defects in hematopoiesis [5-7], endothelial cell formation and organization [8-10], and cardiogenesis [3, 11, 12].

In addition to genetic regulation, mechanical signals imparted through frictional forces created by blood flow are also essential for normal development. If flow is interrupted during embryonic development, heart and vascular defects arise [2, 12-17]. *In vitro* studies have revealed that the shear stress caused by fluid flow can induce changes in the morphology and activity of cultured endothelial cells, causing cell alignment, proliferation, and activation of gene expression and enzyme function [18-22]. Interestingly, several gene products whose expression and activation are influenced by flow in cultured endothelial cells are also necessary for development [18, 19, 22, 23]. All of these data suggest that shear stress may act as a key regulator of development, but very few studies have related shear stress levels to specific cellular events in the embryo.

A large gap exists between the precisely controlled flow and quantitative evaluations performed *in vitro* and the complex dynamic interactions that occur during early circulation *in vivo*. This is largely due to the fact that methods for quantitative hemodynamic analysis of newly formed vessels *in vivo* have not been established. In this study, we show that quantitative flow measurements can be made in early mouse embryos at a time when the cardiovascular system is first forming. Using confocal laser scanning microscopy (CLSM) to image mouse embryos (day 8.5 to 10.5) that express green fluorescent protein (GFP) in primitive erythroblasts [24], velocity measurements were made in vessels ranging from the diameter of a single blood cell (10 μm) up to several hundred microns. Close inspection of velocity profiles revealed that both laminar and disturbed flows are present in the early yolk sac. Therefore, cells are exposed to both laminar and oscillatory shear stress during development. In support of the hypothesis that mechano-sensory signals play a role in development, laminar shear stress levels were consistent with the levels of shear stress known to affect the morphology and molecular signaling of endothelial cells *in vitro*. Thus, it is possible to use quantitative methods to study the remodeling of embryonic vasculature. Moreover, changes in the acceleration and deceleration of flows were seen as the heart matured, showing that velocity measurements can be used to study heart development. The model system described here, in combination with mutant analysis, will provide a powerful approach for studying cardiovascular development and the role of mechano-sensory signals.

Results

Measurement of Blood Velocities in Embryonic Yolk Sac Microvasculature

We have focused our studies on blood flow in the developing yolk sac of the early mouse embryo. In mammals, the first site of red blood cell production is in the yolk sac, an extraembryonic, multi-layered membrane surrounding the embryo proper. Both blood and endothelial cells differentiate in the yolk sac prior to the development of a functional heart (beginning at 7.5 days post coitum (dpc) in the mouse), but vessel remodeling occur after the heart starts beating and blood flow begins.

The yolk sac is an excellent model for studying early hemodynamics because it is a simple system, consisting of only a few different cell types compared to the adult, yet vascular development can be followed from the initial differentiation of endothelial cells to the formation of remodeled vessels in a few short days. In addition, by studying fluid dynamics in the yolk sac, movement artifacts produced by the heart beat are minimized. To aid in visualizing blood flow in the yolk sac, whole mouse embryos expressing GFP in primitive erythroblasts [24] were grown in culture on the stage of a confocal laser scanning microscope [25].

To examine flow regimes and quantify the level of shear stress, the velocities of erythroblasts within the vessel and the hematocrit must be determined. To accomplish this, we have adapted a technique originally developed for measuring blood flow in adult microcirculation in which a confocal laser scanning microscope is used to scan a single line parallel with the flow in a vessel to measure flow velocity [26]. We altered the

technique by scanning perpendicular, rather than parallel, to the direction of flow in order to measure vessel size, hematocrit and the flow profile through the vessel, all of which are necessary for calculating shear stress.

In traditional confocal laser scanning microscopy (CLSM), a laser that excites a given fluorochrome in a cell is scanned across a field of view while a detector simultaneously collects the emission signal, pixel by pixel, to produce a two-dimensional image (Figure 1B). For instance, for a single image that is 512 x 512 pixels, the laser scans across the field of view, collecting 512 pixels worth of data in a straight line and then moves to the next line to acquire the next row of pixels. Therefore, the time to acquire the whole image depends on the acquisition time for each line, the number of lines and the time it takes for the laser to turn around to scan the next line. Scanning the whole field of view is often too slow for capturing very rapid dynamic events, but line scanning, (repeatedly scanning a single line) can be used as an alternative if enough image data is gathered from a single row of pixels.

For the method described here, the laser was used to repeatedly scan along a single line positioned perpendicular to vessels of various sizes in the mouse yolk sac (white line, Figure 1A). The scan line acts like a photo-finish camera at a race, imaging a single row of pixels and collecting partial images of blood cells as they pass that point in the vessel. Slower moving blood cells are imaged more often than rapidly moving cells as they cross the scan line. Velocity can be measured by determining how many times the same cell was imaged and, thus, how long it took for the cell to cross through the line scan. To determine the velocity of a cell, line scans are reconstructed as 2-dimensional images (L vs. t) (Figure 1B). The length of the streak that is produced by the image of

the cell can be directly related to velocity, given that the line scanning speed, pixel size, any movement perpendicular to the vessel, and the cell diameter are known (Figure 1C) (see also Materials and Methods). This calculation is simplified by the fact that early embryonic erythroblasts are spherical throughout all embryonic stages imaged (Figure 2) and do not appear to deform significantly during flow (data not shown). Therefore, the optical plane of the cell being imaged is inconsequential, because the two-dimensional image of the cell will always be circular and the distance traveled can be related to the diameter.

Using this method, the minimum velocity that can be measured will be determined by the number of scans, whereas the maximum limit is determined by scan speed of the instrument (see Materials and Methods). Routinely, 3000 lines are scanned, giving a theoretical lower limit of 3.7 μm/s, while the fastest velocity that can be measured by our current system is 13000 μm/s. In the yolk sac, measured flow velocities ranged between 18.5 and 6000 μm/s. Since measurements of the fastest velocities in the yolk sac were well under the theoretical limit, we made velocity measurements in the dorsal aorta at 8.5 dpc, where measurements showed that flow traveled up to 9400 μm/s. To determine the error rate for these measurements, a mass balance analysis was performed (see Material and Methods). Less than 7% error was observed, indicating that this method provides valid measurements of flow velocity.

Line scanning was used to assess the velocity of the blood in yolk sac vessels in embryos at 8.5, 9.5 and 10.5 dpc (Figure 3A-C). We observed a range of velocities in the embryo at the three stages examined. At the earliest stage examined, just after circulation begins, the channels in the vascular plexus are of similar size, yet flow

velocities were found to be quite variable. At 9.5 and 10.5 dpc, vessels varied in size from approximately 50 μm to 200 μm. At these stages, both velocities and the size of vessels are highly variable, but blood flow appears to travel at similar velocities in vessels of the same size. It is unknown whether velocity at 8.5 dpc is a predictor of the vessel size at later stages (see Discussion).

Determining Blood Flow Profiles in the Developing Yolk Sac

Line scanning perpendicular to the vessel was used to obtain flow profiles from vessels of the yolk sac. Flow profile is used to show directionality with respect to vessel structure. While it is generally assumed that early embryonic blood flow is laminar [27], this has not been shown directly. Laminar flow is characterized by steady movement with a straight trajectory, without mixing. Flow velocity has a parabolic profile with respect to vessel diameter, such that cells in the middle of the vessel travel faster than cells slowed by friction near the vessel walls. In addition to laminar flow, blood flow can exhibit more complex profiles. Yolk sac vessels are too small and flow is too slow to produce turbulence, but areas of flow separation and vessel branching can produce eddies or other disturbed flows. Disturbed flows can be characterized by cells moving in irregular or circular motions within the vessel. Both laminar and disturbed flows were detected within the yolk sac. Figure 4A shows the L vs. t plots of steady flow along a single axis. Cells move predominately along the axis of the vessel parallel to the wall, with limited movement along the perpendicular axis. Velocity profiles of steady flow regions are parabolic at peak (systole) and non-peak (diastole) velocities (Figure 4B), confirming that flow is indeed laminar in these regions. Figure 4C shows the L vs. t plot of a region where an eddy is present. A disturbed pattern of flow is seen, where the

relative angle of the line scan streaks change with respect to one another. Velocities plotted along the diameter of the vessel do not fit a parabolic profile (Figure 4D) and, therefore, are non-laminar.

Hematocrit Measurements in Embryonic Circulation

To calculate shear stress, hematocrit as well as the flow velocity and flow profile are needed. Hematocrit was measured directly in individual yolk sac vessels from 8.5 to 10.5 dpc. Figure 5A shows hematocrit values found at different stages of development. Hematocrit was observed to increase slightly between 8.5 and 10.5 dpc, from about 15% to 20% of total intra-vascular volume. Furthermore, there is a linear relationship between vessel diameter and hematocrit in individual embryos that is statistically significant (average $p=0.074$) and is independent of developmental stage (Figure 5B). This relationship between vessel size and hematocrit is called the Fahraeus effect [28], and has never been reported in an embryonic system.

Laminar Shear Stress (LSS) in Embryonic Flow

The levels of LSS were calculated in different sized vessels at different times during development (Figure 6) using a correlation to approximate blood viscosity [29] based on shear rate and hematocrit (see Materials & Methods). LSS values ranged from 0.40 to 5.16 dynes/cm^2, consistent with shear stress levels known to modulate the expression and subcellular localization of proteins important in normal vascular development such as Flk-1 and other growth factor receptors. At 8.5 dpc, the levels of shear stress were not related to the vessel size, while at both 9.5 and 10.5 dpc, shear stress values were higher in larger vessels. In addition, the magnitude of shear stress increased from 9.5 dpc to 10.5 dpc, a time when vessels undergo remodeling.

Change in Flow with Heart Development

Between 8.5 and 10.5 dpc, the heart is transformed from a linear tube to a looping heart consisting of multiple chambers and developing valve primordia (endocardial cushions). To determine how the periodicity of flow changes during heart development, blood velocities were plotted with respect to time (Figure 7). Yolk sac vessels were compared that had approximately equal maximum velocities. For the earliest embryos examined (8.5 dpc), when the future heart is still a linear tube, velocity increased and decreased gradually with an irregular frequency (Figure 7A). For 9.5 dpc embryos, in which the endocardial cushions are more pronounced, velocity increased steeply and abruptly, decreasing slowly thereafter (Figure 7B). Finally, for 10.5 dpc embryos, velocity increased steeply and rapidly, and then decreased sharply (Figure 7C). These changes in acceleration and deceleration of the flow cycle likely reflect the improvement in heart function from 8.5 to 10.5 dpc.

Discussion

Here we present novel measurements of fluid dynamics in the early mammalian cardiovascular system. Using confocal line scanning, we can accurately measure flow velocities, flow profiles and hematocrit in embryonic microvasculature. We have characterized changes in blood flow through the yolk sac of early mouse embryos and have calculated levels of shear stress induced by blood flow.

Primitive Erythroblast Movement During Yolk Sac Development

In the mouse embryo, blood cells continue to differentiate and proliferate as circulation begins. Hematocrit measurements in the early embryo increased steadily as the embryos developed further. In addition, even at the earliest stage examined, hematocrit was directly dependent on vessel size. In larger vessels, we observed a higher percentage of erythroblasts. This relationship, the Fahraeus effect [28], has previously been demonstrated *in vivo* in adult tissues [30], but it has never been reported in embryos. Even though individual vessels in a single embryo can vary in size by up to three-fold, the relationship between vessel size and hematocrit is maintained.

The hematocrit measurements presented here reflect those cells that were actively moving through the vasculature. Consistent with previous studies [31], we also observed many primary erythroblasts that did not circulate freely (data not shown). In fact, in some cases, primary erythroblasts remained at the site where they formed and others were carried to new sites and became trapped. It is not known if the fate of circulating vs. non-circulating blood cells is different. For example, non-circulating blood cells eventually may be eliminated by programmed cell death or fail to proliferate.

Flow Patterns and Shear Stress During Embryonic Development

We have measured levels of laminar shear stress between 0-5.5 dyn/cm2 in embryos from 8.5 to 10.5 dpc. Similar levels of LSS have been shown to induce notable responses in cultured endothelial cells. *In vitro*, these levels of shear stress are associated with endothelial cell alignment and have been shown to induce the expression of numerous transcription factors, cell adhesion molecules, enzymes, and

cell signaling molecules, including growth factors and growth factor receptors known to play a role in development (for review, see [32]). For instance, the expression of Platelet Derived Growth Factor (PDGF) A [19] and B receptors [23] is induced in the presence of LSS. In the absence of PDGF signaling in the embryo, the recruitment of mural cells and pericytes that stabilize nascent vessels during remodeling is disrupted.[33, 34] LSS also induces the expression of several members of the TGF-beta signaling pathway, such as TGF-beta1 [18] and its mediators Smad 6 and 7 [20]. TGF-beta signaling is required for the remodeling of the vascular plexus and mature vessels do not form in mice with null mutations in TGF-beta 1 or its receptor [35-37]. Vascular Endothelial Growth Factor Receptor 2 (VEGFR2) is also activated in the presence of shear stress *in vitro*, altering its subcellular localization [22]. Embryos lacking VEGFR2/Flk-1 do not form vessels in the yolk sac [38], but VEGF signaling may be required at later stages of hematopoietic and vascular development, since it remains expressed in endothelial cells throughout embryonic development [39]. Our data shows that the levels of shear stress in developing vessels in the yolk sac are similar to the levels shown *in vitro* to regulate key factors necessary for remodeling.

Interestingly, LSS levels vary in yolk sac vessels of 8.5 dpc embryos, even though the vessels themselves are similar in size. At 9.5 and 10.5 dpc, vessel size becomes highly variable, but LSS values are similar in vessels of the same size. The transition from the uniformly-sized vascular channels in the primitive plexus to the formation of individual vessels of variable size represents a major event in vascular remodeling. It is possible that the level of shear stress within early vessels directly affects the size or extent of remodeling in that same vessel one or two days later. We have begun more in depth studies to determine if the level of shear stress at the plexus stage can be used to

predict vessel size or extent of remodeling that follows. As discussed below, examination of mutants with impaired flow may be critical to understanding precisely how the level of shear stress relates to specific remodeling events.

In addition to laminar flow, we also detected eddies or disturbed flows. From *in vitro* studies, it is known that laminar and disturbed flows produce different types of force or shear stress which in turn have differential effects on endothelial cells. Oscillatory shear stress (OSS) induced by eddies [40] correlates with increased cell proliferation. In fact, both the magnitude of shear stress and local fluctuations in shear stress may be important mechano-sensory signals [40]. Cell proliferation, in addition to other factors, is thought to contribute to the formation of atherosclerotic plaques which often form at branch points in arteries [41]. In development, OSS may play a part in vessel growth at the branch point or may signal the proliferation of endothelial cells during vasculogenesis and remodeling. Although it is possible to calculate the magnitude of laminar stress using line scanning, the line scanning method cannot be used to determine the level of OSS. Continuous particle tracking is needed for measuring forces exerted by particles with circular or irregular trajectories. Others have made measurements of OSS and even turbulent flows using high-speed imaging and correlation techniques such as Digital Particle Image Velocimetry [16]; however, high-speed fluorescence imaging is often hampered by poor sensitivity and may not be feasible for these studies.

Hemodynamics and Cardiac Development

Recently there has been an increased interest in the relationship between blood flow and heart and vessel development. In zebrafish, it has been shown that blocking fluid flow, thereby reducing shear stress, results in heart defects [16]. In *silent heart* mutants,

where flow is impaired [17], patterning defects are seen in the intersegmental arteries. In the mouse, the heart does not form properly if flow is stopped through ablation of Ncx1, a Na+/Ca+ exchanger [12]. Also, in Myosin Light Chain 2a (MLC 2a) mutant embryos, the atria and endocardial cushions do not develop properly [42]. It is noteworthy that these mice also have defects in the yolk sac vasculature even though the MLC 2a gene is only expressed in cells within the heart. These and other mutants provide a unique opportunity to study the relationship between fluid dynamics and vascular development since flow is disrupted in a way that does not also directly interfere with the development of endothelial cells.

In addition to studying shear stress, subtle defects in valve function and cardiac muscle development can be detected by examining the periodicity of flow through the heart, providing greater insights into how flow is disrupted in the presence of cardiac abnormalities. The measurements of flow periodicity shown here are similar to the Doppler waveforms produced by ultrasound [43], but can be obtained using a confocal microscope which is more readily available in many research labs.

Mechano-Sensory Signals and Vascular Remodeling

The data we describe here shows that it is possible to explore the relationship between mechano-sensory and biochemical signals involved in vessel development and patterning at a cellular level. We have shown that mechanical forces that act on endothelial cells can be measured using CLSM. CLSM is also a powerful tool for imaging changes in endothelial cell morphology and expression of signaling molecules, making it possible to study how variations in blood flow effect vascular remodeling.

Thus, we have developed a robust model system for studying how mechano-sensory signals function in the development of the mammalian cardiovascular system.

Materials and Methods

Dissection

Homozygous ε-globin:GFP male breeder mice [24] were mated with CD-1 females overnight. The presence of a vaginal plug was taken as 0.5 dpc. Embryos were collected on the morning of the eighth, ninth or tenth day in a Plexiglas hood heated to 37°C using a chicken incubator heater (Lyon Electric Company # 115-20). Dissecting medium consisted of 90% D-MEM/F-12 (Gibco, #11330032), 8% heat-inactivated fetal bovine serum (Gibco, #16140063), 1% HEPES buffer solution 1M (Irvine Scientific, # 9319) and 1% Pen-Strep solution (Irvine Scientific, # 9366). The medium was warmed to 37°C prior to dissection. Females were euthanized with CO_2 followed by cervical dislocation. The uterine horns were removed and placed in warmed medium and the embryos isolated, keeping yolk sacs intact.

The embryos were stained with Cell Tracker Orange (Molecular Probes, C-2927; 1:500 in dissecting medium) for 15 minutes to visualize the vessel wall. Embryos were kept in a tissue culture incubator at 37°C during staining. The embryos were then washed twice with warm dissecting medium and transferred to culture medium in a Nunc Lab-Tek chamber (2 chambers/ coverglass, #155380). The culture medium consisted of 50% D-MEM/F-12 and 50% rat serum (for production, see [25]) supplemented with 10 μL/mL

Pen-Strep and 10 μL/mL HEPES buffer. Embryos were pre-incubated for 1 hour at 37°C and 5% CO_2 in a tissue culture incubator to allow heart rates to stabilize.

Confocal Microscopy

Embryos were imaged on a Zeiss LSM 510 or a Zeiss LSM PASCAL microscope. The culture system has recently been described by Jones *et al* [25]. Line scan imaging was done at a magnification of 20x. An initial whole field image of the blood flow was made and overlaid with a line to record the position of the line scan. The laser was then located at this position and scanned for 3000 lines. Laser line scan rates were between 384 and 960 μsec per line. Pixel size depended on the length of the laser line.

Velocity Calculation

Line scans were reconstructed as L vs. t images such as the one shown in Figure 1. Pixel data collected from the line scans were arranged into an image with the line data on the horizontal axis and time on the vertical axis. Using this approach, the length of each streak (Δt) can be related to the time it takes for the cell to move across the scan line with a given pixel dimension. Since cells do not always move parallel to the vessel wall, movement along the axis of the scan line must also be accounted for and is given by ΔL. With these measurements, velocity can be calculated using the following equations:

The time for one blood cell to pass over the laser line, $t_{RBC,}$ is calculated using the t-displacement of the streak (Δt, in number of lines) and the scan rate (V_{SCAN}, in μs/line):

$$t_{RBC} = (\Delta t\text{-}1) * V_{SCAN} .$$

Primitive erythroblasts are spherical (Figure 2). Irrespective of which z-plane of the cell is imaged, the distance traveled is equivalent to the cell diameter, D, measured in pixels. Therefore, the distance traveled is given by:

Distance = $D*S_{PIXEL}$,

where S_{PIXEL} is the pixel size (μm/pixel).

To determine the component of the velocity perpendicular to the laser line, V_y, the distance traveled is divided by the time taken to pass over the laser line:

$$V_y = \frac{D * S_{PIXEL}}{(\Delta t - 1) * V_{SCAN}} .$$

If there is also a component of the velocity parallel to the laser line, it can similarly be calculated using:

$$V_x = \frac{\Delta L * S_{PIXEL}}{(\Delta t - 1) * V_{SCAN}} ,$$

where ΔL is the measured displacement in the L- direction.

Using these equations, the overall velocity is given by:

$$V = \frac{S_{PIXEL}\sqrt{\Delta L^2 + D^2}}{(\Delta t - 1) * V_{SCAN}} .$$

Clumps of primitive erythroblasts could not, in general, be analyzed using this technique. It was necessary to disregard a small subset of erythroblasts whose edges could not be clearly distinguished.

Line scan images where the erythroblasts passed over the laser line in fewer than 3 scans were discarded. Under these circumstances, diameter measurements may be inaccurate, as it is impossible to know if the laser has imaged the erythroblast close to the center of the cell. The top line scanning rate of the Zeiss PASCAL LSM is 384 μs/line for a line 512 pixels long. For a red blood cell with a diameter of 10 μm, the theoretical maximum velocity that can be measured is 13021 μm/s if the vessel diameter is less than 20 μm wide (using a 20x lens) or 10400 μm/s if the vessel is up to 460 μm in diameter.

Validation of Method

To validate these measurements, a mass balance on merging yolk sac vessels was calculated. Because inflow must equal outflow, the sum of the volumetric flow rate of the two input vessels at a bifurcation should add to the volumetric flow rate of the larger vessels into which the two smaller vessels merge, as long as differences in density are negligible.

Assuming a parabolic profile, the maximum velocity is twice the average velocity and so the volumetric flow rates can be calculated from:

$$Q = \frac{V_{\max}}{2} \pi r^2 = V_{av} \pi r^2 .$$

The pulsatile nature of the flow can be ignored for this calculation since flow within the embryonic vasculature is within the Stoke's flow regime (Re << 1) and the Womersley parameters is known to be much less than one [27].

Because line scans were performed sequentially, a simultaneous comparison of flow rates could not be made. Therefore, the volumetric flow rate was calculated using two different methods to verify that the calculations were unbiased and the results from each method were comparable, with very little error. In the first method, the average of the top 2% of all measured velocities for a vessel was taken as V_{max}. In the second method, the mean velocity of all the flow rates was taken as V_{av}. The error associated with the mass balance (5% to 7%; data not shown) was minimal, indicating a high level of accuracy in the measurements. Errors in individual velocity measurements were minimized by averaging multiple determinations.

To analyze the components that introduced the most error, a sensitivity analysis was performed. Errors in scan rate and pixel size are related to the microscope software and are expected to be minimal. The most sensitive variable to measurement error was the t-dimension of the streak. At the fastest flow rates that can be measured, streaks often had fewer than 5 line scans, which could easily introduce significant error, especially if the length was underestimated. The strength of this method, however, is that by measuring every single red blood cell, so many measurements are made that errors are minimized through data regression.

Calculation of Hematocrit

A scan through the center of the vessel was used as representative of the flow present in the whole vessel since non-disturbed laminar flow is parabolic (Figure 4). Our calculations assume that the vessel is spherically cylindrical, because the difference in dimension on each axis is on the scale of one or two red blood cells. The center of a vessel along the z-axis was determined by changing the focal plane to reveal the widest

cross-section. The hematocrit was calculated by first cropping the images to include only regions of blood flow as assessed by the location of the vessel walls. The image was then converted to gray-scale and a threshold was applied to the image such that pixels were either pure white or pure black. The intensity at which the threshold was applied was chosen by increasing the zoom on the image to visualize the individual pixels and finding the level at which the size of the red blood cell streaks between the black and white and the grayscale image were in agreement. The percentage of white pixels within the image was used as the hematocrit.

Calculation of Laminar Shear Stress (LSS)

The velocity data during a pulse was plotted versus x- position within the line scan image to give the velocity profile within the blood vessel (as in Figure 4). The location of the pulse was assessed visually and only the velocity data during the peak flow was used. The data was regressed using parabolic profile.

$$V = ar^2 + b,$$

where V is the velocity, r is the radial position of the measurement and a and b are the regression results.

The vessel radius, R, is found from the x-intercept.

$$R = \sqrt{\frac{-a}{b}}.$$

This value was compared to the measured diameter based on cell-tracker orange staining. If there was a large difference between actual and calculated diameter, data

from that pulse was rejected. This occurred in less than 10% of the scans and was generally caused by blood flow in which all the red blood cells were located near the center of the vessel. The shear rate was calculated based on the slope of the regressed line at the vessel wall.

$$\dot{\gamma} = -\left.\frac{dV}{dr}\right|_{r=R} = -2aR,$$

where $\dot{\gamma}$ is the shear rate.

The apparent viscosity for embryonic mouse blood was approximated using data from adult human blood [29] because no relevant work has been done on embryonic mouse blood. The apparent viscosity of human blood is very likely to be similar to embryonic mouse blood, despite the fact that red blood cells in the mouse embryo are nucleated. Studies have shown that at low shear and low hematocrit, viscosity is comparable between nucleated avian blood and enucleated human blood [44]. The shear rate data and the hematocrit data for each pulse were inserted into a 6th order logarithmic regression for calculating blood viscosity at low shear rates [29].

The shear stress is calculated by multiplying the shear rate by the apparent viscosity.

$$\tau = \mu_{app}\dot{\gamma}.$$

Acknowledgements

We thank Chris Waters for technical support and Joaquin Gutierrez for assistance in animal husbandry. This work was supported by NIH (R01-HL62248 to M.H.B.) and the Human Frontiers Science Program (SEF.HFSP1-1-HFSP.000002 to S.E.F). We also thank the Powell foundation for the partial support of this work through the Option of Bioengineering at Caltech.

References

1. Payne, R.M., M.C. Johnson, J.W. Grant, and A.W. Strauss, Toward a molecular understanding of congenital heart disease*. Circulation*, 1995. 91(2): 494-504.
2. Olson, E.N. and D. Srivastava, Molecular pathways controlling heart development*. Science*, 1996. 272(5262): 671-6.
3. Conway, S.J., A. Kruzynska-Frejtag, P.L. Kneer, M. Machnicki, and S.V. Koushik, What cardiovascular defect does my prenatal mouse mutant have, and why? *Genesis*, 2002. 35: 1-21.
4. Justice, M.J., J.K. Noveroske, J.S. Weber, B. Zheng, and A. Bradley, Mouse ENU mutagenesis*. Human Molecular Genetics*, 1999. 8(10): 1955-63.
5. Robb, L., I. Lyons, R. Li, L. Hartley, F. Kontgen, R.P. Harvey, D. Metcalf, and C.G. Begley, Absence of yolk sac hematopoiesis from mice with a targeted disruption of the scl gene*. Proc Natl Acad Science USA*, 1995. 92(15): 7075-9.
6. Shivdasani, R.A., E.L. Mayer, and S.H. Orkin, Absence of blood formation in mice lacking the T-cell leukaemia oncoprotein tal-1/SCL*. Nature*, 1995. 373(6513): 432-4.

7. Warren, A.J., W.H. Colledge, M.B. Carlton, M.J. Evans, A.J. Smith, and T.H. Rabbitts, The oncogenic cysteine-rich LIM domain protein rbtn2 is essential for erythroid development*. Cell*, 1994. 78(1): 45-57.

8. Carmeliet, P., V. Ferreira, G. Breier, S. Pollefeyt, L. Kieckens, M. Gertsenstein, M. Fahrig, A. Vandenhoeck, K. Harpal, C. Eberhardt, C. Declercq, J. Pawling, L. Moons, D. Collen, W. Risau, and A. Nagy, Abnormal blood vessel development and lethality in embryos lacking a single VEGF allele*. Nature*, 1996. 380(6573): 435-9.

9. Ferrara, N., K. Carver-Moore, H. Chen, M. Dowd, L. Lu, K.S. O'Shea, L. Powell-Braxton, K.J. Hillan, and M.W. Moore, Heterozygous embryonic lethality induced by targeted inactivation of the VEGF gene*. Nature*, 1996. 380(6573): 439-42.

10. Suri, C., P.F. Jones, S. Patan, S. Bartunkova, P.C. Maisonpierre, S. Davis, T.N. Sato, and G.D. Yancopoulos, Requisite role of angiopoietin-1, a ligand for the TIE2 receptor, during embryonic angiogenesis*. Cell*, 1996. 87(7): 1171-80.

11. Lyons, I., L.M. Parsons, L. Hartley, R. Li, J.E. Andrews, L. Robb, and R.P. Harvey, Myogenic and morphogenetic defects in the heart tubes of murine embryos lacking the homeo box gene Nkx2-5*. Genes & Development*, 1995. 9(13): 1654-66.

12. Wakimoto, K., K. Kobayashi, O.M. Kuro, A. Yao, T. Iwamoto, N. Yanaka, S. Kita, A. Nishida, S. Azuma, Y. Toyoda, K. Omori, H. Imahie, T. Oka, S.

Kudoh, O. Kohmoto, Y. Yazaki, M. Shigekawa, Y. Imai, Y. Nabeshima, and I. Komuro, Targeted disruption of Na+/Ca2+ exchanger gene leads to cardiomyocyte apoptosis and defects in heartbeat. *J Biol Chem*, 2000. 275(47): 36991-8.

13. Chapman, W.B., The effect of the heart-beat upon the development of the vascular system in the chick. *Am. J. Anat.*, 1918. 23: 175-203.
14. Burggren, W.W., S.J. Warburton, and M.D. Slivkoff, Interruption of cardiac output does not affect short-term growth and metabolic rate in day 3 and 4 chick embryos. *J Exp Biol*, 2000. 203 Pt 24: 3831-8.
15. Hogers, B., M.C. DeRuiter, A.C. Gittenberger-de Groot, and R.E. Poelmann, Unilateral vitelline vein ligation alters intracardiac blood flow patterns and morphogenesis in the chick embryo. *Circ Res*, 1997. 80(4): 473-81.
16. Hove, J.R., R.W. Koster, A.S. Forouhar, G. Acevedo-Bolton, S.E. Fraser, and M. Gharib, Intracardiac fluid forces are an essential epigenetic factor for embryonic cardiogenesis. *Nature*, 2003. 421(6919): 172-7.
17. Isogai, S., N.D. Lawson, S. Torrealday, M. Horiguchi, and B.M. Weinstein, Angiogenic network formation in the developing vertebrate trunk. *Development*, 2003. 130(21): 5281-90.
18. Ohno, M., J.P. Cooke, V.J. Dzau, and G.H. Gibbons, Fluid shear stress induces endothelial transforming growth factor beta-1 transcription and

production. Modulation by potassium channel blockade*. J Clin Invest*, 1995. 95(3): 1363-9.

19. Kraiss, L.W., R.L. Geary, E.J. Mattsson, S. Vergel, Y.P. Au, and A.W. Clowes, Acute reductions in blood flow and shear stress induce platelet-derived growth factor-A expression in baboon prosthetic grafts*. Circ Res*, 1996. 79(1): 45-53.
20. Topper, J.N., J. Cai, Y. Qiu, K.R. Anderson, Y.Y. Xu, J.D. Deeds, R. Feeley, C.J. Gimeno, E.A. Woolf, O. Tayber, G.G. Mays, B.A. Sampson, F.J. Schoen, M.A. Gimbrone, Jr., and D. Falb, Vascular MADs: two novel MAD-related genes selectively inducible by flow in human vascular endothelium*. Proc Natl Acad Science USA*, 1997. 94(17): 9314-9.
21. Gan, L., M. Miocic, R. Doroudi, L. Selin-Sjogren, and S. Jern, Distinct regulation of vascular endothelial growth factor in intact human conduit vessels exposed to laminar fluid shear stress and pressure*. Biochem Biophys Res Commun*, 2000. 272(2): 490-6.
22. Shay-Salit, A., M. Shushy, E. Wolfovitz, H. Yahav, F. Breviario, E. Dejana, and N. Resnick, VEGF receptor 2 and the adherens junction as a mechanical transducer in vascular endothelial cells*. Proc Natl Acad Science USA*, 2002. 99(14): 9462-7.
23. Resnick, N., T. Collins, W. Atkinson, D.T. Bonthron, C.F. Dewey, Jr., and M.A. Gimbrone, Jr., Platelet-derived growth factor B chain promoter

contains a cis-acting fluid shear-stress-responsive element. *Proc Natl Acad Sci USA*, 1993. 90(10): 4591-5.

24. Dyer, M.A., S.M. Farrington, D. Mohn, J.R. Munday, and M.H. Baron, Indian hedgehog activates hematopoiesis and vasculogenesis and can respecify prospective neurectodermal cell fate in the mouse embryo*. Development*, 2001. 128(10): 1717-30.
25. Jones, E.A., D. Crotty, P.M. Kulesa, C.W. Waters, M.H. Baron, S.E. Fraser, and M.E. Dickinson, Dynamic in vivo imaging of postimplantation mammalian embryos using whole embryo culture*. Genesis*, 2002. 34(4): 228-35.
26. Dirnagl, U., A. Villringer, and K.M. Einhaupl, In-vivo confocal scanning laser microscopy of the cerebral microcirculation*. Journal of Microscopy*, 1992. 165(Pt 1): 147-57.
27. Phoon, C.K., O. Aristizabal, and D.H. Turnbull, Spatial velocity profile in mouse embryonic aorta and Doppler-derived volumetric flow: a preliminary model*. Am J Physiol Heart Circ Physiol*, 2002. 283(3): H908-16.
28. Fahraeus, R. and T. Lindqvist, The viscosity of blood in narrow capillary tubes. *Am J Physiol*, 1931. 99: 563-568.
29. Chien, S., S. Usami, H.M. Taylor, J.L. Lundberg, and M.I. Gregersen, Effects of hematocrit and plasma proteins on human blood rheology at low shear rates*. J Appl Physiol*, 1966. 21(1): 81-7.

30. Lipowsky, H.H., S. Usami, and S. Chien, In vivo measurements of "apparent viscosity" and microvessel hematocrit in the mesentery of the cat. *Microvasc Res*, 1980. 19(3): 297-319.

31. McGrath, K.E., A.D. Koniski, J. Malik, and J. Palis, Circulation is established in a stepwise pattern in the mammalian embryo. *Blood*, 2003. 101(5): 1669-76.

32. Topper, J.N. and M.A. Gimbrone, Jr., Blood flow and vascular gene expression: fluid shear stress as a modulator of endothelial phenotype. *Mol Med Today*, 1999. 5(1): 40-6.

33. Lindahl, P., B.R. Johansson, P. Leveen, and C. Betsholtz, Pericyte loss and microaneurysm formation in PDGF-B-deficient mice. *Science*, 1997. 277(5323): 242-5.

34. Crosby, J.R., K.A. Tappan, R.A. Seifert, and D.F. Bowen-Pope, Chimera analysis reveals that fibroblasts and endothelial cells require platelet-derived growth factor receptorbeta expression for participation in reactive connective tissue formation in adults but not during development. *Am J Pathol*, 1999. 154(5): 1315-21.

35. Dickson, M.C., J.S. Martin, F.M. Cousins, A.B. Kulkarni, S. Karlsson, and R.J. Akhurst, Defective haematopoiesis and vasculogenesis in transforming growth factor-beta 1 knock out mice. *Development*, 1995. 121(6): 1845-54.

36. Goumans, M.J., A. Zwijsen, M.A. van Rooijen, D. Huylebroeck, B.A. Roelen, and C.L. Mummery, Transforming growth factor-beta signalling in extraembryonic mesoderm is required for yolk sac vasculogenesis in mice. *Development*, 1999. 126(16): 3473-83.

37. Yang, X., L.H. Castilla, X. Xu, C. Li, J. Gotay, M. Weinstein, P.P. Liu, and C.X. Deng, Angiogenesis defects and mesenchymal apoptosis in mice lacking SMAD5. *Development*, 1999. 126(8): 1571-80.

38. Shalaby, F., J. Rossant, T.P. Yamaguchi, M. Gertsenstein, X.F. Wu, M.L. Breitman, and A.C. Schuh, Failure of blood-island formation and vasculogenesis in Flk-1-deficient mice. *Nature*, 1995. 376(6535): 62-6.

39. Yamaguchi, T.P., D.J. Dumont, R.A. Conlon, M.L. Breitman, and J. Rossant, Flk-1, a flt-related receptor tyrosine kinase is an early marker for endothelial cell precursors. *Development*, 1993. 118(2): 489-98.

40. Chiu, J.J., D.L. Wang, S. Chien, R. Skalak, and S. Usami, Effects of disturbed flow on endothelial cells. *J Biomech Eng*, 1998. 120(1): 2-8.

41. Davies, P.F., A. Remuzzi, E.J. Gordon, C.F. Dewey, Jr., and M.A. Gimbrone, Jr., Turbulent fluid shear stress induces vascular endothelial cell turnover in vitro. *Proc Natl Acad Sci USA*, 1986. 83(7): 2114-7.

42. Huang, C., F. Sheikh, M. Hollander, C. Cai, D. Becker, P.H. Chu, S. Evans, and J. Chen, Embryonic atrial function is essential for mouse embryogenesis cardiac morphogenesis and angiogenesis. 2003.

43. Phoon, C.K., O. Aristizabal, and D.H. Turnbull, 40 MHz Doppler characterization of umbilical and dorsal aortic blood flow in the early mouse embryo*. Ultrasound in Med & Biol.*, 2000. 26(8): 1275-1283.

44. Usami, S., V. Magazinovic, S. Chien, and M.I. Gregersen, Viscosity of turkey blood: rheology of nucleated erythrocytes*. Microvascular Research*, 1970. 2(4): 489-99.

Figure 1. Line Scanning Image to Measure of Blood Flow. Line scans were performed perpendicular to the direction of blood flow on transgenic embryos that express GFP in their primitive erythroid cells [24]. The white line represents the location of the scans within an x-y image of the yolk sac (A). The green fluorescence represents red blood cells and the red color is cell tracker orange staining used to visualize the vessel walls. Line scanning at this location yields a L vs. t image (B). Several measurements were made on these L- vs. t images. They include the L- and t- location of the beginning of the streak, the L- and t- dimensions of the streak, and the diameter of the streak (C).

Figure 2. Confocal Image of Primitive Red Blood Cells Showing Spherical Shape. A confocal z-series was taken of red blood cells in 8.5 dpc (A) and 10.5 dpc (B) transgenic embryo that expresses GFP in primitive erythroblasts, to confirm their spherical shape. Both an x-y frame and an x-z frame are shown. For the 8.5 dpc, slices were taken at 40x magnification and were 0.2 μm apart with a total of 145 slices. The 10.5 dpc embryo was imaged using a 63x lens and the slices were 0.83 μm apart with a total of 20 slices. The 8.5 dpc image has been digitally zoomed 150% to bring it onto the same scale as the 10.5 dpc image.

Figure 3. Comparison of Velocities at Different Embryonic Stages. The velocity of the blood flow versus vessel diameter was plotted for 8.5 dpc (A), 9.5 dpc (B) and 10.5 dpc (C) embryos. Vmax represents the maximum velocity during the pulses, which was calculated by regressing the velocity profile according to a parabolic profile.

Figure 4. Imaging Flow Pattern Within the Vessels. An L. vs. t image of the line scanning across two vessels (A) shows blood cells moving uni-directionally in one vessel

(left), indicating the presence of a laminar flow and re-circulating in the other vessel (right), indicating the presence of an eddy within the flow. The velocity of blood in a vessel with steady, unidirectional flow was plotted both in systole and diastole (B) with regard to position within the blood vessel. The velocity shows a parabolic profile that fits the expected shape for laminar flow.

Figure 5. Hematocrit Measurements from the Line Scans. The average hematocrit was plotted with respect to age (A) and shows a slight increase. The hematocrit vs. diameter was plotted (B) for a typical 10.5 dpc embryo. The plot exhibits the Fahraeus-Lindqvist effect for blood flow in small tubes.

Figure 6. Shear Stress Values. Shear stress was calculated in vessels of different size at 3 stages of development. Data from older embryos (E9.5 and E10.5) increases with increasing diameter. Shear stress values before the capillary plexus has remodeled (E8.5) however, are more scattered, showing no defined pattern.

Figure 7. Blood Flow Velocity Changes With Heart Development. The measured velocity vs. time was plotted for embryos at stage 8.5 dpc (A), 9.5 dpc (B) and 10.5 dpc (C). The pulse is visible at all ages; however, it becomes more discrete as embryos develop.

Figure 1

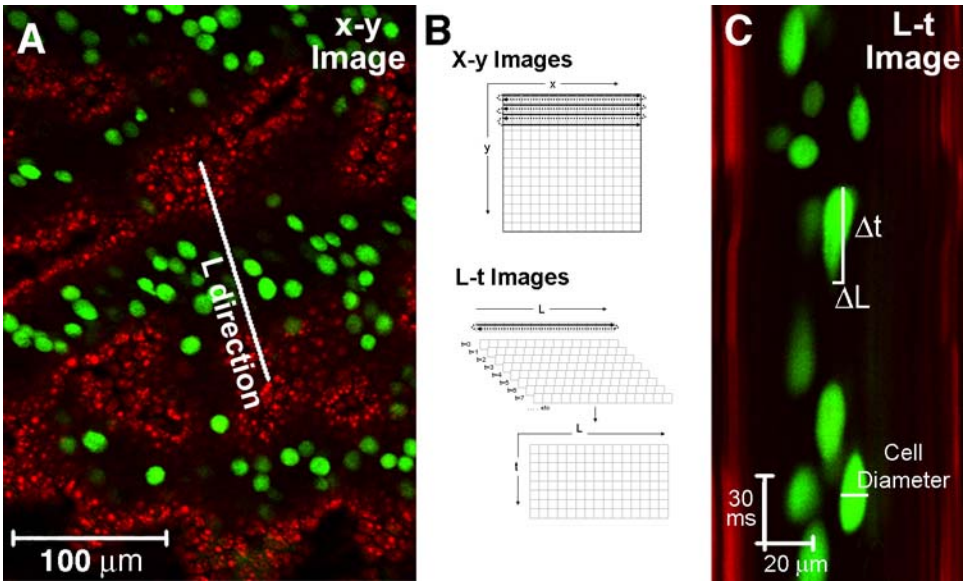
A
x-y Image
L direction
100 µm
B
X-y Images
x
y
L-t Images
L
t
C
L-t Image
Δt
ΔL
Cell Diameter
30 ms
20 µm

Figure 2

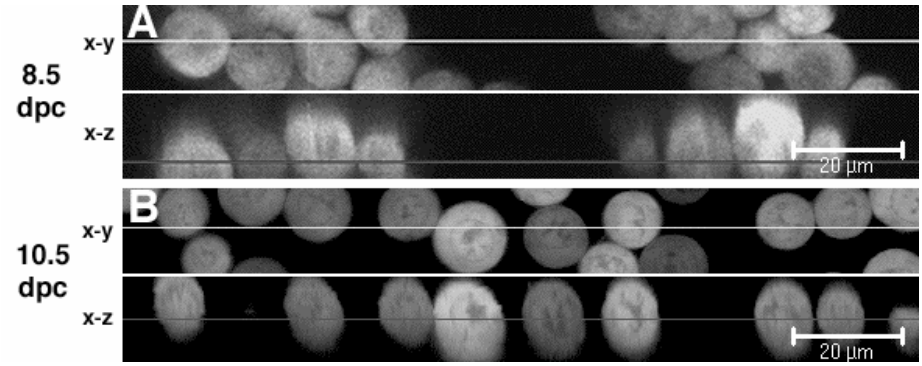

Figure 3

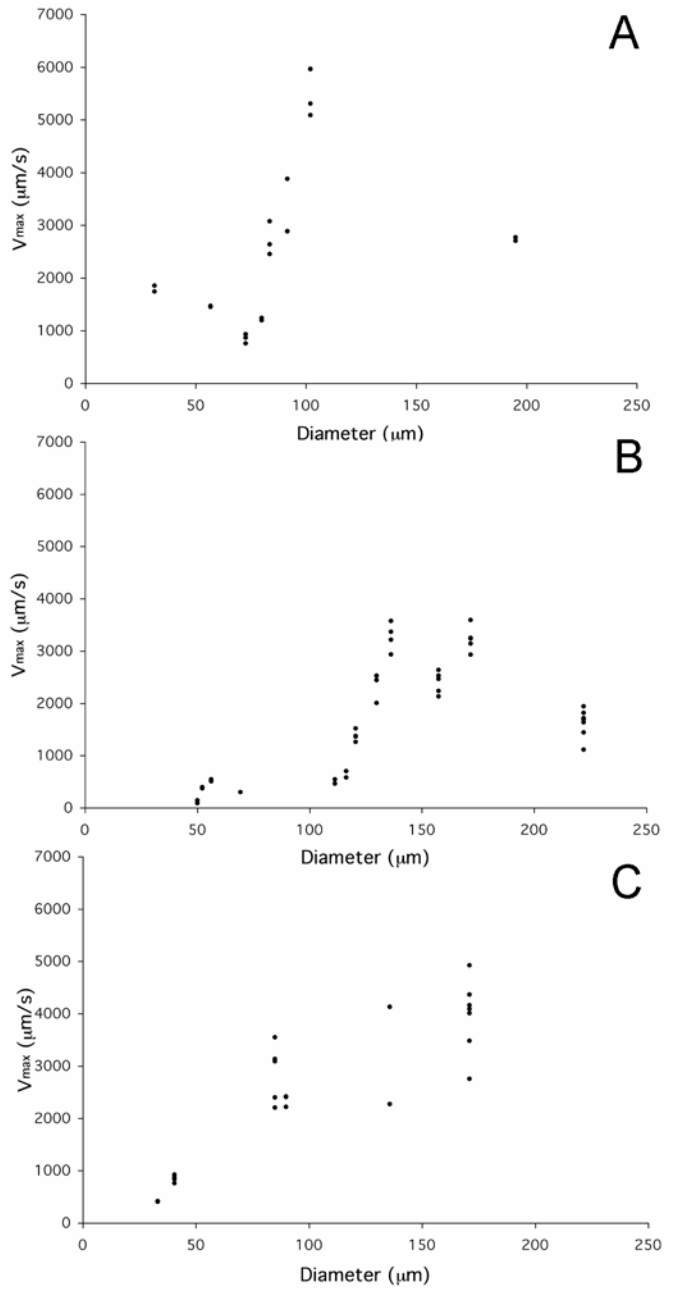
A
B
C
Vmax (μm/s)
Diameter (μm)
0
1000
2000
3000
4000
5000
6000
7000
0
50
100
150
200
250

Figure 4

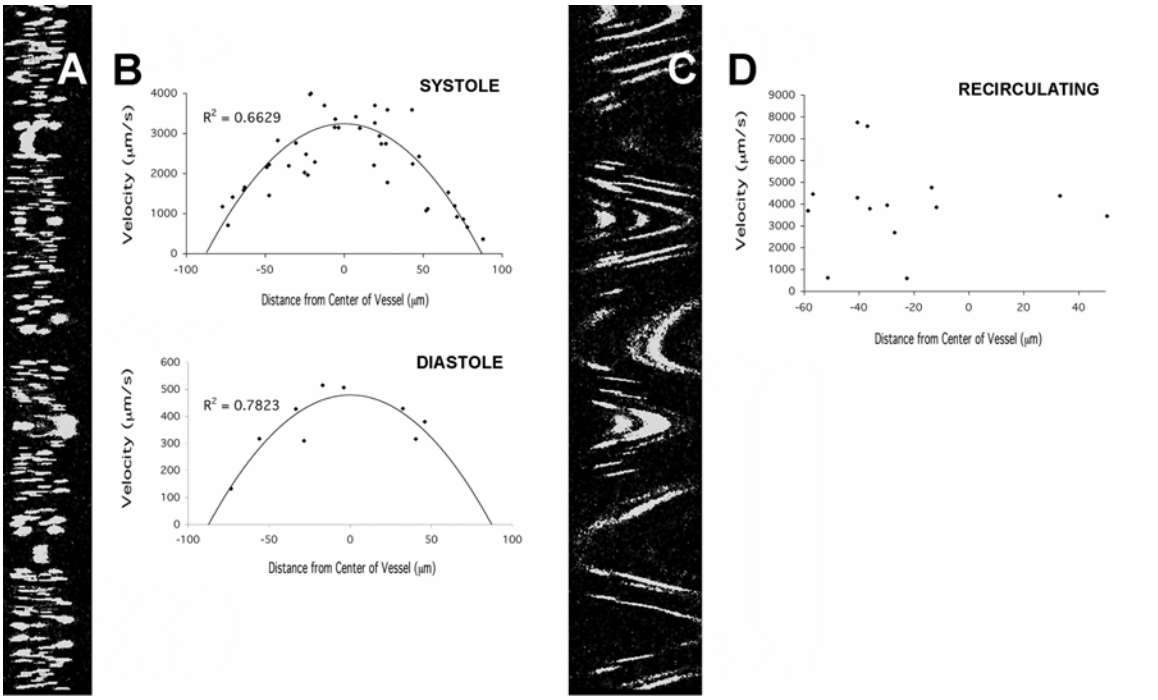
A
B
SYSTOLE
R^2 = 0.6629
Velocity (μm/s)
Distance from Center of Vessel (μm)
DIASTOLE
R^2 = 0.7823
Velocity (μm/s)
Distance from Center of Vessel (μm)
C
D
RECIRCULATING
Velocity (μm/s)
Distance from Center of Vessel (μm)

Figure 5

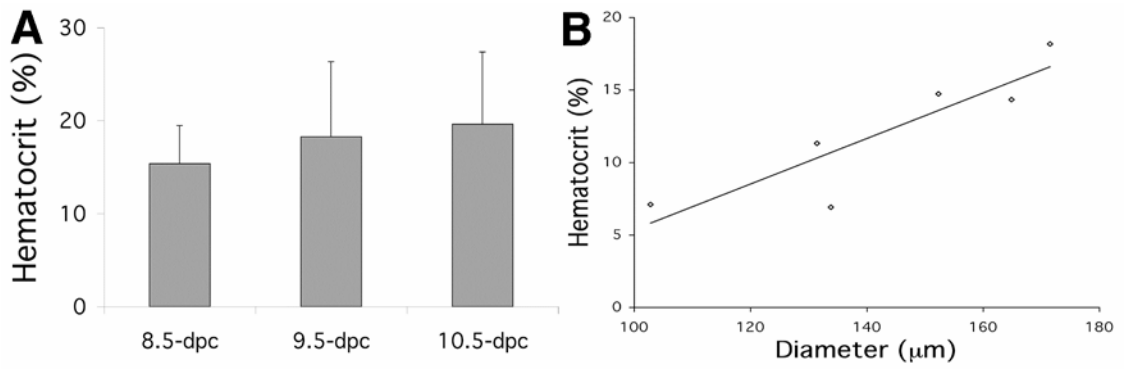
A
Hematocrit (%)
30
20
10
0
8.5-dpc
9.5-dpc
10.5-dpc
B
Hematocrit (%)
20
15
10
5
0
100
120
140
160
180
Diameter (μm)

Figure 6

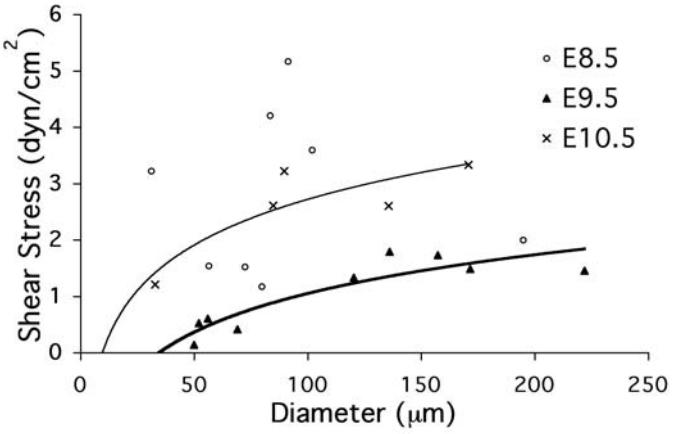
Shear Stress (dyn/cm^2)
Diameter (μm)
E8.5
E9.5
E10.5
0
1
2
3
4
5
6
0
50
100
150
200
250

Figure 7

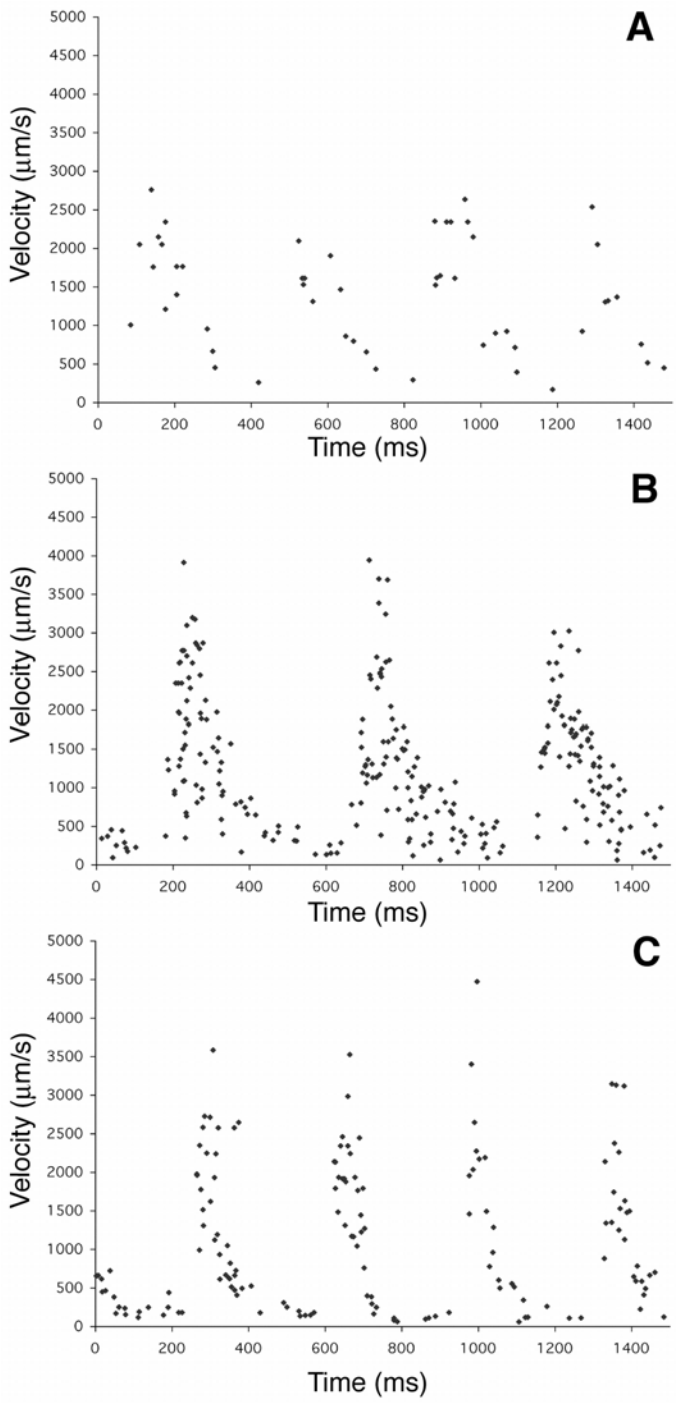
A
B
C
Velocity (µm/s)
Time (ms)
0
500
1000
1500
2000
2500
3000
3500
4000
4500
5000
0
200
400
600
800
1000
1200
1400

Chapter 4

Initiation of Circulation and Vascular Remodeling in Mammalian Embryos.

Summary

The role of hemodynamics, or blood fluid dynamics, in cardiovascular development remains controversial. It is known that early event in angiogenesis and vascular remodeling are dependent on blood flow, however, mechanisms for the induction of remodeling by blood flow have not been established. Mechanical cues, such as shear stress, are imparted on early endothelial cells by blood flow. The timing of initiation of vascular remodeling, the exact onset of blood flow and the relationship between these two events must be considered together in order to understand what signaling cues are available to the vasculature to initiate remodeling. Here we analyze the initiation of blood flow using a transgenic mouse that expresses GFP in primitive erythroblasts and measure the shear stress levels when circulation is first established. We show that both morphological changes in the vasculature and the appearance of molecular markers of remodeling correlate to periods of high shear stress.

Introduction

Formation of a functional vascular system is a critical and complex process. During murine development, both vasculogenesis and hematopoesis begin in the extra-embryonic yolk sac. Angioblasts and primitive erythroblasts first appear at E7.0 [1, 2], initially forming together in blood islands, and are thought to form from a common precursor, the hemangioblast, that derives from the primitive streak of the embryo proper [1, 3, 4]. As the population of endothelial precursors expands through the yolk sac, cells aggregate and interconnect to form angioblastic cords [5], which then form intracellular lumens [6], creating a channel for blood flow. This honeycomb-shaped network of blood vessels that connects the embryo to the yolk sac is known as the capillary plexus.

A vital step in the development of the embryo is the remodeling of the yolk sac capillary plexus. On a gross level, vascular remodeling is characterized by both changes in vessel size and in branch angles between vessels [7]. Some vessels regress, while others are transformed from small caliber vessels to large ones. The remodeling process occurs quickly; the most prominent changes are apparent within twenty-four hours in both chick and mouse embryos. In mutant strains, embryos that fail to undergo remodeling die between E10.5 and E11.5, two to three days after the onset of blood flow [8-12]. Mutations that effect vascular remodeling can be grouped into two distinct categories, mutations in

genes that function directly in endothelial cells and precursors [9-11], and mutations that effect heart function [8, 12]. It has been hypothesized that vascular defects in the second class of mutants occur because of abnormal blood flow patterns. This idea is supported by several studies that show that blood flow is necessary for proper vascular development. If the heart is removed [13] or the outflow of the heart is blocked [14, 15], remodeling does not occur. Thus, vascular remodeling in the yolk sac depends both on genetic and epigenetic signaling events, but little is known about how these pathways are related.

In vitro studies performed with cultured endothelial cells show that these cells are able to sense mechanical force such as shear stress (for review, see [16]), a tangential force imported on the vessel wall by the flowing blood. Shear stress can cause cells to align to direction of flow [17] and can activate signaling pathways that are important for cardiovascular development [18-22]. Identifying when these mechanical cues are first present and whether the levels are consistent with those shown to act as signals is essential for understanding how mechanical cues relate to vascular remodeling.

Though flow is essential, exactly when erythroblasts begin circulating is not firmly established. Primitive erythroblasts have been observed outside the blood islands in fixed embryos at four somites although it is not known if they had been

actively circulating before fixation [23]. Using Doppler Ultrasound, flow has been observed as early as the 7 somite stage [24], however, it is not clear if this method has enough resolution necessary to measure the initiation of slow flows in small caliber vessels. Because remodeling is at least partially dependent on proper blood flow, it is essential to establish the precise time when flow begins.

In this paper, we have used high-resolution, confocal time-lapse microscopy to ascertain the precise stage at which blood flow begins, to measure changes in shear stress in yolk sac vessels and to define dynamic changes in vessels soon after flow begins. We show that primitive erythroblasts enter into circulation (7-10 somite stage) after a prolonged period of plasma flow that begins as soon as the heart starts beating (3 somite stage). By measuring the levels of shear stress in the early yolk sac, we show that endothelial cells are exposed to a transient rise in shear stress soon after erythroblasts begin circulating. Furthermore, cellular changes associated with remodeling (vessel regression, changes in vessel orientation and expression of junction and support cell markers) occur coincident with peak levels of shear stress. By developing a timeline of events using methods with high temporal and spatial resolution, it is possible to establish which developmental changes are related to flow and those that are independent. From these studies, it is clear that vascular remodeling initiates just after erythroblasts enter circulation, suggesting that forces produced by flow signal changes in vascular morphology.

Results

Initiation of Blood Flow

To determine the series of events in early circulation, we took confocal time-lapse images of epsilon-globin: GFP transgenic embryos starting at approximately the 6 somite stage (Movie 1, Figure 1). During the first hour of the time-lapse movie, the heart beats but no circulating erythroblasts are seen (Figure 1A, H). A single immobile erythroblast is visible within one of the vessels (red arrow, Figure 1A), however, the rest of the blood remains in the blood islands (outside the field of view). As erythroblasts begin to enter the circulation, the hematocrit, or volume percentage of red blood cells in vessels, is initially low and fluctuates from one frame to another (Figure 1B). The initial immobile erythroblast remains stationary for 3.5 hours as other erythroblasts circulate in adjacent vessels. Finally, all erythroblasts within the field of view are circulating, increasing the hematocrit within individual vessels.

To verify the results from our time-lapse analysis, we examined several litters of live embryos at early somite stages to determine precisely when circulating blood cells were observed (Table I). Until the 4 somite stage, erythroblasts are mainly confined to the blood islands. Isolated erythroblasts were occasionally observed outside the blood islands and even in the dorsal aorta from the 4-6 somite stage agreeing with previously published results [23], but these cells were immobile

and were not actively circulating. Primitive erythroblasts are not found moving continuously throughout the capillary plexus until the 7 or 8-somite stage. Hence, the presence of erythroblasts outside the blood islands at early stages (4-6 somites) was not a reliable indicator of erythroblast circulation, which begins at 7-8 somites.

Once circulation begins, the circulating fraction of erythroblasts steadily increases. Both the change in hematocrit as well as improvement in heart performance will dramatically affect the mechanical forces acting on endothelial cells. Thus, we measured shear stress in the embryonic vessels using confocal line scanning as described in Jones *et al.* 2004 (Chapter 3, Figure 2). At 8 somites, a significant systole and diastole is not present within the blood flow and hematocrit fluctuates. Therefore, it is necessary to use average shear stress measurements based on the location of the erythroblast within the vessel. From 10 somites onward, peak shear stress during systole is reported. The highest measured shear stress occurs at the 11 somite stage, with shear stress levels reaching 3.2 dyn/cm^2 (Figure 2). These levels remain high until the 13 somite stage. After this stage, there is a reduction in shear stress and a smaller range of values in any given embryo. When the data is plotted with respect to diameter, shear stress is related to vessel size after this point (data not shown), as previously reported for E9.5 and E10.5 embryos [25].

Presence of Plasma Flow

Our data from above clearly indicates that erythroblasts do not begin to circulate until the 7-8 somite stage, yet the heart starts beating at the 3 somite stage (Table 1). Since a functioning pump is present, we tested whether plasma circulation could be detected prior to the flow of erythroblasts. Fluorescent dextran was injected into the heart of the early stage embryos (Figure 3). Embryos were allowed to recover only ten minutes after injection and then were imaged to determine if the dextran spreads through the plexus. A ten minute incubation period prevents the vessels from filling by diffusion such that the presence of fluorescence in the yolk sac can only be explained by fluid flow. In 0 and 1 somite stage embryos, injected dextran remained confined to the site of injection in the heart (data not shown). In most embryos at the 2 somite stage, dextran did not flow into the yolk sac (5 of 6 embryos, Figure 3A-B), but flow was observed in one embryo at this stage (Figure 3D-E). From 3 somites onward, dextran reliably filled the capillary plexus in the ten minutes following injection into the heart (20 of 20 embryos; Figure 3C & F).

To confirm the presence of plasma flow in early vessels, we used Fluorescence Recovery After Photobleaching (FRAP) (for review, see [26]). For this method, the plexus is filled with fluorescent dextran and a 100μm^2 area is bleached within a fluorescent field of view. The recovery of fluorescence in the bleached area is

measured to calculate the rate of diffusion. When flow is present, the apparent diffusion coefficient, referred to here as the perfusion coefficient, is much higher than in the case of pure diffusion. To determine the pure diffusion coefficient in the absence of flow, FRAP was performed using in embryos where the heart beat was intentionally arrested. Dextran diffused at 51 $\mu m^2/s$ (n=8, std dev= 21) in embryonic blood plasma at 37°C. From the 3 somite stage onward, perfusion coefficients were an order of magnitude higher than measurements for pure diffusion (Figure 4A). By 6 somites, some flows were too fast to be measured by FRAP. The variability of plasma flow measurements are likely to relate to the proximity to the heart (Figure 4B). These experiments establish that there is circulation between the embryo and the yolk sac by the 3 somite stage, long before the embryonic blood contains primitive erythroblasts.

Timing of Remodeling Events

To understand how early hemodynamic events relate to remodeling, we investigated when remodeling of the vasculature was first apparent using molecular markers. ZO-1 is a protein that is localized at cell-cell junctions and is upregulated in endothelial cells exposed to pressure [27]. Immunostaining for ZO-1 indicates that intercellular junctions between endothelial cells increases by the 13 somite stage (Figure 5A-C, red). Endothelial cells lining the blood vessels express much higher levels of ZO-1 than surrounding mesenchyme, and cell

shapes are elongated in the direction of the blood vessel (Figure 5B). Before this time, ZO-1 staining can be seen in cuboidal endoderm cells in the yolk sac (Figure 5A).

Another step in the remodeling process is the recruitment of support cells, smooth muscle cells and pericytes. Using an antibody to α-smooth muscle actin, α-SMA (Figure 5D-F, red), we examined when support cells first appear. α-SMA positive cells are not apparent in the yolk sac of 11 somite embryos (Figure 5D). The first α-SMA positive cells appear at 13 somites in loose clusters within the mesenchyme (Figure 5E). α-SMA positive support cells do not appear fully differentiated until E9.5, at which time they surround major vessels (Figure 5F).

The markers that we have used above establish that there are clear changes in endothelial and support cells that occur coincident with the onset of peak shear stress flow. To examine these dynamic events more closely, we used time-lapse imaging of embryos expressing GFP in endothelial cells under the control of the Tie-2 promoter [28]. Coincident with the entry of erythroblasts into the circulation, dynamic changes occur in the vascular plexus (Figure 6, Movie 2, embryo is initially at 8 somites). The endothelial marker, Tie-2, is not strong enough at early somite stages, but dextran injections show no significant changes in vascular morphology until blood cells start flowing (data not shown). At the start of the time-lapse sequence, large vascular spaces are present

separated by small avascular regions. Within several minutes of the start of the movie, avascular spaces enlarge as vessels become more defined. Most vessels reduce in diameter, with some vessels regressing almost completely (arrow, Figure 6A-D). Though vessels regress during this period, no vessel sprouting can be seen. Cell divisions within endothelial cells are prevalent, as can be seen by the bright dividing nuclei (asterick, Figure 6C, D). Cells appear to remain associated with neighbors during divisions.

In order to quantify changes in early vessels, the average vessel diameter (Figure 6E), the branch angle between vessels (Figure 6F) and the long axis of the avascular regions, called Feret's diameter (Figure 6G), were measured from the frames of the time-lapse movie. The average diameter reduces during the angiogenic process, with larger changes occurring early (within the first 4 hours) in the time-lapse movie. The growth of the avascular space, as measured by Feret's diameter, occurs at a regular, linear pace. The branch angle between vessels, however, did not change significantly during the time-lapse sequence indicating that, at least initially vessel morphology is modified without significant changes in the branch pattern.

Discussion

The Initiation of Circulation

Linking changes in blood flow with changes in vascular morphology is critical to understanding the role of hemodynamics in vessel remodeling. In this work, we have established the precise timeline for blood flow between the embryo and the yolk sac and we have discovered that blood flow starts in two phases, an initial plasma flow phase (3 somites) which presumably is low viscosity and low shear stress, and a later higher viscosity, peak shear stress erythroblast circulation phase (7-10 somites) (Figure 8). We find that the earliest morphological changes in vessel structure, judged by cellular dynamics and molecular markers, occur coincident with the onset of erythroblast circulation. We also show that there is transient peak in shear stress following the entry of blood cells into circulation, suggesting that the initiation of vascular remodeling events is related to changes in shear stress.

The high-resolution, dynamic methods that we employed have allowed us to both observe when flows begin as well as quantify the velocity of flows. Previous studies assumed that flow began at 4 somites, because blood cells were found in the embryo [23]. We also observed a number of non-circulating, globin-positive erythroblasts adjacent to vessel walls in the yolk sac and the embryo at the 4-6 somite stage, but these cells were stationary and possibly differentiated in situ.

While it is generally assumed that most blood cells form in the blood islands, others have shown that endothelial cells isolated from the yolk sac can give rise to hematopoetic lineages [29]. Our data is consistent with the presence of hemogenic endothelium in the early yolk sac and embryo.

Dynamic Morphological Changes Related to Remodeling

We have shown that several key morphological changes in vessel structure occur directly after erythroblasts enter into circulation. Using time-lapse imaging, we have shown that there is a dynamic reduction in the average vessel diameter in the early plexus, despite obvious cell proliferation. Decreasing vessel diameter correlates with the appearance of ZO-1 expression in endothelial cells suggesting the decrease in vessel diameter results from cells forming tight junctions with their neighbors. Close associations between endothelial cells are necessary to prevent fluid from leaking from the vessel walls, an important event in remodeling.

Mechanical vs. Biochemical Signals

Instead of providing mechanical stimulus, blood flow could be necessary for remodeling because key signaling molecules are delivered to early vessels. The data presented here show that plasma circulation, capable of carrying nutrients, proteins and small molecule signals, is established for many hours before overt signs of remodeling are observed. While it is still formally possible that the

release of signaling molecules into the circulation is a precisely timed event, the data presented here show a strong correlation between the initiation of remodeling and the entry of erythroblasts into circulation, suggesting that this transition is necessary for vascular remodeling to begin. Though it is unlikely that paracrine signals induce remodeling, plasma flow could carry factors that have a role in priming or sensitizing the endothelial cells to react to later stimuli.

The Role of Mechanical Forces in Early Development

Quantitative measurements of shear stress levels in early vessels show a transient peak in shear stress soon after cells enter the circulation. The levels of shear stress are highest as the capillary plexus initiates remodeling and correlate strongly with morphological change in the plexus. Shear stress is capable of regulating the expression of many proteins, some of which are known to be essential for proper cardiovascular development [30]. For instance several studies have shown that shear stress can induce the transcription of Flk-1, a tyrosine kinase receptor for Vascular Endothelial Growth Factor (VEGF) [31], as well as activate the receptor and cause nuclear translocation [20]. Flk-1 is involved in the initial formation of hematopoetic and endothelial cell lineages in the embryo [1, 2]. Because early cell differentiation is disrupted in Flk-1 null mutant embryos, its role in remodeling is poorly understood. Interestingly, recent evidence from ES cell differentiation studies indicates that the proliferation of Flk-1+ cells was dramatically increased upon exposure to low levels of shear stress,

1.5 dyn/cm^2 [32]. These studies showed that it was the shear stress and not shear rate which affected proliferation of Flk1 positive cells. Shear rate is dependent only on the velocity of the fluid, whereas shear stress is dependent on both shear rate and viscosity. We find that changes in vascular morphology correlate with the entry of erythroblasts into circulation which dramatically affects fluid viscosity and hence, the shear stress. Thus, it is possible that the proliferation of Flk-1+ cells in the yolk sac depend on shear stress signals. Proliferating Tie-2 positive cells are clearly seen at the onset of flow (Figure 1; Movie 1).

In addition to Flk-1 signaling, transcription of PDGF signaling molecules have also been shown to be modified by shear stress. PDGF can act as a smooth muscle mitogen [33] and mutants in components of the PDGF signaling pathway have significantly reduced numbers of α-SMA-positive support cells that are needed for vessel stabilization [34, 35]. mRNA transcription of PDGF is graded with respect to shear stress in endothelial cells exposed to levels between 0 and 6 dyn/cm^2, but constant at higher shear stress [36]. Recent studies have also shown that abrupt changes in shear stress may be even more instructive to endothelial cells than chronic shear stress [37] and PDGF-A is differentially regulated by step increases in shear stress as compared to gradual increases in shear stress [38]. Here we have shown that α-SMA positive cells appear in the yolk sac by 11 somites, at times when shear stress levels are at a transient peak

(~3.5 dyn/cm^2). Soon after, support cells are recruited to surround vessels in the yolk sac. Thus, shear stress may induce the transcription of PDGF, which then recruits the migration of peripheral cell types toward the vessel.

Although there is a strong correlation between shear stress and the initiation of remodeling, it is likely that this is not the only mechanical force involved in remodeling. Endothelial cells are also known to respond to circumferential strain, a perpendicular force caused by fluid pressure (for review, see [39]). Circumferential strain can increase cell-cell junctions [40] and can cause the upregulation of junction proteins such as ZO-1 [27]. Thus, an increase in pressure could be responsible for some of the dynamic events in remodeling that we have described; however, it is not currently feasible to measure pressure levels in such small vessels making it difficult to test this hypothesis.

Blood Flow in Vessel Patterning and Arterio-Venous Differentation

The role of fluid dynamics in vascular development has also been studied in other systems such as in Avians and in Zebrafish [41, 42]. It is generally accepted that the initial pattern of the vasculature is laid down without influence from flow dynamics. We studied Flk1 expression in the early embryos and found that Flk1 positive cells were present throughout the yolk sac by the 3 somite stage and lined vessels when plasma flow is initiated (data not shown). These results agree with data from chick, zebrafish and mouse showing that the pre-

pattern of endothelial lined vessels is present before the onset of flow [5, 43-45]. Thus, the initial patterning of vessels is not determined by fluid flow; however, as suggested above, the subsequent control of proliferation, vessel growth, and regression which are needed for remodeling are likely to depend on fluid derived forces.

Since even low levels of plasma flow are present by 3 somites, it is essential to re-investigate whether arterio-venous (A-V) differentiation is genetically pre-determined. By our staging criteria many markers of A-V identity are not expressed until after erythroblasts circulate, well after plasma circulation has begun. EphrinB2, an arterial marker, is expressed in the heart and dorsal aorta, but not yet in the yolk sac, at the 7 somite stage. Notch4 expression, another arterial marker, is restricted to the heart, vitelline vein and dorsal aorta in the 3 to 5 somite mouse embryo [46]. Interestingly, one would expect the dorsal aorta and heart, the first locations of A-V markers, to experience relatively high pressure from plasma flow as compared to the yolk sac. Thus, the temporal correlation between fluid flow and the expression of these markers needs to be re-examined before it can be determined if A-V identity is determined prior to flow and thus, is purely genetically determined.

Conclusions

Here we have shown that the initiation of vascular remodeling coincides with the entry of erythroblasts into circulation; an event that is preceded by a significant period of plasma flow. These data do not show that shear stress provides a necessary signal for remodeling, but by building a timeline of hemodynamic and morphological events during remodeling, we can constrain our model and focus on those events that are likely to depend on fluid flow. Currently, we are exploring ways to alter hemodynamic properties to test how cells respond to these changes and to build a better understanding of the events that are necessary for proper vessel remodeling.

Materials And Methods

Dissection and Embryonic Culture

Breeding pairs of mice were mated overnight. The presence of a vaginal plug in the morning was taken as 0.5 dpc. Embryos were collected on the morning of the eight day and cultured as previously described [47]. ImageJ software (http://rsb.info.nih.gov/ij/) was used to calculate the Feret's diameter for avascular spaces on images to which a black and white threshold was applied. Objects that were smaller than the area of 2 erythroblasts (less than 200 μm^2) were ignored since some erythroblasts do not express GFP. Average diameter and average branch angle was measured using Adobe Photoshop.

Shear Stress Calculations

Embryos were dissected and placed in culture media and allowed to recover for one hour in the incubator. They were then transferred to the heated microscope stage. An initial image at 20x magnification was taken and the location of the velocity measurement marked. The laser line was set to line scanning mode, and the single laser line across a vessel was scanned repeatedly for 3000 lines. The amount of time that an erythroblast is imaged is directly related to the velocity of the erythroblast, as previously described [25].

Dye Injection

After dissection, embryos were allowed to recover in dissecting media for 30 minutes. A pulled quartz needle (Sutter Instruments) was filled with 10,000 MW Texas Red dextran or fluorescein dextran (Molecular Probes, No. D-1828 and D-1281, respectively) and a picospritzer II (General Valve Corp.) was used to inject small volumes of dye into the heart tube. Embryos were then returned to the incubator for 10 minutes before imaging.

Fluorescence Recovery After Photobleaching

Embryos were injected with 10,000MW fluorescein dextran (Molecular Probes, No. D-1821), and transferred to Nunc Lab-Tek chambers (No. 155380) with culture media. The embryos were allowed to recover in a tissue incubator for an hour, to ensure that dye was present in all vessels and that heart rates were normal. The microscope (Zeiss LSM5 PASCAL) was preheated to 37°C using a heater box [47]. Using a 20x lens, an initial image of the plexus was taken, and the location of the bleach marked. Scan speeds were set to 100 msec per frame and the aperture was set fully open. The region of interest was scanned repeatedly at 10% laser power to obtain initial fluorescence levels. The laser power was increased to 100% to bleach. The laser power was subsequently

returned to 10% and 500-600 frames were collected. Embryos were transferred to separate wells and somites were counted.

Mean fluorescence with respect to time for the region of interest was exported to a spreadsheet. The recovery curve was fit to the equation:

$$\frac{F(t)-F_0}{F_F-F_0} = e^{\frac{-2\tau}{t}}\left(I_0\left(\frac{2\tau}{t}\right)+I_1\left(\frac{2\tau}{t}\right)\right),$$

where F(t) is the fluorescence intensity, F_0 is the initial post-bleach fluorescence intensity, F_F is the final level of fluorescence recovery, I_0 and I_1 are zeroth and first order Bessel's Functions, and τ is the characteristic diffusion time.

The bleach area was divided by characteristic diffusion time to give the measured diffusion rate. This is subsequently referred to as a perfusion rate since flow is present.

Immunohistochemical Staining

For ZO-1 staining, embryos were fixed overnight in methanol:DMSO (4:1), and then stored in methanol. Embryos were rehydrated and blocked with 2% nonfat dried milk in PBS. Embryos were incubated overnight at 4°C with primary

antibodies (Zymed, No. 61-7300) at a 1:100 dilution with dried milk in PBS. Embryos were washed with 0.5% Triton and 2% nonfat dried milk in 10mM Tris. Embryos were incubated overnight at 4°C with secondary antibodies (Molecular Probes, No. A-11009) and then washed.

For staining of α-SMA, embryos were fixed in 4% PFA overnight at 4°C. Embryos were washed 4-5 times with 0.1% Triton in PBS and then incubated overnight at 4°C with fluorescently conjugated primary antibodies (Sigma, No. C6198) at 1:100 dilution in 0.1% Triton. Embryos were washed 4-5 times, for 1 hour each.

Acknowledgments

We thank Chris Waters for technical support and Joaquin Gutierrez for assistance in animal husbandry. This work was supported by the Human Frontiers Science Program (RG0146/2000-B102), the American Heart Association (0315023Y) and NIH (R01 HL078694). We also thank the Powell foundation for the partial support of this work through the Option of Bioengineering at Caltech.

References

1. Yamaguchi, T.P., D.J. Dumont, R.A. Conlon, M.L. Breitman, and J. Rossant, Flk-1, a flt-related receptor tyrosine kinase is an early marker for endothelial cell precursors*. Development*, 1993. 118(2): 489-98.
2. Shalaby, F., J. Rossant, T.P. Yamaguchi, M. Gertsenstein, X.F. Wu, M.L. Breitman, and A.C. Schuh, Failure of blood-island formation and vasculogenesis in Flk-1-deficient mice*. Nature*, 1995. 376(6535): 62-6.
3. Huber, T.L., V. Kouskoff, H.J. Fehling, J. Palis, and G. Keller, Haemangioblast commitment is initiated in the primitive streak of the mouse embryo*. Nature*, 2004. 432(7017): 625-30.
4. Kallianpur, A.R., J.E. Jordan, and S.J. Brandt, The SCL/TAL-1 gene is expressed in progenitors of both the hematopoietic and vascular systems during embryogenesis*. Blood*, 1994. 83(5): 1200-8.
5. Ferkowicz, M.J., M. Starr, X. Xie, W. Li, S.A. Johnson, W.C. Shelley, P.R. Morrison, and M.C. Yoder, CD41 expression defines the onset of primitive and definitive hematopoiesis in the murine embryo*. Development*, 2003. 130(18): 4393-403.
6. Haar, J.L. and G.A. Ackerman, A phase and electron microscopic study of vasculogenesis and erythropoiesis in the yolk sac of the mouse*. Anat Rec*, 1971. 170(2): 199-223.
7. Risau, W., Mechanisms of angiogenesis*. Nature*, 1997. 386(6626): 671-4.

8. Tanaka, M., Z. Chen, S. Bartunkova, N. Yamasaki, and S. Izumo, The cardiac homeobox gene Csx/Nkx2.5 lies genetically upstream of multiple genes essential for heart development. *Development*, 1999. 126(6): 1269-80.

9. Wang, H.U., Z.F. Chen, and D.J. Anderson, Molecular distinction and angiogenic interaction between embryonic arteries and veins revealed by ephrin-B2 and its receptor Eph-B4. *Cell*, 1998. 93: 741-753.

10. Krebs, L.T., J.R. Shutter, K. Tanigaki, T. Honjo, K.L. Stark, and T. Gridley, Haploinsufficient lethality and formation of arteriovenous malformations in Notch pathway mutants. *Genes Dev*, 2004. 18(20): 2469-73.

11. Fischer, A., N. Schumacher, M. Maier, M. Sendtner, and M. Gessler, The Notch target genes Hey1 and Hey2 are required for embryonic vascular development. *Genes Dev*, 2004. 18(8): 901-11.

12. Huang, C., F. Sheikh, M. Hollander, C. Cai, D. Becker, P.H. Chu, S. Evans, and J. Chen, Embryonic atrial function is essential for mouse embryogenesis, cardiac morphogenesis and angiogenesis. *Development*, 2003. 130(24): 6111-9.

13. Chapman, W.B., The effect of the heart-beat upon the development of the vascular system in the chick. *Am. J. Anat.*, 1918. 23: 175-203.

14. Hogers, B., M.C. DeRuiter, A.C. Gittenberger-de Groot, and R.E. Poelmann, Unilateral vitelline vein ligation alters intracardiac blood flow

patterns and morphogenesis in the chick embryo*. Circ Res*, 1997. 80(4): 473-81.

15. Wakimoto, K., K. Kobayashi, O.M. Kuro, A. Yao, T. Iwamoto, N. Yanaka, S. Kita, A. Nishida, S. Azuma, Y. Toyoda, K. Omori, H. Imahie, T. Oka, S. Kudoh, O. Kohmoto, Y. Yazaki, M. Shigekawa, Y. Imai, Y. Nabeshima, and I. Komuro, Targeted disruption of Na+/Ca2+ exchanger gene leads to cardiomyocyte apoptosis and defects in heartbeat*. J Biol Chem*, 2000. 275(47): 36991-8.
16. Resnick, N., H. Yahav, A. Shay-Salit, M. Shushy, S. Schubert, L.C.M. Zilberman, and E. Wofovitz, Fluid shear stress and the vascular endothelium: for better and for worse*. Prog Biophys Mol Biol.*, 2002. 81(3): 177-99.
17. Dewey, C.F., Jr., S.R. Bussolari, M.A. Gimbrone, Jr., and P.F. Davies, The dynamic response of vascular endothelial cells to fluid shear stress*. J Biomech Eng*, 1981. 103(3): 177-85.
18. Resnick, N., T. Collins, W. Atkinson, D.T. Bonthron, C.F. Dewey, Jr., and M.A. Gimbrone, Jr., Platelet-derived growth factor B chain promoter contains a cis-acting fluid shear-stress-responsive element. *Proc Natl Acad Sci USA*, 1993. 90(10): 4591-5.
19. Feng, Y., V.J. Venema, R.C. Venema, N. Tsai, and R.B. Caldwell, VEGF induces nuclear translocation of Flk-1/KDR, endothelial nitric oxide

synthase, and caveolin-1 in vascular endothelial cells. *Biochem Biophys Res Commun*, 1999. 256(1): 192-7.

20. Shay-Salit, A., M. Shushy, E. Wolfovitz, H. Yahav, F. Breviario, E. Dejana, and N. Resnick, VEGF receptor 2 and the adherens junction as a mechanical transducer in vascular endothelial cells. *Proc Natl Acad Science USA*, 2002. 99(14): 9462-7.
21. Lee, H.J. and G.Y. Koh, Shear stress activates Tie2 receptor tyrosine kinase in human endothelial cells. *Biochem Biophys Res Commun*, 2003. 304(2): 399-404.
22. Shyy, J.Y. and S. Chien, Role of integrins in endothelial mechanosensing of shear stress. *Circ Res*, 2002. 91(9): 769-75.
23. McGrath, K.E., A.D. Koniski, J. Malik, and J. Palis, Circulation is established in a stepwise pattern in the mammalian embryo. *Blood*, 2003. 101(5): 1669-76.
24. Ji, R.P., C.K. Phoon, O. Aristizabal, K.E. McGrath, J. Palis, and D.H. Turnbull, Onset of cardiac function during early mouse embryogenesis coincides with entry of primitive erythroblasts into the embryo proper. *Circ Res*, 2003. 92(2): 133-5.
25. Jones, E.A., M.H. Baron, S.E. Fraser, and M.E. Dickinson, Measuring hemodynamic changes during mammalian development. *Am J Physiol Heart Circ Physiol*, 2004. 287(4): H1561-9.

26. Lippincott-Schwartz, J. and G.H. Patterson, Development and use of fluorescent protein markers in living cells*. Science*, 2003. 300(5616): 87-91.

27. DeMaio, L., J.M. Tarbell, R.C. Scaduto, Jr., T.W. Gardner, and D.A. Antonetti, A transmural pressure gradient induces mechanical and biological adaptive responses in endothelial cells*. Am J Physiol Heart Circ Physiol*, 2004. 286(2): H731-41.

28. Motoike, T., Loughna, S., Perens, E., Roman, B.L., Liao, W., Chau, T.C., Richardson, C.D., Kawate, T., Kuno, J., Weinstein, B.M., Stainier, D.Y. & Sato, T.N., Universal GFP reporter for the study of vascular development. *Genesis*, 2000. 28: 75-81.

29. Nadin, B.M., M.A. Goodell, and K.K. Hirschi, Phenotype and hematopoietic potential of side population cells throughout embryonic development*. Blood*, 2003. 102(7): 2436-43.

30. Garcia-Cardena, G., J. Comander, K.R. Anderson, B.R. Blackman, and M.A. Gimbrone, Jr., Biomechanical activation of vascular endothelium as a determinant of its functional phenotype*. Proc Natl Acad Sci USA*, 2001. 98(8): 4478-85.

31. Chen, K.D., Y.S. Li, M. Kim, S. Li, S. Yuan, S. Chien, and J.Y. Shyy, Mechanotransduction in response to shear stress. Roles of receptor tyrosine kinases, integrins, and Shc*. J Biol Chem*, 1999. 274(26): 18393-400.

32. Yamamoto, K., T. Sokabe, T. Watabe, K. Miyazono, J.K. Yamashita, S. Obi, N. Ohura, A. Matsushita, A. Kamiya, and J. Ando, Fluid Shear Stress Induces Differentiation of Flk-1-Positive Embryonic Stem Cells into Vascular Endothelial Cells In Vitro. *Am J Physiol Heart Circ Physiol*, 2004.

33. Berk, B.C., R.W. Alexander, T.A. Brock, M.A. Gimbrone, Jr., and R.C. Webb, Vasoconstriction: a new activity for platelet-derived growth factor. *Science*, 1986. 232(4746): 87-90.

34. Soriano, P., Abnormal kidney development and hematological disorders in PDGF beta-receptor mutant mice. *Genes Dev*, 1994. 8(16): 1888-96.

35. Leveen, P., M. Pekny, S. Gebre-Medhin, B. Swolin, E. Larsson, and C. Betsholtz, Mice deficient for PDGF B show renal, cardiovascular, and hematological abnormalities. *Genes Dev*, 1994. 8(16): 1875-87.

36. Hsieh, H.J., N.Q. Li, and J.A. Frangos, Shear stress increases endothelial platelet-derived growth factor mRNA levels. *Am J Physiol*, 1991. 260(2 Pt 2): H642-6.

37. White, C.R., M. Haidekker, X. Bao, and J.A. Frangos, Temporal gradients in shear, but not spatial gradients, stimulate endothelial cell proliferation. *Circulation*, 2001. 103(20): 2508-13.

38. Bao, X., C. Lu, and J.A. Frangos, Temporal gradient in shear but not steady shear stress induces PDGF-A and MCP-1 expression in endothelial cells: role of NO, NF kappa B, and egr-1. *Arterioscler Thromb Vasc Biol*, 1999. 19(4): 996-1003.

39. Lehoux, S. and A. Tedgui, Signal transduction of mechanical stresses in the vascular wall. *Hypertension*, 1998. 32(2): 338-45.

40. Suttorp, N., T. Hessz, W. Seeger, A. Wilke, R. Koob, F. Lutz, and D. Drenckhahn, Bacterial exotoxins and endothelial permeability for water and albumin in vitro. *Am J Physiol*, 1988. 255(3 Pt 1): C368-76.

41. Isogai, S., N.D. Lawson, S. Torrealday, M. Horiguchi, and B.M. Weinstein, Angiogenic network formation in the developing vertebrate trunk. *Development*, 2003. 130(21): 5281-90.

42. le Noble, F., D. Moyon, L. Pardanaud, L. Yuan, V. Djonov, R. Matthijsen, C. Breant, V. Fleury, and A. Eichmann, Flow regulates arterial-venous differentiation in the chick embryo yolk sac. *Development*, 2004. 131(2): 361-75.

43. Fouquet, B., B.M. Weinstein, F.C. Serluca, and M.C. Fishman, Vessel patterning in the embryo of the zebrafish: guidance by notochord. *Dev Biol*, 1997. 183(1): 37-48.

44. Eichmann, A., C. Marcelle, C. Breant, and N.M. Le Douarin, Two molecules related to the VEGF receptor are expressed in early endothelial cells during avian embryonic development. *Mech Dev*, 1993. 42(1-2): 33-48.

45. Drake, C.J. and P.A. Fleming, Vasculogenesis in the day 6.5 to 9.5 mouse embryo. *Blood*, 2000. 95(5): 1671-9.

46. Shirayoshi, Y., Y. Yuasa, T. Suzuki, K. Sugaya, E. Kawase, T. Ikemura, and N. Nakatsuji, Proto-oncogene of int-3, a mouse Notch homologue, is expressed in endothelial cells during early embryogenesis. *Genes Cells*, 1997. 2(3): 213-24.

47. Jones, E.A., D. Crotty, P.M. Kulesa, C.W. Waters, M.H. Baron, S.E. Fraser, and M.E. Dickinson, Dynamic in vivo imaging of postimplantation mammalian embryos using whole embryo culture. *Genesis*, 2002. 34(4): 228-35.

48. Dyer, M.A., S.M. Farrington, D. Mohn, J.R. Munday, and M.H. Baron, Indian hedgehog activates hematopoiesis and vasculogenesis and can respecify prospective neurectodermal cell fate in the mouse embryo. *Development*, 2001. 128(10): 1717-30.

Tables

Table I – Expansion of blood islands and onset of erythroblast circulation

Somite stage	**0-2**	**3**	**4**	**5**	**6**	**7**	**8**	**9**	**10**	**11**
Average Heart Rate (bpm)	**0**	**18**	**32**	**38**	**36**	**40**	**38**	**53**	**60**	**64**
Blood islands only	6	3	3	3						
Some expansion proximal to blood islands			1	2	2					
Extensive blood island expansion				3	4	1				
Some flow, in distal yolk sac				1		8	5	3	1	
Full flow present							3	5	6	4
Total (number of embryos observed)	6	3	4	8	6	9	8	8	7	4

Figure 1 – Time-Lapse of the Initiation of Erythroblast Circulation. The initiation of erythroblast circulation was followed using time-lapse microscopy (Movie2) in an embryo expressing GFP (green) in its erythroblasts [48]. The embryo starts at 6 somites, before erythroblasts circulate. The time-lapse is focused on the yolk sac (YS), and the heart (H) and somites (S) can be seen. Erythroblasts enter circulation within 11 frames. Images were taken every 6 minutes at 10x magnification on a Zeiss LSM5 PASCAL for a total of 12.1 hrs.

Figure 2 – Shear Stress with Respect to Somite Stage. Shear stress was calculated using confocal line scanning [25]. Shear stresses are highest, up to 3.5 dyn/cm^2, during the initial stages of vascular remodeling between 10 and 13 somites.

Figure 3 – Dextran Injection Into The Cardiac Crescent. 10,000MW fluorescent dextran was injected into the heart (Hrt) of embryos at various stages. The embryos were incubated for 10 minutes, and imaged to determine when dextran would fill the yolk sac capillary plexus (YS) by plasma flow. Examples of plexus that do not fill (A & B, arrow) and that do fill (D & E, arrow) at the 2 somite stage are shown. Head folds (HF) are also visible. The plexus fills consistently from 3 somites onward (3 somites, C; 7 somites, F).

Figure 4 – Perfusion Coefficients Measured Using FRAP. Fluorescence Recovery After Photobleaching (FRAP) was used to calculate perfusion coefficients within the early embryonic blood vessels to assess the presence of

flow with respect to somite stage (A). The wide range of perfusion coefficients is thought to arise from the more or less tortuous paths of flow through the yolk sac between the heart and dorsal aorta (B).

Figure 5 – Antibody Staining of Remodeling Markers. Antibodies stain for ZO-1 (red, A-C) and α-SMA (red, D-F) in the vasculature of the yolk sac at 11 somites (A, D), 13 somites (B, E) and 21-29 somites (C, F). Erythroblasts that express GFP (green) are also present. ZO-1 initially highlights cell-cell junctions in all tissues, but becomes elevated in endothelial cells by 13 somites. The expression becomes significantly higher in endothelial cells than surrounding tissues by E9.5 (F). α-SMA stains for the recruitment of peripheral cells and can first be observed at 13 somites (E). By E9.5 (F), α-SMA positive cells envelope the large vessels of the yolk sac.

Figure 6 – Time-Lapse of Microvascular Remodeling. Endothelial cells of the yolk sac were followed through time-lapse microscopy (A-D, Movie 1) using a transgenic mouse that expresses GFP (green) in its endothelial cells [28]. The embryo is initially at 8 somites stage. Vessel diameters reduce and endothelial cells divide during remodeling (bright spots). Images were taken every 10 minutes at 10x magnification on a Zeiss LSM5 PASCAL for a total of 11.7 hrs. The average vessels diameter (E), Feret's diameter for the avascular region (F) and the branch angle between vessels (G), was followed through the frames to assess changes in morphology.

Figure 7 – Model of Cardiovascular Development. As the heart begins contracting at 3 somites, it induces flow of the primordial plasma. The flow increases in magnitude and by 7 somites, erythroblasts begin entering the circulation. At 9 somites, remodeling of the vascular network begins. Shear stress levels are high when erythroblasts first circulate, but begin to reduce at the 13 somite stage.

Figure 1

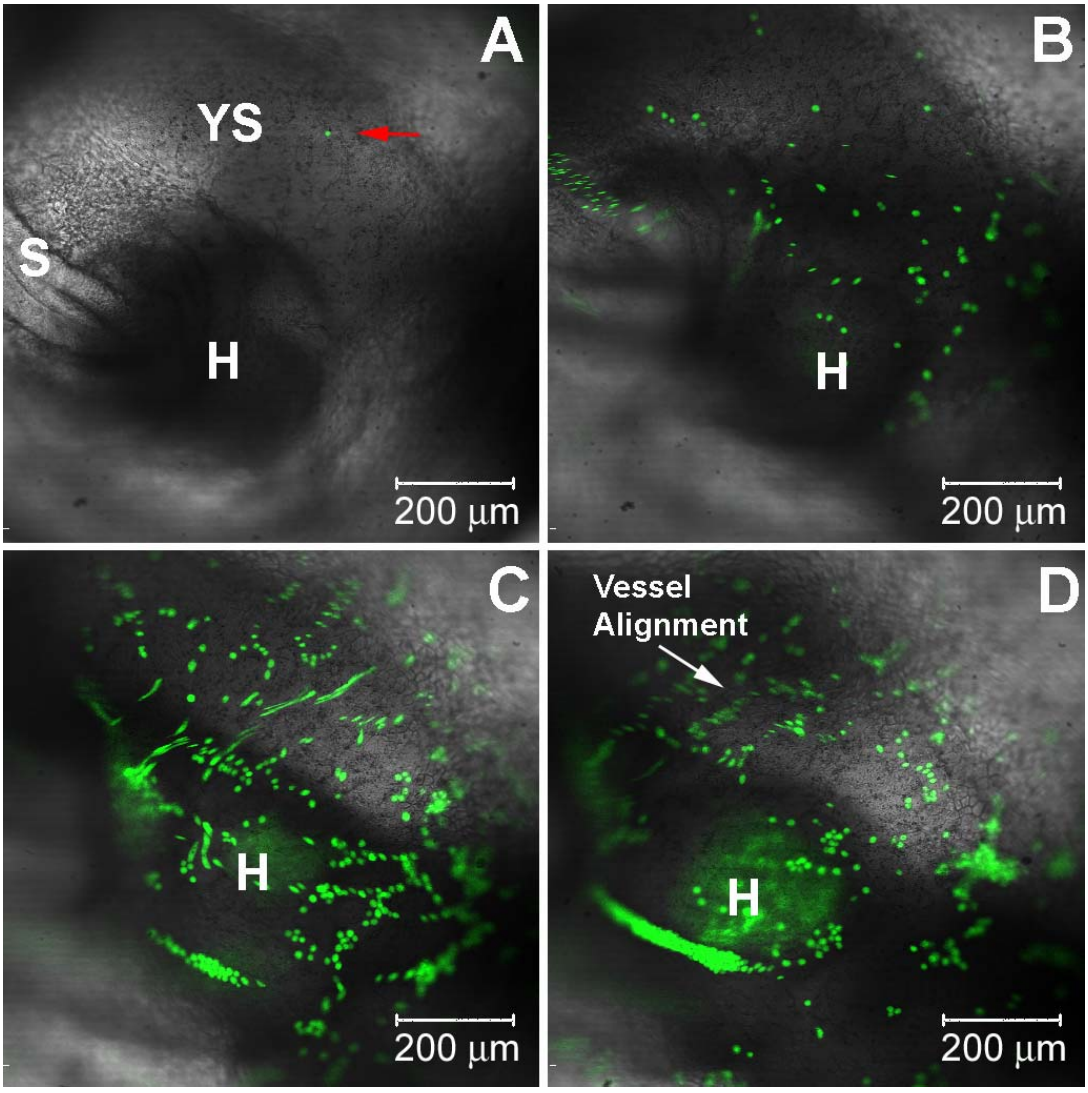

Figure 2

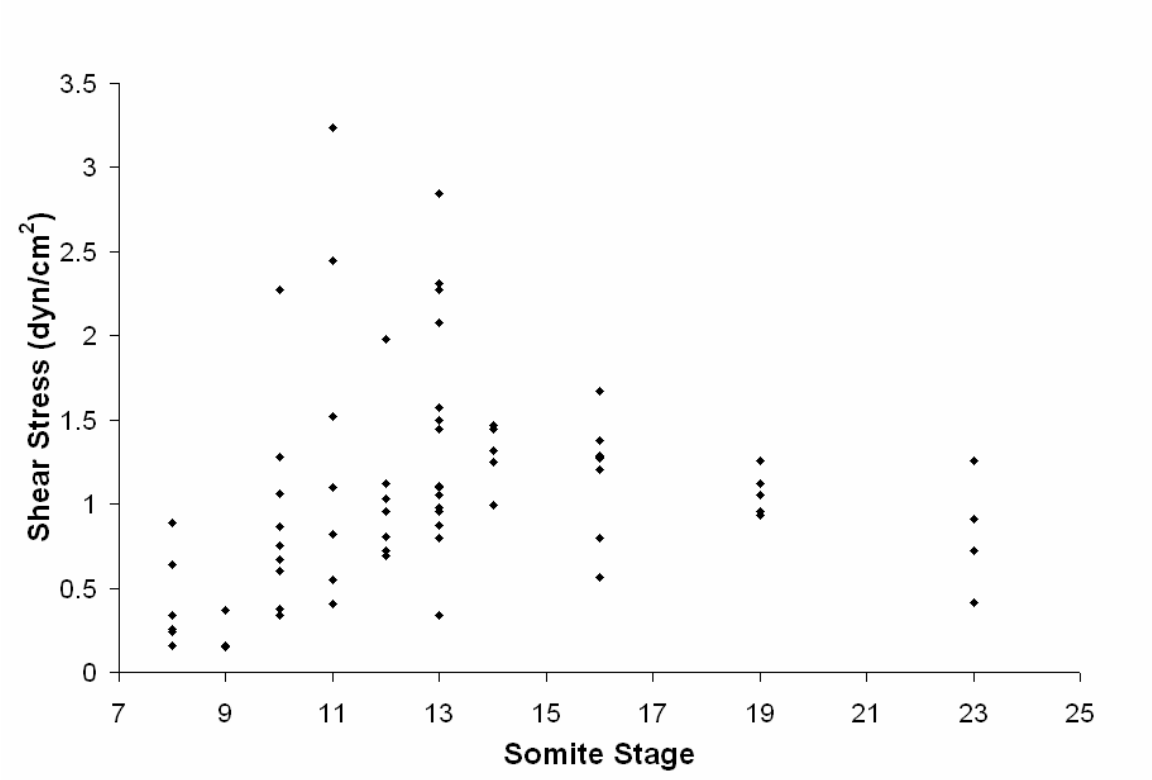
Shear Stress (dyn/cm^2)
3.5
3
2.5
2
1.5
1
0.5
0
7
9
11
13
15
17
19
21
23
25
Somite Stage

Figure 3

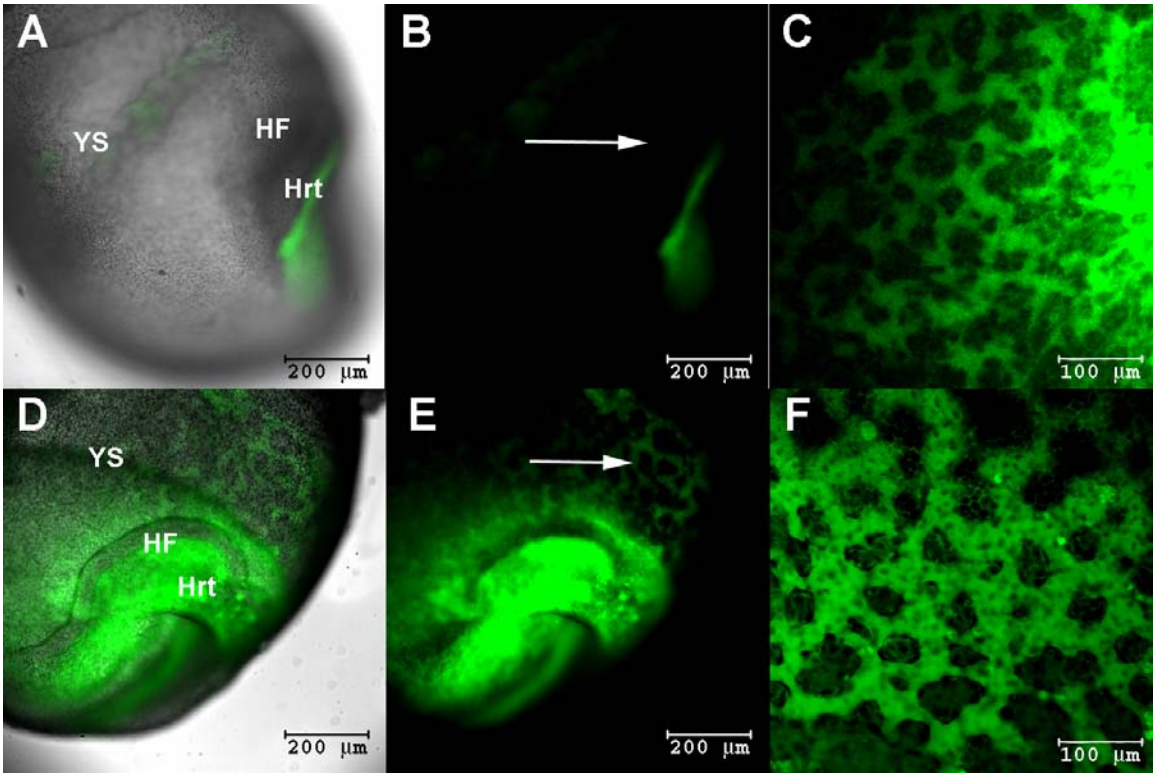
A
YS
HF
Hrt
200 µm
B
200 µm
C
100 µm
D
YS
HF
Hrt
200 µm
E
200 µm
F
100 µm

Figure 4

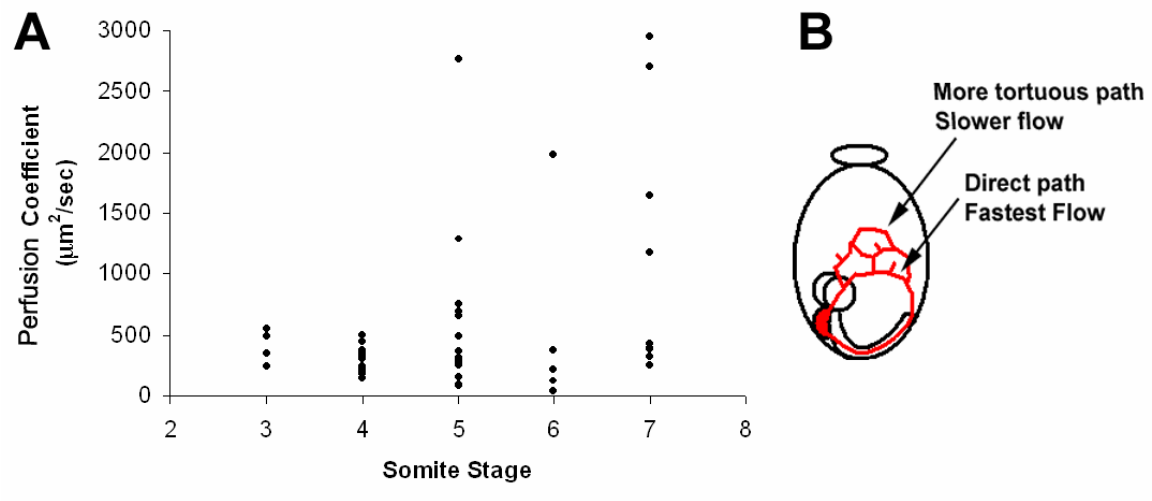
A
Perfusion Coefficient
(μm²/sec)
3000
2500
2000
1500
1000
500
0
2
3
4
5
6
7
8
Somite Stage
B
More tortuous path
Slower flow
Direct path
Fastest Flow

Figure 5

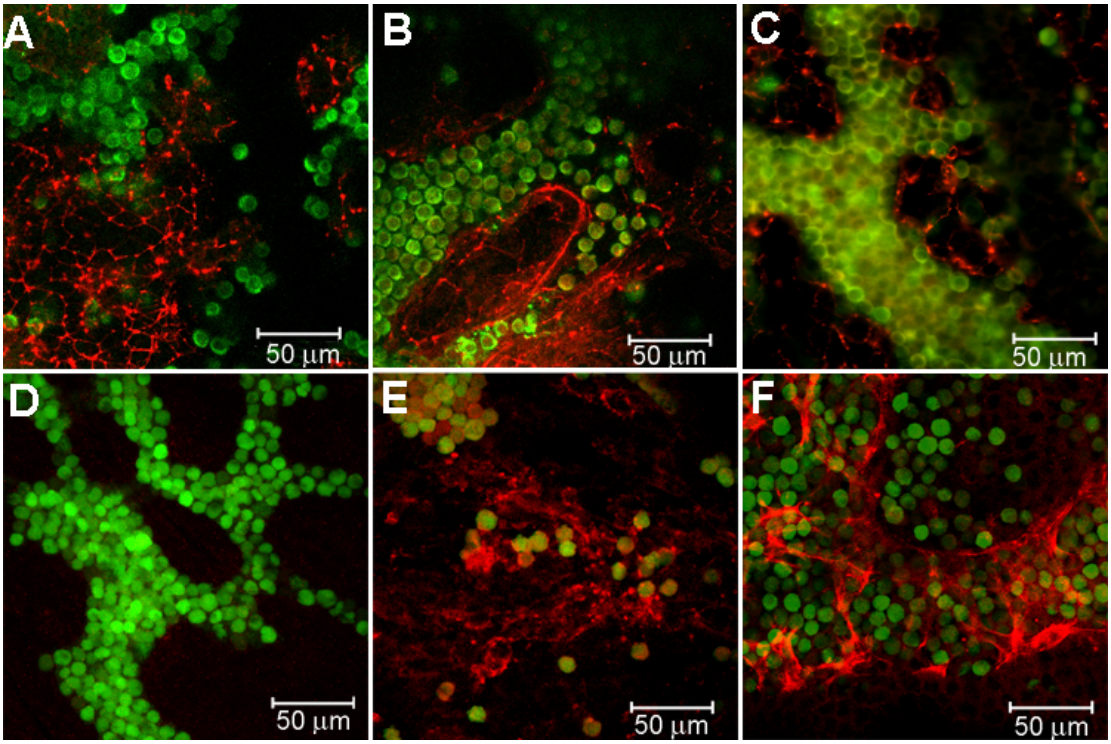

Figure 6

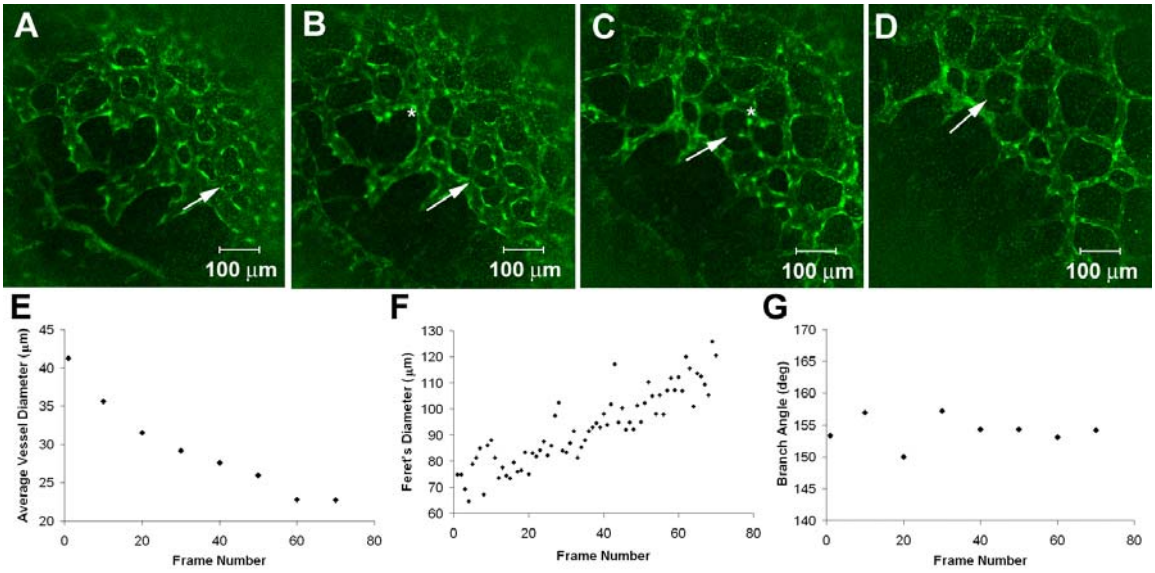
A
B
C
D
100 µm
100 µm
100 µm
100 µm
E
Average Vessel Diameter (µm)
Frame Number
F
Feret's Diameter (µm)
Frame Number
G
Branch Angle (deg)
Frame Number

Figure 7

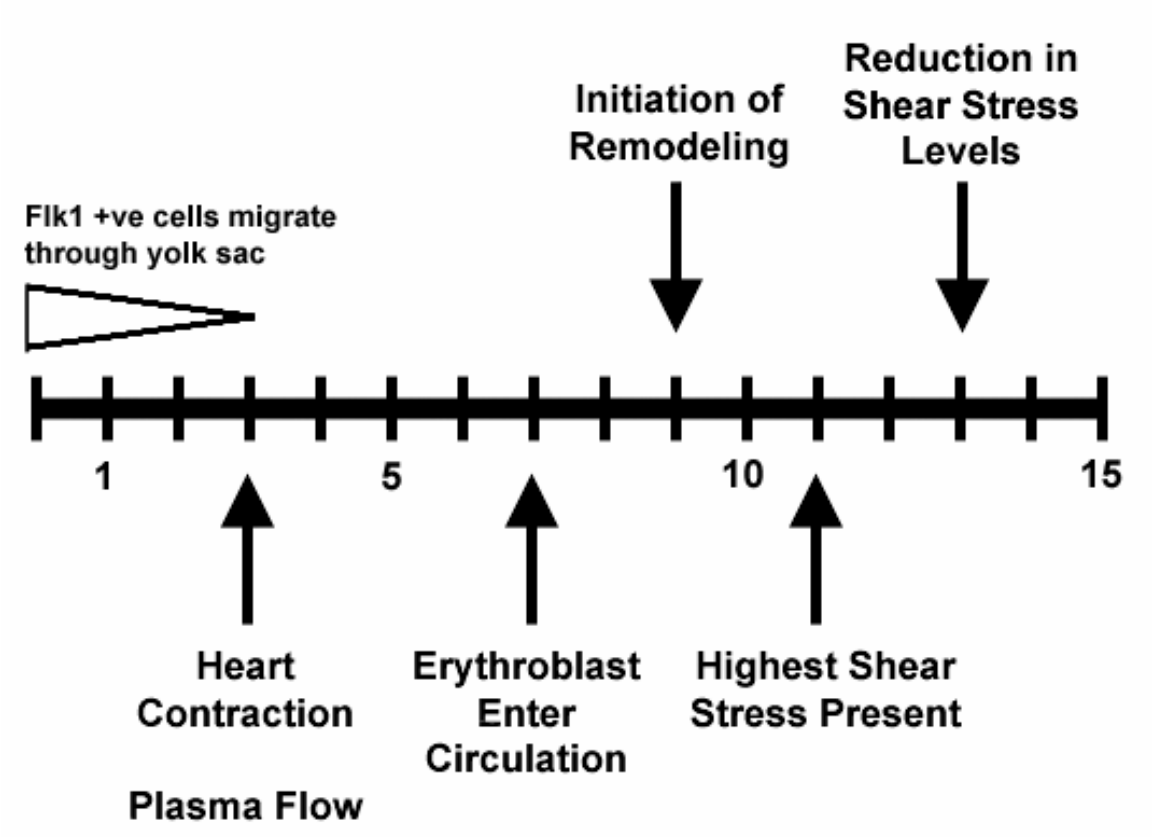
Reduction in Shear Stress Levels
Initiation of Remodeling
Flk1 +ve cells migrate through yolk sac
1
5
10
15
Heart Contraction
Erythroblast Enter Circulation
Highest Shear Stress Present
Plasma Flow

Chapter 5

Hemodynamic Analysis of MLC2a Knockout Phenotype.

Summary

Many cardiovascular mutants exist in which the embryonic vascular plexus fails to remodel due to altered cardiac function. Vascular defects are assumed to be secondary to cardiac defects, due to altered fluid dynamics in the vasculature. Presumably, the altered flow produced in these mice is unable to induce proper mechanical signaling within the vasculature and this mechanical signaling is required to initiate vascular remodeling. This hypothesis, however, has not been tested because of the difficulty in measuring fluid dynamic aspects of the phenotypes. Using a transgenic mouse that expresses GFP in primitive erythroblasts, we characterize hemodynamic inefficiencies in Myosin Light Chain 2a knock-out mice. Null mutations in MLC2a result in a specific heart defect; atrial contraction of the heart is silent, but the ventricle can beat normally. We find that these mice exhibit increased oscillatory flow, decreased plasma flow velocities and a failure of erythroblasts to enter the circulation. In order to link the flow phenotype to the vascular deficiencies, we have phenocopied individual aspects of the hemodynamic insufficiencies in order to establish the importance of the individual flow defects to vascular remodeling and link these to changes in proliferation and protein expression. We show that it is not only important for flow to be present, but that viscous flow, as provided by the entry of erythroblast into circulation, is essential for proper vascular remodeling.

Introduction

The early embryonic vasculature is established through two processes: vasculogenesis, which consists of de novo formation of blood vessels, and angiogenesis, which involves both the remodeling of existing vessels and the sprouting of new vessels [1]. The first site of vasculogenesis in the mouse is the yolk sac and this process consists of the specification of angiogenic cells, and subsequently of the migration and interconnection of these angiogenic cells leading to the formation of a honeycomb-shaped network of blood vessels known as the vascular plexus. During angiogenesis, the early plexus remodels to form a network resembling more mature vasculature with larger vessels branching to form progressively smaller vessels. The remodeling process happens quickly, with the most prominent changes occurring within twenty-four hours in both chick and mouse embryos, and is critical to embryonic survival, such that embryos that fail to remodel die as early as E10.5 (for example, see [2-6]). Remodeling involves changes in vessel morphology and recruitment of peripheral cell types [7]. The mechanism through which remodeling occurs, however, is poorly understood.

Remodeling of the vascular plexus is dependent on the presence of blood flow. When the heart is removed [8, 9] or prevented from beating [5], remodeling does not occur. Gene ablation studies in mouse have shown that disrupting early heart function can lead to vascular defects in the yolk sac as well. Mutations in several genes, including $Ncx1^{-/-}$ [5], $MEF2c^{-/-}$ [10], $Cx45^{-/-}$ [4], $MLC2a^{-/-}$ [11], and $Titin^{-/-}$ [12] all show a failure in yolk sac remodeling due to poor circulation. In one such study, the vascular abnormalities caused by the deletion of N-cadherin were rescued by cardiac specific expression of

either N- or E-cadherin [13] indicating that the vascular defects were secondary to the heart defects and probably due to abnormal blood flow.

While it is well accepted that proper blood flow is required for remodeling of the vascular plexus, it is not known what aspect of blood flow is necessary. Blood serves as an oxygen and nutrient carrier and improper flow could result in increased hypoxia or nutrient starvation. Flowing blood also produces mechanical forces on the endothelial cells, such as shear stress which is a force tangential to the endothelial cells, and pressure which is a force perpendicular to the endothelial cells. It is known that endothelial cells can perceive both these forces and such mechanical triggers are able to induce changes in gene expression within endothelial cells (for review, see [14]). Many of the genes that can be controlled by shear stress are essential to proper cardiovascular development, including PDGF-β [15], connexin43 [16] and Flk1 [16]. In addition, flow causes changes in endothelial cell morphology such that the cells flatten and align with the direction of flow [17]. In Titin$^{-/-}$ embryos, a protein involved in cardiac contraction, abnormal endothelial morphology is present such that endothelial cells are more globular and do not flatten, reminiscent of cell shapes associated with migrating angioblasts rather than differentiated endothelial cells [12]. There is strong reason to suspect, therefore, that the forces caused by flowing blood during development are important and essential for proper vascular development. The issue lies in the fact that fluid dynamic phenotype has never been measured and linked to changes in the vascular morphology.

Measuring blood flow dynamics in the early embryo is problematic. For older embryos or in larger vessels, it is possible to use Doppler Ultrasound to measure flow dynamics and this technique has been used to measure the flow abnormalities which lead to embryonic lethality in the NFATC1$^{-/-}$ embryo [18]. The small vessels of the remodeling yolk sac are not, however, accessible to ultrasound measurements. In order to measure flow dynamics in these small vessels, we have previously developed a technique based on confocal line scanning using an embryo that expresses GFP in its primitive erythroblasts (Chapter 3, [19]). This technique allows us to measure the hemodynamic phenotype of mutant embryos and ascertain the effect of these changes on the vascular morphology. Linking the changes in blood flow dynamics directly to the phenotype is critical to understand the role that blood flow plays in vascular remodeling.

We now report on hemodynamic analysis of a mutant mouse, MLC2a$^{-/-}$, which has cardiac deficiencies leading to vascular defects [11]. MLC2a is the atrial-specific myosin light chain, which is expressed specifically in the early embryonic heart and not the vasculature [20]. By breeding an erythroblast-specific GFP marker [21] into the MLC2a$^{+/-}$ background, we have been able to analyze the flow present in these mice. We find that these mice exhibit decreased plasma velocity, increased oscillatory flow and a failure of erythroblasts to circulate properly. We then proceeded to phenocopy aspects of these fluid dynamic deficiencies, either by inducing weakened blood flow without oscillatory flow or by preventing entry of the erythroblasts into circulation without weakening the heart, in order to establish which factors were the primary causes of the vascular phenotype. The presence of increased oscillatory flow was not found to be the primary cause of the phenotype of the MLC2a$^{-/-}$ embryos since weakening the heart

alone was sufficient to induce the phenotype. We find that preventing the entry of the erythroblasts into circulation can produce most aspects of the lack of remodeling phenotype. This works shows that not only is flow important for vascular remodeling but that the viscous increase caused by the entry of the red blood cells is essential.

Results

The knock-out mice of atrial-specific myosin light chain (MLC2a) show a vascular phenotype in which angiogenic remodeling is inhibited [11]. Since the MLC2a gene does not normally function outside the heart, the vascular phenotype was thought to arise from altered blood flow. Our previous analysis of yolk sac circulation shows that in normal development blood circulation is established through a multi-step process. First, plasma flow begins as the heart begins to beat (2-3 somites) and increases as the heart contractions become stronger. Erythroblasts enter the circulation over the course of several hours (6 to 9 somite stage), increasing shear stress and perhaps acting as a signal for the initiation of vessel remodeling. By the 13 somite stage, shear stress levels are reduced as vessel remodeling is underway (Jones *et al*., submitted, Chapter 4). The nature of the circulatory defect in the MLC2a$^{-/-}$ embryos is unknown, including the stage at which MLC2a$^{-/-}$ circulatory development diverges from normal development. If plasma flow is abnormal, erythroblast circulation could fail to be established. Alternatively, the lack of atrial contraction in the MLC2a$^{-/-}$ embryos could result in lowered shear stress which could alter the mechanosensory signals necessary for triggering vascular remodeling. Another possibility is that poor atrial function could cause excessive regurgitation, leading to increased oscillatory shear stress within developing vessels.

To evaluate the potential role of altered flow in the abnormal development of the MLC2a knock-out embryos, we mated these mice to the ϵ-globin::GFP mice [21], which express GFP in primitive erythroblasts, in order to analyze fluid dynamics in the yolk sac vasculature. We first dissected the mice at various stages to observe the expansion of the blood islands and the formation of the plexus (Figure1, Table I). Before 7 somites, in both heterozygous (Figure 1A) and homozygous knock-out mice (Figure 1B), the blood islands are tightly clustered in the proximal end of the yolk sac. By 10 somites, the blood islands expand to fill the entire plexus and appear phenotypically normally in both heterozygous and homozygous mutant embryos (Figure 1D). Homozygous knock-out embryos, however, fail to establish flowing erythroblasts by this stage, as seen in wild-type embryos (Table I). Defects in vascular remodeling can first be seen by the 13 somite stage. Wild-type and mutant embryos compared at E9.5 indicate that the vascular plexus does not remodel into mature vessels (Figure 1F). Somites in mutant embryos are produced at the same rate as wild-type littermates, indicating that development as a whole is not delayed at this stage and that the phenotype is specific to the cardiovascular system.

Next, we examined how erythroblasts fill the plexus since culture and observation under fluorescence microscopy of MLC2a homozygous null embryos showed that erythroblasts do not circulate freely (Table I). Some small oscillatory motions are present; however, laminar flow that is normally established is not sustained. Using time-lapse video microscopy as previously described (Chapter 2, [19]), we examined blood flow within wild-type and mutant yolk sacs. Movie 1, Figure 2 shows the results of a time-lapse analysis of blood island expansion in MLC2a$^{-/-}$ embryos. During the first part of the time-

lapse movie, erythroblasts appear and disappear very quickly from one frame to the next, indicative of some limited erythroblast motion. Regions containing immobile erythroblasts appear and quickly expand to fill the plexus. This causes an increasing number of erythroblasts to become trapped. The plexus fills quickly (within 22 frames, or 2 hours) and most erythroblasts are stationary after this point (Figure 2, C-F). While some limited erythroblast motion is initiated, erythroblasts appear to be taken up by the flow only briefly and motion of erythroblasts is intermittent.

To determine the precise nature of the erythroblast motion in the yolk sac of MLC2a$^{-/-}$ embryos, time-lapse sequences were taken at a higher magnification (40x) using a faster frame rate of acquisition (2 Hz) to resolve the flows and to track individual cells. Image sequences taken at 2 frames per second (Figure 3, Movie 2) indicate that erythroblasts oscillate back and forth (Figure 3B). In wild-type embryos, the net motion of erythroblasts during a cardiac cycle is forward. We find that in MLC2a$^{-/-}$ embryos as much retrograde (backward) motion is present as anterograde (forward) motion. The erythroblasts thus seem to oscillate in place rather than to flow within the early vessels. Though erythroblasts move with the blood flow in the mutant embryos, the net displacement within a cardiac cycle is limited because of the large amount of retrograde flow.

Since defects were seen in the initial stages of erythroblast circulation, we next investigated whether plasma flow was normal in these embryos using Fluorescence Recovery After Photobleaching (FRAP). FRAP is a technique in which a small area of a fluorescent field of view is bleached and the recovery curve of the fluorescence is

measured [22]. Fluorescence recovery can arise either from flow of fluorescent molecules into the field of view or through diffusion. In cases where flow is known to be absent, the rate of fluorescence recovery can be used to calculate a diffusion coefficient for fluorescently tagged molecules. The presence of plasma flow can be assessed by the presence of large increases in the apparent or measured diffusion coefficients, called a perfusion coefficient, as compared to measurements for pure diffusion, with the magnitude of the increase indicative of the general level of flow present. We injected 10,000MW fluorescein-dextran into the heart of the embryos and then bleached square regions of interest within the vascular channels and followed the fluorescence recovery (Figure 4). To measure the value for pure diffusion, we performed FRAP on embryos in which we specifically stopped cardiac contraction. In these embryos, we find that purely diffusive fluorescent recovery results in a diffusion coefficient of 51 $\mu m^2/s$ (n=8, std dev= 21) for 10,000MW dextran in embryonic blood plasma at 37 °C. In wild-type embryos, we find perfusion coefficients between 100 and 3500 $\mu m^2/s$ (Figure 4A). Since this is considerably higher than the pure diffusion rate in the absence of flow, we find that there is flow present at these stages. The measured perfusion coefficients are comparable between wild-type (Figure 4A) and knock-out (Figure 4B) littermates at the 4 somite stage. As the embryos develop, however, there is a significant increase in the measured perfusion coefficient of wild-type embryos which is not matched in the knock-out embryos. At the older somite stages, some vessels of wild-type embryos had flow that was too fast to measure (perfusion coefficient > 9000 $\mu m^2/s$). In knock-out embryos, the measured perfusion coefficients were never higher than 1000 $\mu m^2/s$. The measured perfusion coefficients represent an order of magnitude increase in measured perfusion coefficient over the purely diffusive case, indicating that flow is present. While these

data indicate that the plasma is flowing in the MLC2a$^{-/-}$embryos, we also find that the flow induced by the heart is much slower than normal.

Slow plasma flow indicated that heart performance was reduced in MLC2a mutant embryos and we sought to determine whether the remodeling phenotype could be induced solely by reduced cardiac ejection volume. We treated the embryos with KB-R7943, an Ncx1-specific inhibitor [23]. Ncx1 is a calcium-sodium exchange pump expressed specifically in cardiac tissue during early development [20]. Embryos that are treated with this compound develop normally and increase somite number at the same rate as control embryos (data not shown), but show reduced strength of cardiac contractions. Though the vast majority of erythroblasts remain immobile (Figure 5C), as with the MLC2a$^{-/-}$ mice, a small number of erythroblasts flow within the embryonic vasculature (data not shown). This is similar to the occasional erythroblasts that oscillate in the MLC2a$^{-/-}$ embryos, however, in the KB-R7943 embryos; these erythroblasts do not exhibit increased retrograde flow. Blood islands expand from the initial tight band of erythroblasts, but most erythroblasts never circulate. After culture, control embryos have several large diameter vessels coming off the dorsal aorta and feeding the yolk sac, a regular branching pattern and enlarged avascular spaces, all of which are characteristics consistent with vascular remodeling (Figure 5A, B). In treated embryos after culture, the vascular plexus lacks the large diameter feeding vessels and exhibits large vascular spaces separated by very small avascular regions (Figure 5C) similar to the unremodeled phenotype seen in the MLC2a$^{-/-}$ embryos. Plasma flow, as measured by FRAP (Table II), was in the same range for the KB-R7943 treated embryos (average, 750 $\mu m^2/s$) as for MLC2a$^{-/-}$ embryos (average, 560 $\mu m^2/s$) indicating that

slower plasma flow was induced by this treatment. These results indicate that the phenotype after treatment with the Ncx inhibitor is similar to that of the MLC2a$^{-/-}$ embryos. As such, the reduction in circulation caused by the weakened heart was sufficient to induce remodeling defects.

Next, we sought to investigate whether the remodeling phenotype observed in the MLC2a mutant embryos results from lowered shear stress or the poor circulation of nutrients necessary for proper remodeling. The viscosity of blood is significantly dependent on the hematocrit, or the percent of the volume taken up by the erythroblasts [24]. To test whether the viscous increase caused by the entry of the erythroblasts into circulation was essential, we prevented their entry by focally polymerizing acrylamide around the blood islands (see methods). Experimental embryos were injected with acrylamide and ammonium persulfate (APS) into the heart and TEMED into the blood islands. Control embryos were injected with only acrylamide/APS into the heart, or injected with only TEMED into the blood islands or left uninjected. All control embryos developed normally, showing that the treatment did not injure the embryos. The polymerization of the blood islands results in the majority of the erythroblasts remaining fixed in the proximal end of the yolk sac even at the 14 somite stage (Figure 6D) when most erythroblasts circulate in wild-type embryos (Figure 6A). Since this treatment aimed to prevent entry of the erythroblasts into circulation without affecting heart function, we used FRAP to measure perfusion coefficients and perfusion coefficients which were similar to wild-type embryos of the same stage (Table II). FRAP measurements on treated embryos measured perfusion coefficients (n=16) between 400 and 6000 $\mu m^2/s$ (av. 3167, Table II) consistent with plasma perfusion coefficients

present when erythroblasts are fluidized in untreated embryos. Some vessels in treated embryos contain flow too fast to measure using FRAP which is also seen in uninjected embryos. As such, plasma flow was normal in treated embryos. In all control embryos, we observe the presence of large diameter vessels (Figure 6B), a more regular branching pattern and enlarged avascular spaces (Figure 6C), consistent with vascular remodeling. In treated embryos, avascular spaces are enlarged and the dilated vascular spaces of the unremodeled plexus disappear, consistent with the initial phase of vascular remodeling (Figure 6F). The large blood vessels that form directly off the heart and dorsal aorta and feed the yolk sac, however, are not present by 14 somites (Figure 6E). This phenotype is not equivalent to the phenotype of MLC2a$^{-/-}$ embryos. The two phenotypes, however, share many common characteristics. Vessels are able to initiate remodeling some aspects of vascular remodeling without high shear flow, but do not form large caliber vessels.

Oscillatory flows have been shown to induce proliferation in cultured endothelial cells [25]. Since the MLC2a $^{-/-}$ embryos showed a similar phenotype to the KB-R7943 treated embryos that do not have oscillatory flow, we investigated whether there were secondary effects present in the form of increased cell proliferation. Using an antibody to phospho-histone 3 to highlight replicating cells, GFP to identify red blood cells and DAPI to determine the total number of cells within an image, the percent of non-erythroblast cells that were replicating was measured in wild-type, mutant, KB-R7943 treated and acrylamide treated embryos (Figure 7). MLC2a$^{-/-}$ embryos showed increased levels of proliferation as compared to all other experimental embryos. Proliferation was more than two-fold higher in MLC2a$^{-/-}$ embryos than in stage-matched control embryos.

Discussion

In trying to understand what aspects of blood flow are important for the vascular remodeling process, it is necessary to separate the various features of blood flow. The MLC2a$^{-/-}$ mice have several defects in blood flow including: i) a weakened heart that leads to lower plasma flow velocities, ii) the lack of entry of the erythroblasts into circulation that leads to lower viscosity, and iii) the increase in retrograde flow, each of which could theoretically cause hemodynamic insufficiencies. By phenocopying various aspects of the knock-out mice, we are able to investigate the role of each of these hemodynamic deficiencies.

The presence of lower levels of plasma flow indicates that the heart could not induce regular plasma flow within the vasculature. This is likely one of the reasons that the red blood cells do not enter circulation since a minimum flow velocity is required to suspend particles in a flowing fluid, known as the fluidization velocity. We phenocopied the MLC2a$^{-/-}$ embryos without inducing oscillatory flow using treatment with the Ncx1 inhibitor, KB-R7943. The vascular phenotype of these treatments is identical to the MLC2a$^{-/-}$ mice, indicating that reduced cardiac output alone is sufficient to induce the failure of vascular remodeling.

In order to separate the effects of the weaker heart from those of the entry of erythroblasts into circulation, we used focal polymerization around the blood islands. Plasma flow levels are similar to wild-type after polymerization, as indicated by the high perfusion rates measured by FRAP (Table II). The results of the focal polymerization experiments show that some aspects of vascular remodeling are present without

erythroblast motion. The embryonic plexus initially consists of large vascular regions separated by small avascular spaces. As remodeling begins, the diameter of most vessels within the plexus decreases. This is accompanied by growth of the avascular regions. These changes are present when the erythroblasts are prevented from entering circulation through polymerization. In the MLC2a$^{-/-}$ mice, this process does not occur and the vessels of the plexus remain dilated. A strong heart does not only produce higher velocity flow, but would also produce higher pressure flow, and we are not able to establish which of the two is essential. These results do, however, indicate a role for strong plasma flow during early vascular remodeling.

It is important to note, however, that the appearance of large caliber vessels coming directly off the dorsal aorta does not occur in embryos where the blood islands have been immobilized. Erythroblasts carry oxygen to the tissues as well as playing a role in the hemodynamics of the flowing blood. The entry of erythroblasts into circulation increases the viscosity of the blood [24], and since the calculation of shear stress is dependent on both the velocity and viscosity of the fluid, this causes an increase in the shear stress on the endothelial cells. The lack of large diameter vessels is not consistent with the role of erythroblasts as oxygen carriers since hypoxia is believed to stabilize the formation of large vessels [26] and lack of HIF1α signaling results in the failure of large caliber vessel formation [27, 28]. As well, whole embryo culture at this stage in the presence of carbon monoxide, which ablates oxygen carrying ability of the erythroblast, does not affect remodeling (unpublished results). Increased shear stress, on the other hand, leads to increased vessel diameter [29]. We therefore believe the

lack of large vessel formation is due to the low viscosity, and therefore low shear stress, flow that is present due to absence of erythroblasts in circulation.

Through embryo culture and time-lapse microscopy, we are able to detect the presence of oscillatory flow in the yolk sac of MLC2a$^{-/-}$ embryos. When erythroblasts first begin circulating, the heart valves are not yet formed. Though we observe significant retrograde flow in wild-type embryos (unpublished results), the net flow is forward. In the MLC2a$^{-/-}$ embryos, there does not appear to be a net forward motion of the circulating erythroblasts. The presence of this retrograde flow puts an abnormal load on the embryonic heart and may explain the severe chest edema observed in the knock-out embryos [11]. These results highlight the role of atrial contraction in preventing retrograde flow before the formation of the heart valves. In the zebrafish *wea* mutants, the *atrial myosin heavy chain (amhc)* gene is disrupted leading to a silenced atrial contraction. Circulation is present in these embryos, though inefficient [30]. The presence of increased retrograde flow, however, was not specifically investigated. Our results suggest that the atrial contraction is essential in blocking retrograde flow before valve formation.

The presence of retrograde flow is especially important to vascular remodeling because this type of flow is known to be biologically active for mature endothelial cells (for review, see [14]). A significant amount of work has been done on the effect of oscillatory flows on endothelial cells because atherosclerotic plaques tend to form in regions where oscillatory eddies are present in the blood flow [31]. Since the failure to remodel required only reduced heart function and not oscillatory flow as shown by the KB-R7943

treatment, we do not believe that the presence of oscillatory flow was the primary reason for the failure of the yolk sac to remodel. This is not to say that increased oscillatory flow does not have an effect during remodeling as indicated by the increased level of proliferation in the MLC2a$^{-/-}$ embryos as compared to the wild-type embryos, KB-R7943 treated embryos and the acrylamide treated embryos. We believe that the increase in proliferation is due to the oscillatory flow since reduced nutrient and oxygen delivery due to altered flow might result in lower, not higher levels of proliferation. The effect of the increased proliferation, however, was not as significant as the effects caused by the weakened heart contraction.

Taken together, our findings support an early role for fluid dynamics and more specifically shear stress during vascular development. The presence of plasma flow alone, without the increase in viscosity caused by the entry of erythroblasts into circulation, does not allow for proper remodeling. The presence of proper plasma flow in these embryos, as shown by the large perfusion coefficients, indicate that nutrients and growth factors can circulate and these components alone cannot induce remodeling. Thus, it is likely that the role of the early circulation of erythroblasts is to increase the blood viscosity in order to establish a proper and energy efficient cardiovascular loop before circulation is needed for nutrient and oxygen delivery.

The other physical force which may be important for proper cardiovascular development is tangential strain caused by pressure. Since pressure cannot currently be measured in vessels as small as those present in the early vasculature, it is difficult to establish the exact role pressure may play during development. The presence of some aspects of

vascular remodeling in acrylamide treated embryos, such as the initial reduction in the diameter of many of the vessels in the yolk sac that is accompanied by growth of avascular regions, indicate a role for pressure as well as shear stress. These changes are not present when heart contractions are weak which should cause lower pressure, such as in the MLC2a$^{-/-}$ embryos. This work thus implicates a role for both pressure and shear stress during cardiovascular development.

Though blood flow is known to be essential for embryonic vascular remodeling, the role of blood fluid dynamics remains controversial. Many knock-out phenotypes that fail to remodel the yolk sac vasculature are believed to have abnormal fluid dynamics, however, these are rarely investigated. By analyzing the fluid dynamics of the MLC2a$^{-/-}$ embryos, we are able not only to assess why these mice lack vascular remodeling but also assess the importance of various aspects of blood flow in the remodeling process.

Materials And Methods

Dissection and Embryonic Culture

Breeding pairs of MLC2a$^{+/-}$:ε-globin::GFP mice [11, 21] were mated together and the presence of a vaginal plug in the morning was taken as 0.5 dpc. Embryos were collected on the morning of the eighth day and cultured as previously described [32].

For time-lapse microscopy, single images were taken every 6 minutes at a magnification of 20x (Plan-Neofluar 20x/0.5NA) on a Zeiss LSM 5 PASCAL. Real time images of oscillatory motion were taken with 40x magnification, and individual cells were tracked

manually by connecting the center of the same cell in subsequent images. Overlay of tracking images was performed using Adobe Photoshop.

Fluorescence Recovery After Photobleaching

Embryos were injected with 10,000MW dextran conjugated to fluorescein (Molecular Probes, No. D-1821) and put in culture. FRAP was performed as previously described (Jones *et al*., submitted; Chapter 4).

KB-R7943 Inhibition

For KB-R7943 treatment, embryos were cultured in roller culture (BCI Engineering) rather than static embryo culture. Embryos were somite stage matched between treated and control before culture, and three embryos were cultured in each vial. Initial somite counts were between 5 and 7 somites. Each vial contained 2 mL of cultured media, and for treated embryos 5 µL of 6 mM KB-R7943 (EMB Bioscience, No. 420336) was added to the media. Embryos were kept in culture for 6 to 10 hours. After culture, heart rates were measured and the expansion of the blood islands was imaged on a fluorescent dissecting microscope. Texas Red-conjugated 10,000 MW dextran (Molecular Probes, No. D1828) was then injected into the heart of the embryos using a pulled glass needle and a Picospritzer II (General Valve Corp.). Embryos were placed in a tissue culture incubator for 30 minutes, and then the plexus was imaged on a confocal microscope (Zeiss LSM 5 PASCAL) at 20x magnification (Plan-Neofluar 20x/0.5NA).

Acrylamide Immobilization

Embryos were dissected at a stage between 3 and 5 somites. A 98.8 v/v% acrylamide/bis-acrylamide (National Diagnostics, No. EC-890) and 1.2 v/v% ammonium persulfate (stock 20 w/v%) solution was prepared and injected directly into the heart of the embryos using a Picospritzer II (General Valve Corp.). Two to three small volume injections were used rather than a single large volume injection to prevent damage to the heart. Single large injections caused the heart muscle to stretch and even control embryos which were injected with only acrylamide did not develop normally in this case. Embryos were placed in a tissue culture incubator for 30 minutes to allow the acrylamide solution to circulate. Embryos were then injected with TEMED directly into the blood islands of the yolk sac. The blood islands were visualized using an ϵ-globin::GFP transgenic line [21] on a fluorescent dissecting scope. Several focal injections were performed in order to polymerize the entire circumference of the blood islands. Three sets of controls were performed: a) uninjected embryos, b) embryos injected only with the acrylamide solution into the heart, and c) embryos injected with TEMED into the blood islands. For all controls and experimental sets, embryos were then cultured in roller culture. Three embryos were placed per vial with 2 mL of culture media. Embryos were cultured for 10 hrs, until approximately the 14 somite stage. After culture, the expansion of the blood islands was imaged on a fluorescent dissecting microscope using the GFP marker. The vessel morphology was imaged in the same manner as with the KB-R7943 treated embryos.

Analysis of Replication in Yolk Sac

Embryos expressing ε-globin::GFP were fixed for one hour in 4% PFA at 4°C and then washed 4-5 times in PBS. Embryos were blocked with 2% nonfat dried milk in PBS and then incubated overnight at 4°C with primary antibodies to Flk1 (PharMingen, No. 555307) and phospho-histone 3 (Upstate, No. 06-570) at a 1:100 dilution with dried milk in PBS. Embryos were washed with 0.5% Triton and 2% nonfat dried milk in 10mM Tris. Embryos were incubated overnight at 4°C with secondary antibodies conjugated to Cy3 and Cy5 respectively and then washed. Embryos were then stained with DAPI and imaged at 40x on a Zeiss LSM510 META. The total number of cells (DAPI) and the total number of replicating cells (phospho-histone 3) were counted. The number of replicating cells expressing erythroblast markers (ε-globin:GFP) or endothelial cell markers (Flk1) were also recorded. The number of non-erythroblast cells that were replicating was calculated by subtracting the replicating erythroblasts from the total number of cells that are replicating, and dividing this number by total number of cells minus the number of erythroblast present.

Acknowledgments

We thank Chris Waters for technical support and Joaquin Gutierrez for assistance in animal husbandry. This work was supported by the Human Frontiers Science Program (RG0146/2000-B102), the American Heart Association (0315023Y) and NIH (R01 HL078694). We also thank the Powell foundation for the partial support of this work through the Option of Bioengineering at Caltech.

References

1. Risau, W. and I. Flamme, Vasculogenesis*. Annual Review of Cell & Developmental Biology*, 1995. 11: 73-91.
2. Huang, C., F. Sheikh, M. Hollander, C. Cai, D. Becker, P.H. Chu, S. Evans, and J. Chen, Embryonic atrial function is essential for mouse embryogenesis, cardiac morphogenesis and angiogenesis*. Development*, 2003. 130(24): 6111-9.
3. Kotch, L.E., N.V. Iyer, E. Laughner, and G.L. Semenza, Defective vascularization of HIF-1alpha-null embryos is not associated with VEGF deficiency but with mesenchymal cell death*. Dev Biol*, 1999. 209(2): 254-67.
4. Kruger, O., A. Plum, J.S. Kim, E. Winterhager, S. Maxeiner, G. Hallas, S. Kirchhoff, O. Traub, W.H. Lamers, and K. Willecke, Defective vascular development in connexin 45-deficient mice*. Development*, 2000. 127(19): 4179-93.
5. Wakimoto, K., K. Kobayashi, O.M. Kuro, A. Yao, T. Iwamoto, N. Yanaka, S. Kita, A. Nishida, S. Azuma, Y. Toyoda, K. Omori, H. Imahie, T. Oka, S. Kudoh, O. Kohmoto, Y. Yazaki, M. Shigekawa, Y. Imai, Y. Nabeshima, and I. Komuro, Targeted disruption of Na+/Ca2+ exchanger gene leads to cardiomyocyte apoptosis and defects in heartbeat*. J Biol Chem*, 2000. 275(47): 36991-8.

6. Yang, X., L.H. Castilla, X. Xu, C. Li, J. Gotay, M. Weinstein, P.P. Liu, and C.X. Deng, Angiogenesis defects and mesenchymal apoptosis in mice lacking SMAD5*. Development*, 1999. 126(8): 1571-80.

7. Risau, W., Mechanisms of angiogenesis*. Nature*, 1997. 386(6626): 671-4.

8. Chapman, W.B., The effect of the heart-beat upon the development of the vascular system in the chick. *Am. J. Anat.*, 1918. 23: 175-203.

9. Manner, J., W. Seidl, and G. Steding, Formation of the cervical flexure: an experimental study on chick embryos*. Acta Anat*, 1995. 152(1): 1-10.

10. Bi, W., C.J. Drake, and J.J. Schwarz, The transcription factor MEF2C-null mouse exhibits complex vascular malformations and reduced cardiac expression of angiopoietin 1 and VEGF*. Dev Biol*, 1999. 211(2): 255-67.

11. Huang, C., F. Sheikh, M. Hollander, C. Cai, D. Becker, P.H. Chu, S. Evans, and J. Chen, Embryonic atrial function is essential for mouse embryogenesis cardiac morphogenesis and angiogenesis*.* 2003.

12. May, S.R., N.J. Stewart, W. Chang, and A.S. Peterson, A Titin mutation defines roles for circulation in endothelial morphogenesis*. Dev Biol*, 2004. 270(1): 31-46.

13. Luo, Y., M. Ferreira-Cornwell, H. Baldwin, I. Kostetskii, J. Lenox, M. Lieberman, and G. Radice, Rescuing the N-cadherin knockout by cardiac-specific expression of N- or E-cadherin*. Development*, 2001. 128(4): 459-69.

14. Resnick, N., H. Yahav, A. Shay-Salit, M. Shushy, S. Schubert, L.C.M. Zilberman, and E. Wofovitz, Fluid shear stress and the vascular endothelium: for better and for worse*. Prog Biophys Mol Biol.*, 2002. 81(3): 177-99.

15. Resnick, N., T. Collins, W. Atkinson, D.T. Bonthron, C.F. Dewey, Jr., and M.A. Gimbrone, Jr., Platelet-derived growth factor B chain promoter contains a cis-acting fluid shear-stress-responsive element. *Proc Natl Acad Sci USA*, 1993. 90(10): 4591-5.

16. Gabriels, J.E. and D.L. Paul, Connexin43 is highly localized to sites of disturbed flow in rat aortic endothelium but connexin37 and connexin40 are more uniformly distributed*. Circ Res*, 1998. 83(6): 636-43.

17. Dewey, C.F., Jr., S.R. Bussolari, M.A. Gimbrone, Jr., and P.F. Davies, The dynamic response of vascular endothelial cells to fluid shear stress*. J Biomech Eng*, 1981. 103(3): 177-85.

18. Phoon, C.K., R.P. Ji, O. Aristizabal, D.M. Worrad, B. Zhou, H.S. Baldwin, and D.H. Turnbull, Embryonic heart failure in NFATc1-/- mice: novel mechanistic insights from in utero ultrasound biomicroscopy*. Circ Res*, 2004. 95(1): 92-9.

19. Jones, E.A., M.H. Baron, S.E. Fraser, and M.E. Dickinson, Measuring hemodynamic changes during mammalian development*. Am J Physiol Heart Circ Physiol*, 2004. 287(4): H1561-9.

20. Kubalak, S.W., W.C. Miller-Hance, T.X. O'Brien, E. Dyson, and K.R. Chien, Chamber specification of atrial myosin light chain-2 expression precedes septation during murine cardiogenesis*. Journal of Biological Chemistry*, 1994. 269(24): 16961-70.

21. Dyer, M.A., S.M. Farrington, D. Mohn, J.R. Munday, and M.H. Baron, Indian hedgehog activates hematopoiesis and vasculogenesis and can respecify prospective neurectodermal cell fate in the mouse embryo*. Development*, 2001. 128(10): 1717-30.

22. Axelrod, D., D.E. Koppel, J. Schlessinger, E. Elson, and W.W. Webb, Mobility measurement by analysis of fluorescence photobleaching recovery kinetics. *Biophysical Journal*, 1976. 16: 1055-1069.

23. Linask, K.K., M.D. Han, M. Artman, and C.A. Ludwig, Sodium-calcium exchanger (NCX-1) and calcium modulation: NCX protein expression patterns and regulation of early heart development*. Dev Dyn*, 2001. 221(3): 249-64.

24. Chien, S., S. Usami, H.M. Taylor, J.L. Lundberg, and M.I. Gregersen, Effects of hematocrit and plasma proteins on human blood rheology at low shear rates*. J Appl Physiol*, 1966. 21(1): 81-7.

25. DePaola, N., M.A. Gimbrone, Jr., P.F. Davies, and C.F. Dewey, Jr., Vascular endothelium responds to fluid shear stress gradients. *Arteriosclerosis & Thrombosis*, 1992. 12(11): 1254-7.

26. Elson, D.A., G. Thurston, L.E. Huang, D.G. Ginzinger, D.M. McDonald, R.S. Johnson, and J.M. Arbeit, Induction of hypervascularity without leakage or inflammation in transgenic mice overexpressing hypoxia-inducible factor-1alpha. *Genes Dev*, 2001. 15(19): 2520-32.

27. Carmeliet, P., Y. Dor, J.M. Herbert, D. Fukumura, K. Brusselmans, M. Dewerchin, M. Neeman, F. Bono, R. Abramovitch, P. Maxwell, C.J. Koch, P. Ratcliffe, L. Moons, R.K. Jain, D. Collen, E. Keshert, and E. Keshet, Role of HIF-1alpha in hypoxia-mediated apoptosis, cell proliferation and tumour angiogenesis. *Nature*, 1998. 394(6692): 485-90.

28. Ryan, H.E., J. Lo, and R.S. Johnson, HIF-1 alpha is required for solid tumor formation and embryonic vascularization. *Embo J*, 1998. 17(11): 3005-15.

29. Kamiya, A. and T. Togawa, Adaptive regulation of wall shear stress to flow change in the canine carotid artery. *Am J Physiol*, 1980. 239(1): H14-21.

30. Berdougo, E., H. Coleman, D.H. Lee, D.Y. Stainier, and D. Yelon, Mutation of weak atrium/atrial myosin heavy chain disrupts atrial function and influences ventricular morphogenesis in zebrafish. *Development*, 2003. 130(24): 6121-9.

31. Cornhill, J.F. and M.R. Roach, A quantitative study of the localization of atherosclerotic lesions in the rabbit aorta. *Atherosclerosis*, 1976. 23(3): 489-501.

32. Jones, E.A., D. Crotty, P.M. Kulesa, C.W. Waters, M.H. Baron, S.E. Fraser, and M.E. Dickinson, Dynamic in vivo imaging of postimplantation mammalian embryos using whole embryo culture. *Genesis*, 2002. 34(4): 228-35.

Tables

Table I – Expansion of Blood Islands and Erythroblast Circulation in MLC2a$^{-/-}$ Embryos

KO Phenotype

Somite stage	**4-5**	**6-7**	**8-9**	**10-11**	**12-13**
Blood islands only	8	1		1	
Some expansion proximal to blood islands	1	6	5	1	
Extensive blood island expansion			2	5	
Full plexus			2		5
Percent with circulating erythroblasts	0%	0%	0%	0%	0%
N total	**9**	**7**	**9**	**7**	**5**

WT Phenotype

Somite stage	**4-5**	**6-7**	**8-9**	**10-11**	**12-13**
Blood islands only	6	2			
Some expansion proximal to blood islands	7	4	1	1	
Extensive blood island expansion		6	17	4	
Full plexus			2	12	19
Percent with circulating erythroblasts	0%	33%	85%	82%	100%
N total	**13**	**12**	**20**	**17**	**19**

Table II – Phenotypic Comparison of Treatments

	Average Perfusion Coefficient (um^2/s)	**Std Dev**
Wild-type	1400	1300 (n=12)
MLC2a $^{-/-}$	560	270 (n=6)
KB-R7943 Inhibition	750	510 (n=8)
Blood Island Polymerization	3200	1400 (n=7)

Figure 1 – Phenotype of MLC2a -/- Embryos. Heterozygous (A, C, E) and knock-out (B, D, F) littermates at 7 somites (A-B), 10 somites (C-D) and approximately 23 somites (E-F). Plexus is highlighted by GFP-expressing erythroblasts [21]. Blood islands form properly (A, B) and expand within the plexus (C, D) however, the blood vessels of the plexus fail to remodel (E, F) as evidenced by the honeycomb pattern of the vessels and the lack of large diameter vessels (F).

Figure 2 – Time-lapse of MLC2a Expansion from Blood Islands. The expansion of the erythroblasts from the blood islands was followed using a transgenic mouse that expresses GFP in its erythroblasts [21]. The embryo is initially at the 9 somite stage. Erythroblasts enter the field of view within singles frames, indicative of the presence of flow. They quickly become immobilized, however, and form blockages within the vessels. As these blockages expand, an increasing number of erythroblasts are seen immobilized within the plexus. Images were taken every 6 minutes at 10x magnification on a Zeiss LSM5 PASCAL for a total duration of 7 hrs. Panel represents every 23rd frame or 2.3 hours.

Figure 3 – Cell Tracking of Erythroblast Motion. The motion of erythroblasts (green) within the vessels was imaged at 2Hz using a 40x objective lens on a Zeiss LSM5 PASCAL. Panels represent every 5th frame. The motion of some of the erythroblasts was tracked (B). The cell tracking showed erythroblasts oscillating with as much retrograde (backward) motion as anterograde (forward).

Figure 4 – Perfusion Coefficients of Blood Plasma Measured by FRAP. Fluorescence Recovery After Photobleaching (FRAP) was used to calculate perfusion coefficients with respect to somite stage within the early embryonic blood vessels in wild-type (A) and knock-out embryos (B). The higher perfusion coefficients present in wild-type embryos indicate the presence of faster plasma flow.

Figure 5 – KB-R7943 Inhibition of Cardiac Function. KB-R7943 was used to reduce cardiac function in embryos. KB-R7943 is an Ncx1 specific inhibitor which causes weak cardiac contractions [23]. Embryos were cultured for 6-10 hrs both without inhibitor (A, B) and with 9 μM KB-R7943 (C, D). This concentration was found through dose response experiments to reduce the strength of cardiac contraction without causing cardiac arrest. Control embryos show vascular remodeling where large diameter vessels appear (A) and avascular spaces enlarge (B). Erythroblasts fail to enter circulation in treated embryos and remain as blood islands (C). The vasculature remains completely unremodeled, showing small avascular pillars (D).

Figure 6 – Polymerization of Blood Islands. Erythroblasts were prevented from entering circulation by focal polymerization of acrylamide in the blood islands (D). Control embryos (A) show vascular remodeling including the formation of large diameter vessels (B) and enlargement of avascular spaces (C). Treated embryos never establish large diameter vessels (E), but do undergo some remodeling as evidenced by the increase in avascular diameter as compared to vascular diameter (E-F).

Figure 7 – Analysis of Cell Division Rate in Yolk Sacs. The presence of proliferation of non-erythroblast cells in the yolk sac of wild-type (WT), MLC2a$^{-/-}$ embryos, KB-R7943 treated and acrylamide treated embryos embryos was assessed using antibodies to phospho-histone 3. The percentage of undergoing cell division was assessed using a counterstain to DAPI. The percentage of non-erythroblast cells undergoing division is much higher in the yolk sacs of MLC2a$^{-/-}$ embryo than in somite stage matched wild-type embryos, KB-R7943 treated embryos and acrylamide treated embryos.

Figure 1

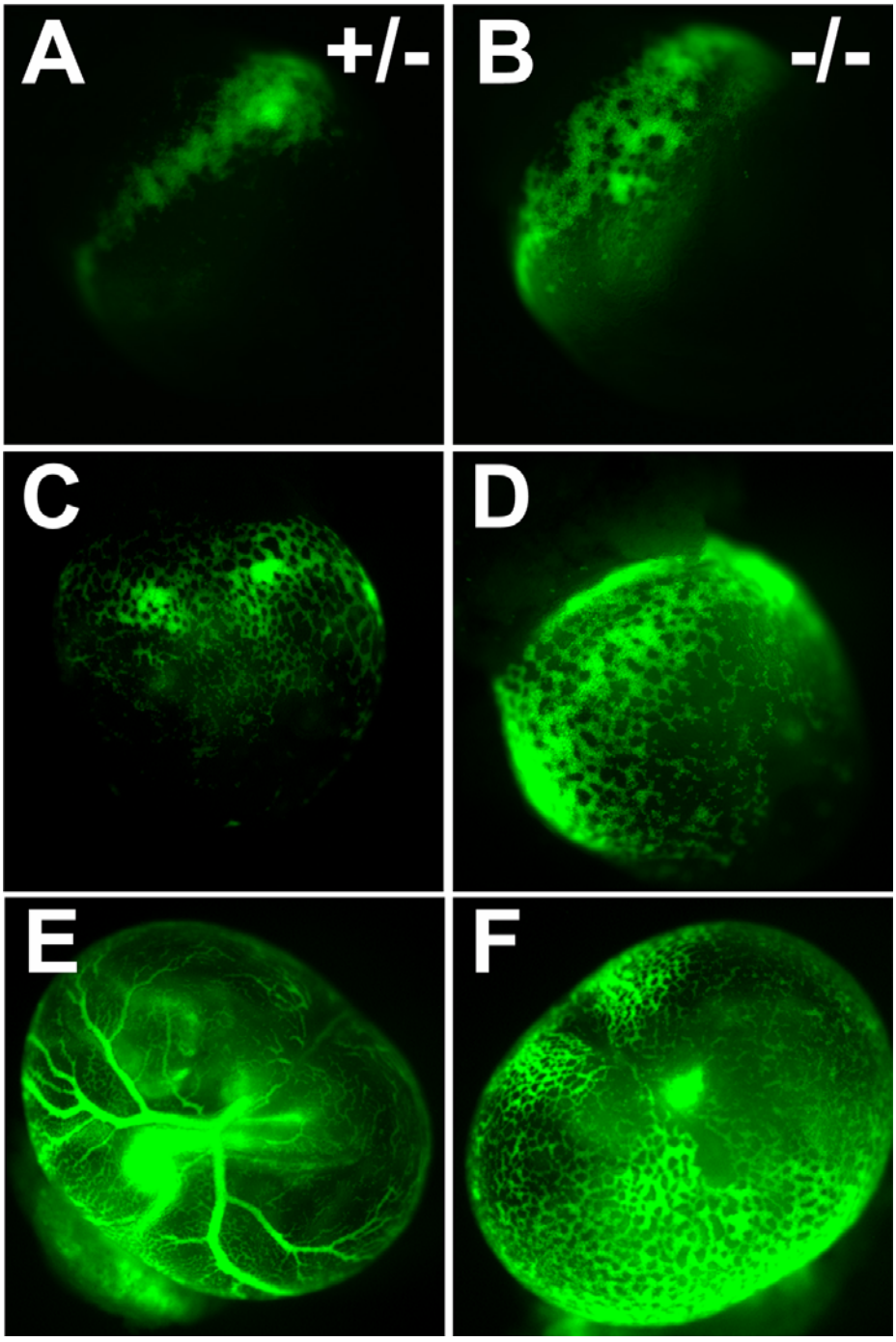

Figure 2

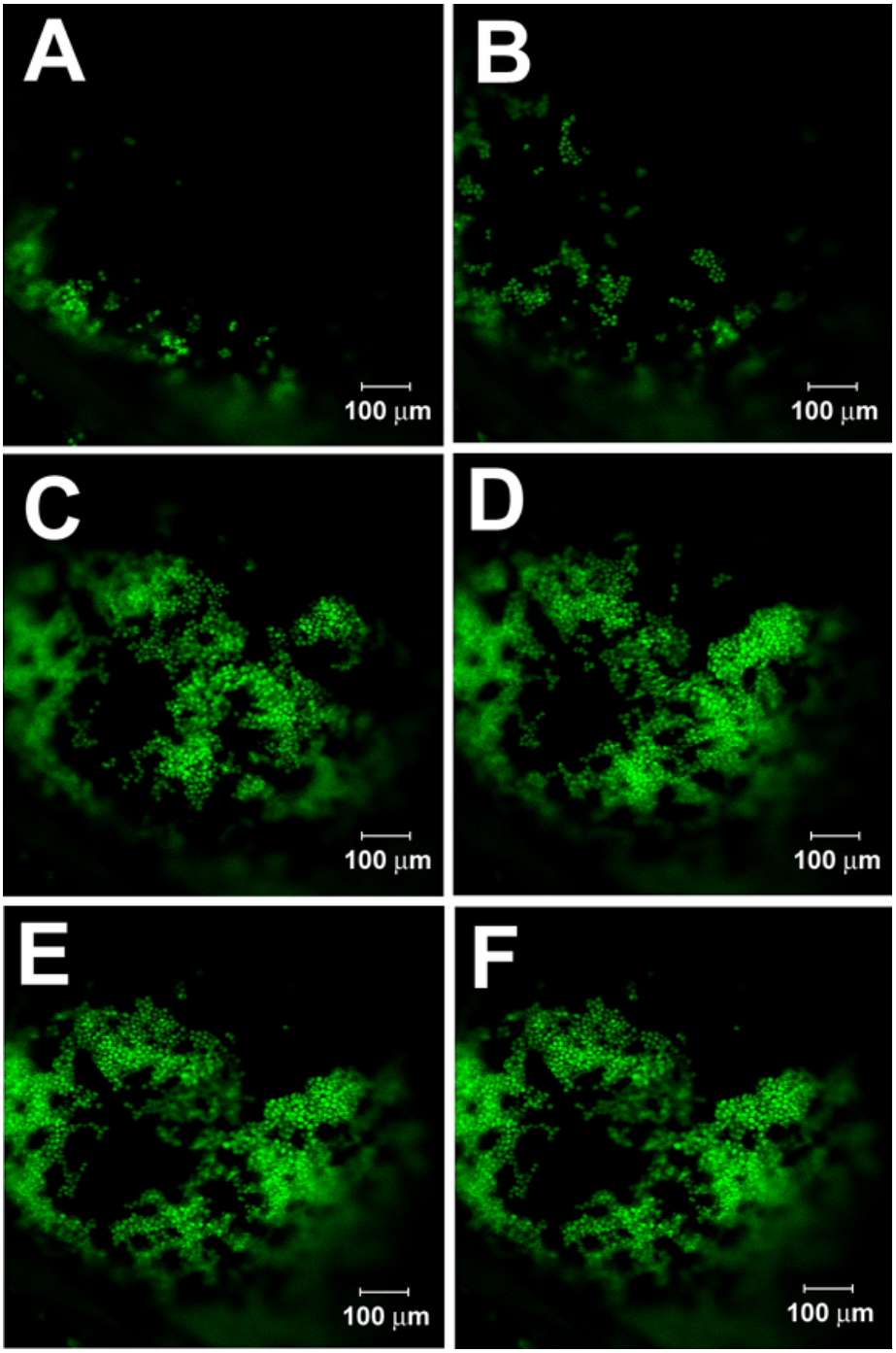

Figure 3

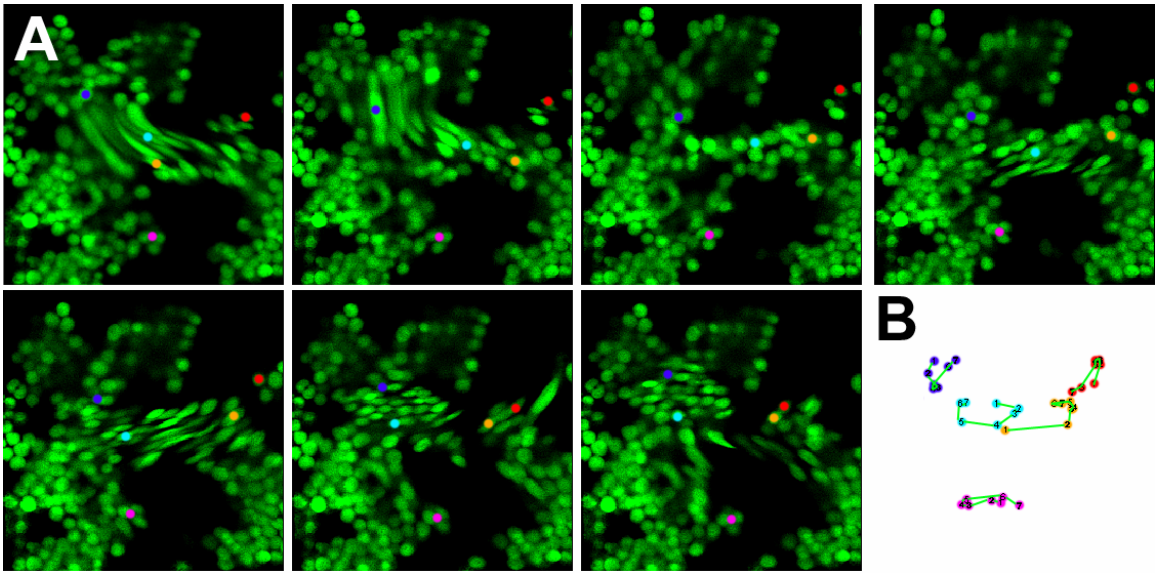

Figure 4

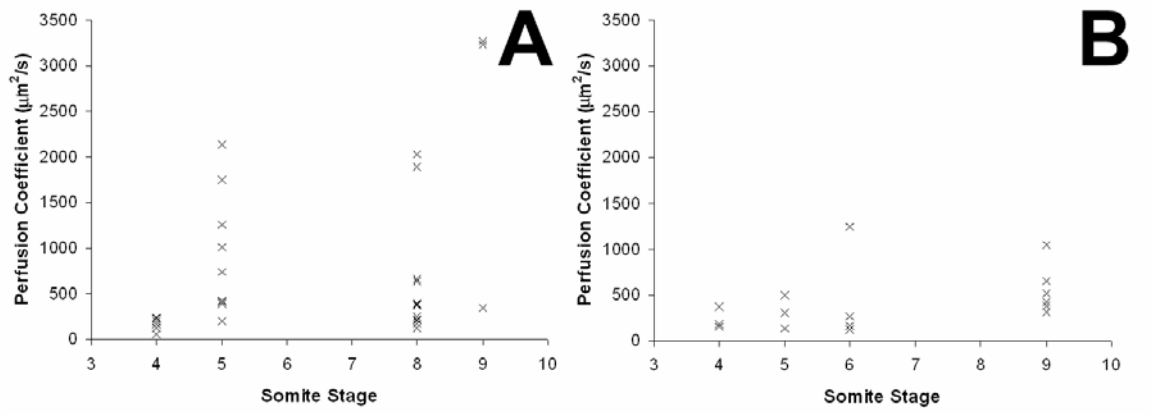
A
B
Perfusion Coefficient (μm²/s)
Somite Stage
0
500
1000
1500
2000
2500
3000
3500
3
4
5
6
7
8
9
10

Figure 5

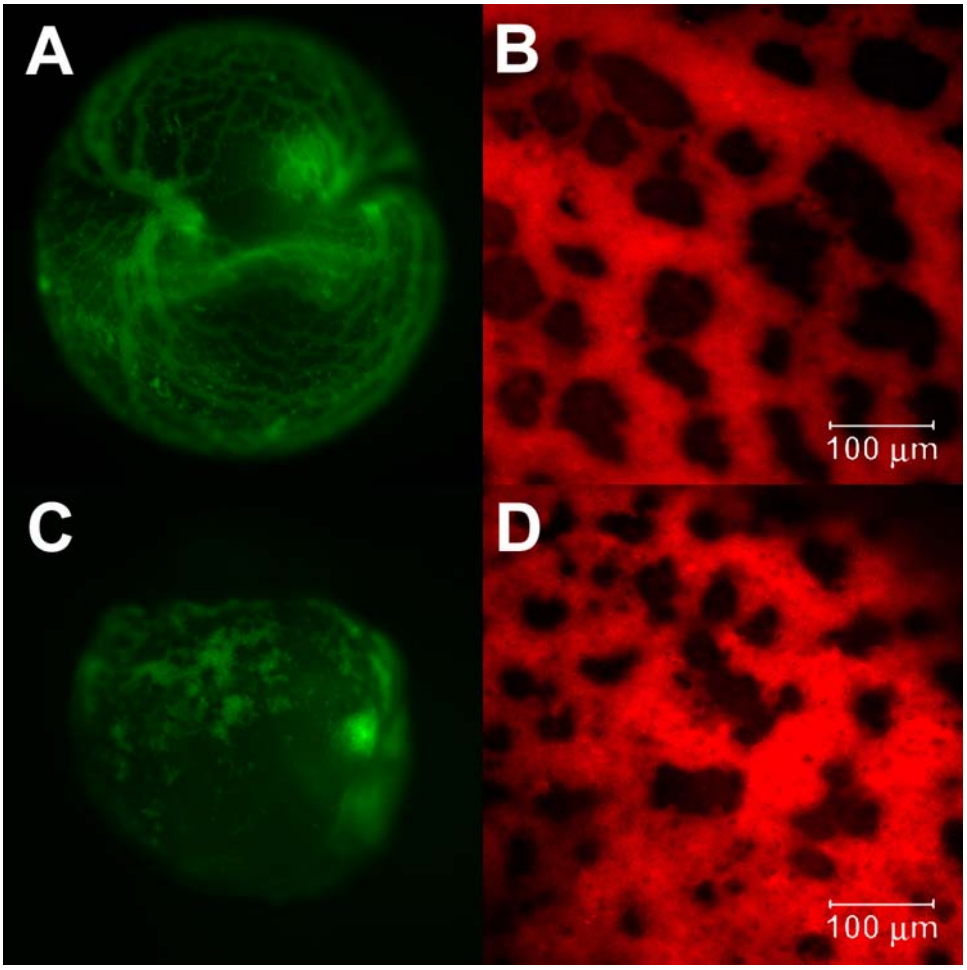

Figure 6

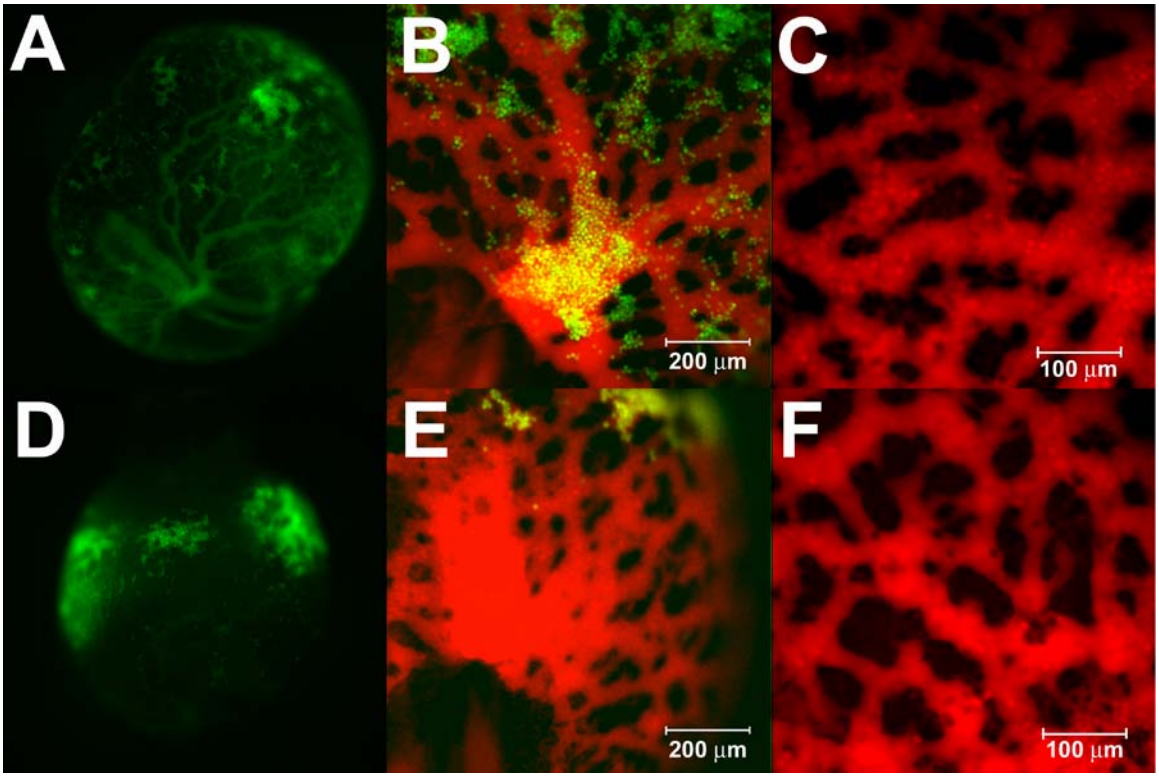

Figure 7

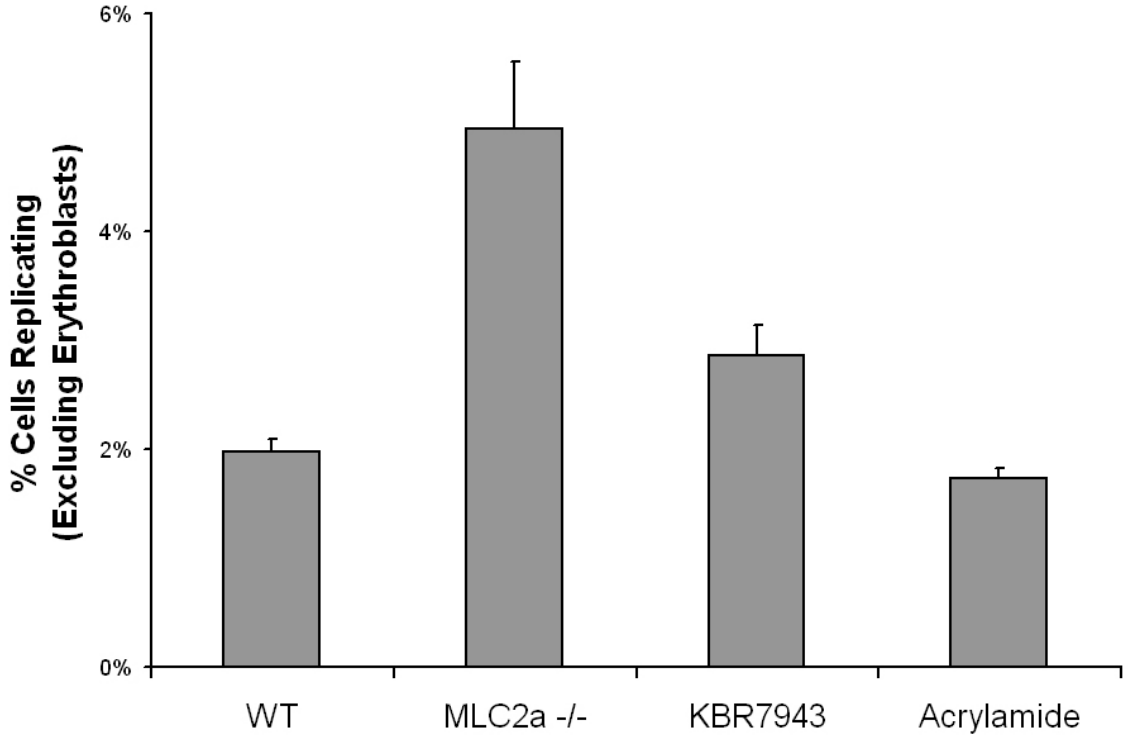
% Cells Replicating
(Excluding Erythroblasts)
6%
4%
2%
0%
WT
MLC2a -/-
KBR7943
Acrylamide

Chapter 6

Conclusions

Although it has been recognized for over a hundred years that blood flow is necessary for vascular remodeling, it is only recently that researchers have begun to investigate how endothelial cells respond to mechanical forces generated by blood flow. The work described here focuses on relating quantitative differences in shear stress with the response of neighboring endothelial cells. Biologists have many tools available to them for understanding changes in gene and protein expression within cells. The equivalent instruments for measuring biological forces, however, are not present. Thus, the first step to understanding the role of mechanical forces in biology is to find methods to measure these forces. The ability to measure blood flow velocity and shear stress in mammalian embryos provides one such technique ([1], Chapter 3). This work has allowed velocity profiles and shear stresses to be calculated for the first time every within developing mammalian embryos and established that shear stress levels were within the range known to activate cell signaling.

This work then continued to look at changes in vascular morphology during embryonic development in the context of the changes in blood flow that occur (Chapter 4). This worked established that the initiation of vascular remodeling coincides with the entry of erythroblasts into circulation; an event that is preceded by a significant period of plasma flow. The presence of this plasma flow constrained possible models of which events could be dependent on fluid flow, more specifically ruling out the possibility that paracrine signaling factors were carried by the blood in order to initiate remodeling events.

Having established that remodeling began just after the entry of erythroblasts into circulation, we tested whether the role of entry of the erythroblasts into circulation was to induce higher mechanical forces. This was done using MLC2a mutant mice, which lack an atrial contraction in the heart, and specific chemical techniques to reduce shear stress (Chapter 5). We found that whenever erythroblasts were prevented from entering the circulation, proper vascular remodeling was inhibited, even if the heart was normal. Other problems associated with the MLC2a$^{-/-}$ embryos, such as increased oscillatory flow, were secondary to problems associated with low shear stress flow. This work showed that changes in viscosity due to the entry of erythroblasts into circulation are essential for the formation of large vessels. Thus, by dissecting abnormal flow patterns, we begin to understand how blood flow, and the mechanical forces it imparts, are involved in normal cardiovascular development.

Outstanding Issues

Increasing Shear Forces During Vascular Remodeling

The shear stress exerted on the blood vessels during development is dependent on several factors, including the velocity profile of the blood, the viscosity of the blood and the pulsatility of the flow, all of which change during development. Though this makes it difficult to understand the role of fluid forces during development, it also gives us several parameters to adjust in order to change the shear force on the early blood vessels. Though my work has looked at altered shear stress, I was only successful at decreasing

shear stresses. In order to understand the role of shear stress in cardiovascular development, it will be necessary to find methods to increase shear stress as well.

The most obvious method to increase the shear stress on endothelial cells is to change blood flow velocity by altering the heart rate. The embryonic heart rate can be altered by temperature and by exogenous chemical. Changes in temperature, however, affect the viability of all cells in the embryo. Also, chemicals known to increase the heart rate of adults often operate on proteins that are either not expressed in the heart at the early stages of heart development or their expression is not specific to the heart early in development. Thus, the non-specificity of the effect of temperature and chemicals made interpretation of the results difficult. As we begin to gain a better understanding of the molecules involved in heart development and contractile function, it should be possible to find compounds that control the embryonic heart rate specifically without additional side-effects.

Shear stress levels can be altered not only by changing the velocity of the blood flow, but also by changing the viscosity of the blood. In a similar way, it should be possible to increase the shear stresses by increasing the viscosity of the blood. The use of erythropoietin, a protein involved in the control of red blood cell production, was used unsuccessfully in an attempt to increase embryonic blood production. The injection of foreign substances that could affect the blood viscosity, including dextran, microspheres and liposomes, was also attempted. The increases were never significant enough to affect development. Several options, however, still exist. Mouse mutants for the erythropoietin receptor exist that exhibit increased red blood cell production at birth [2].

The level of embryonic blood production has not been investigated in these mice. Another possibility is the use of materials whose viscosity can be altered after injection into the cardiovascular system, by catalyst addition or UV polymerization. Therefore, it is technically feasible that a method for increasing the viscosity of blood in the embryo be found.

Non-laminar Flow Patterns

Disturbed flow patterns are known to be very biologically active (for review see [3]) and induce cell proliferation as well as apoptosis [4]. Disturbed flow patterns include turbulent flows as well as eddies caused by laminar flow separation. The confocal line scanning technique we have used to calculate hemodynamic parameter ([1], Chapter 3) cannot measure shear stress present with such flow patterns. This requires high-speed imaging and complicated cell tracking algorithms, technology that until recently was unavailable. With the advent of these new tools, it should be possible to investigate where within the yolk sac disturbed patterns of flow are present and whether these locations correlate to areas of increased cell proliferation or gene upregulation.

It will also be interesting to investigate the role of oscillatory flow during cardiovascular development. MLC2a$^{-/-}$ embryos exhibit increased oscillatory flow (Chapter 5). We found that this was not the primary cause of the defect but that it was biologically active. A model is required in which oscillatory flow is not accompanied by lower flow velocity. The knowledge that the atrial contraction is important for producing net forward flow aids in the search for an appropriate model organism. Zebrafish models exist where atrial and ventricular contractions are not coupled as well as other models where defects

cause regurgitant flow in the heart. Blood flow patterns in these fish have not been reported but may provide models for the effect of increased oscillatory flow during development.

Oxygen Signaling and Vascular Remodeling

In mature circulation, red blood cells function to carry oxygen to cells, however, it is not clear that this role is essential in the first few days of embryonic blood flow. In chick [5], frog [6] and mouse embryos (unpublished results), culture with carbon monoxide, which effectively ablates oxygen transport by the blood, does not affect the early embryo or the remodeling of the vasculature. Mouse embryos also undergo a process of axial rotation, or turning, in which the embryo rotates such that it detaches from the yolk sac and the only access to the extra-embryonic circulation is through two large vessels called the vitelline vessels. Remodeling begins before the embryo turns, however, when both the yolk sac and the embryo proper have equal access to the maternal circulation. These observations have lead to the idea that the initial role of the entry of erythroblasts into circulation is simply to increase the viscosity of the blood, and not to carry oxygen.

The role of oxygen during remodeling can be investigated in several different ways. If erythroblasts truly represent particles whose only initial function is to increase the viscosity of the blood, then the addition of microspheres should rescue mutants which lack erythroblast circulation. One such mutant is the Scl/Tal$^{-/-}$ mouse in which no primitive erythroblasts form [7]. Secondly, a mutant mouse exists that has constituently active HIF-1α [8], which is the protein responsible for sensing low oxygen levels. These mice are viable, though hypervascularized. If mice that constitutively express HIF-1α

are mated to mice with problems with flow dynamics, the presence of vascular abnormalities would indicate that the problems were related to the flow dynamics and not caused by improper signaling for oxygen. This is especially true if cell viability in surrounding tissues is unaffected.

Linking Fluid Dynamics To Genetics

While understanding how mechanical forces are involved in remodeling is important, it is necessary to determine how epigenetic signals relate to genetic signaling cascades. As in vitro studies unravel how endothelial cells sense shear stresses (for review, see [3]), it will be important to extend this work in vivo and establish whether similar signaling mechanisms are at work during development. Enhancer elements have been isolated that are shear responsive [9, 10]. Using these enhancer elements to drive a reporter gene would give an in vivo marker of the location where fluid flow is most active. This would not only show that shear stress is genetically active within the embryo but indicate the type of flow patterns that is most biologically important within the embryo.

While it is still not clear how endothelial cells sense and transduce signals from mechanical force, many genes that are essential for this process are known, including VE-cadherin and integrins (for review, see [3]). Endothelial cells which lack VE-cadherin fail to activate several shear-responsive genes, including Flk1, p38 and Akt1 [11]. Lack of VE-cadherin function in embryos causes embryonic lethality. In these mutants, endothelial cells of the vasculature detach from their basement membrane [12]. Genes that are important for mechanotransduction, however, are expressed in both the heart and the vasculature, leading to cardiac defects that cause flow abnormalities. Therefore,

if in vitro work on mechanotransduction is to be extended to developmental systems, it will require the production of mice in which the function of these genes important in shear stress sensing is removed specifically in the vasculature.

The study of external stimuli, such as mechanical forces, on development has only recently begun to be addressed. It represents an exciting intersection between various sciences, including physics, engineering and biology. By studying early blood fluid dynamics, this work contributes to our understanding of how an efficient and functional cardiovascular system is established. The many outstanding issues regarding the role of mechanical forces in cardiovascular development raised by this work will be the subject of further study.

References

1. Jones, E.A., M.H. Baron, S.E. Fraser, and M.E. Dickinson, Measuring hemodynamic changes during mammalian development*. Am J Physiol Heart Circ Physiol*, 2004. 287(4): H1561-9.
2. Divoky, V., Z. Liu, T.M. Ryan, J.F. Prchal, T.M. Townes, and J.T. Prchal, Mouse model of congenital polycythemia: Homologous replacement of murine gene by mutant human erythropoietin receptor gene*. Proc Natl Acad Science USA*, 2001. 98(3): 986-91.
3. Resnick, N., H. Yahav, A. Shay-Salit, M. Shushy, S. Schubert, L.C.M. Zilberman, and E. Wofovitz, Fluid shear stress and the vascular endothelium: for better and for worse*. Prog Biophys Mol Biol.*, 2002. 81(3): 177-99.
4. Davies, P.F., A. Remuzzi, E.J. Gordon, C.F. Dewey, Jr., and M.A. Gimbrone, Jr., Turbulent fluid shear stress induces vascular endothelial cell turnover in vitro*. Proc Natl Acad Sci USA*, 1986. 83(7): 2114-7.
5. Cirotto, C. and I. Arangi, Chick embryo survival under acute carbon monoxide challenges*. Comp Biochem Physiol A*, 1989. 94(1): 117-23.
6. Territo, P.R. and W.W. Burggren, Cardio-respiratory ontogeny during chronic carbon monoxide exposure in the clawed frog Xenopus laevis*. J Exp Biol*, 1998. 201(Pt 9): 1461-72.
7. Shivdasani, R.A., E.L. Mayer, and S.H. Orkin, Absence of blood formation in mice lacking the T-cell leukaemia oncoprotein tal-1/SCL*. Nature*, 1995. 373(6513): 432-4.

8. Elson, D.A., G. Thurston, L.E. Huang, D.G. Ginzinger, D.M. McDonald, R.S. Johnson, and J.M. Arbeit, Induction of hypervascularity without leakage or inflammation in transgenic mice overexpressing hypoxia-inducible factor-1alpha. *Genes Dev*, 2001. 15(19): 2520-32.
9. Resnick, N., T. Collins, W. Atkinson, D.T. Bonthron, C.F. Dewey, Jr., and M.A. Gimbrone, Jr., Platelet-derived growth factor B chain promoter contains a cis-acting fluid shear-stress-responsive element. *Proc Natl Acad Sci USA*, 1993. 90(10): 4591-5.
10. Shyy, J.Y., Y.S. Li, M.C. Lin, W. Chen, S. Yuan, S. Usami, and S. Chien, Multiple cis-elements mediate shear stress-induced gene expression. *J Biomech*, 1995. 28(12): 1451-7.
11. Shay-Salit, A., M. Shushy, E. Wolfovitz, H. Yahav, F. Breviario, E. Dejana, and N. Resnick, VEGF receptor 2 and the adherens junction as a mechanical transducer in vascular endothelial cells. *Proc Natl Acad Science USA*, 2002. 99(14): 9462-7.
12. Carmeliet, P., M.G. Lampugnani, L. Moons, F. Breviario, V. Compernolle, F. Bono, G. Balconi, R. Spagnuolo, B. Oostuyse, M. Dewerchin, A. Zanetti, A. Angellilo, V. Mattot, D. Nuyens, E. Lutgens, F. Clotman, M.C. de Ruiter, A. Gittenberger-de Groot, R. Poelmann, F. Lupu, J.M. Herbert, D. Collen, and E. Dejana, Targeted deficiency or cytosolic truncation of the VE-cadherin gene in mice impairs VEGF-mediated endothelial survival and angiogenesis. *Cell*, 1999. 98(2): 147-57.